

Decoupled Continuous-Time Reinforcement Learning via Hamiltonian Flow

Minh Nguyen^{1,2}

Abstract

Many real-world control problems, ranging from finance to robotics, evolve in continuous time with non-uniform, event-driven decisions. Standard discrete-time reinforcement learning (RL), based on fixed-step Bellman updates, struggles in this setting: as time gaps shrink, the Q -function collapses to the value function V , eliminating action ranking. Existing continuous-time methods reintroduce action information via an advantage-rate function q . However, they enforce optimality through complicated martingale losses or orthogonality constraints, which are sensitive to the choice of test processes. These approaches entangle V and q into a large, complex optimization problem that is difficult to train reliably. To address these limitations, we propose a novel decoupled continuous-time actor-critic algorithm with alternating updates: q is learned from diffusion generators on V , and V is updated via a Hamiltonian-based value flow that remains informative under infinitesimal time steps, where standard max/softmax backups fail. Theoretically, we prove rigorous convergence via new probabilistic arguments, sidestepping the challenge that generator-based Hamiltonians lack Bellman-style contraction under the sup-norm. Empirically, our method outperforms prior continuous-time and leading discrete-time baselines across challenging continuous-control benchmarks and a real-world trading task, achieving 21% profit over a single quarter—nearly doubling the second-best method.

1. Introduction

Many learning and control problems in scientific computing, robotics, and finance evolve in continuous time with continuous state and action spaces. In markets, decisions are often made only when new signals arrive or positions need rebalancing, so holding times vary even when prices are ob-

¹Google ²University of Texas at Austin. Correspondence to: Minh Nguyen <minhpnguyen@utexas.edu>.

served per minute. Robots face the same pattern: often they can move with coarse updates, but when terrain becomes unstable or contacts change, they need small corrective steps to keep balance and recover. Similarly, autonomous vehicles take larger control steps on empty roads but update more frequently near intersections or in dense traffic. Across these domains, we need RL methods that learn reliably with both irregular decision times and small step sizes.

Standard reinforcement learning algorithms, however, are built on a discrete-time Markov decision process (MDP) abstraction with a fixed step size Δt . This mismatch creates practical and theoretical issues when decisions occur at irregular times and when the data mixes multiple time scales. With large Δt , the model can miss important dynamics between decisions; with very small Δt , Bellman targets change little from one step to the next, weakening learning signals and making training sensitive to noise. More fundamentally, the fixed-step Bellman recursion does not naturally account for non-uniform holding times, so the resulting updates can depend heavily on the choice of discretization rather than the underlying continuous-time control problem.

To address these issues, recent continuous-time RL work recasts learning as stochastic control. Building on the controlled-diffusion formulation of Wang et al. (2020), Jia & Zhou (2023) introduce the advantage-rate function $q(x, a)$, which restores state-action discrimination lost when the discrete-time Q -function collapses to V as $\Delta t \rightarrow 0$. This q -function underlies both value-based methods with martingale constraints (Jia & Zhou, 2023) and policy-gradient variants such as entropy-regularized PPO (CPPO) (Zhao et al., 2023). These formulations provide a foundation for learning under irregular decision times and small timesteps, without relying on a fixed discretization.

However, a central technical challenge remains. Under diffusion dynamics, minimizing the usual squared temporal-difference (TD) error does not directly enforce the dynamic programming principle: in continuous time, such losses can primarily control variance terms induced by Brownian noise rather than true Bellman errors. Prior work addresses this by imposing martingale-based objectives or martingale orthogonality conditions that characterize the optimal solution (Jia & Zhou, 2023). While theoretically motivated, these modifications make optimization substantially harder in practice.

Martingale objectives couple q and V into a single functional optimization problem, which is difficult to simplify into standard TD-style updates and can be challenging to optimize with modern function approximation and off-policy training. This motivates seeking continuous-time learning rules that keep the stochastic-control foundation, but admit a more modular and scalable optimization structure.

In this paper, we resolve these difficulties by **decoupling** the learning of q and V , replacing a single coupled objective with a sequence of simple updates. With V fixed, the correct q is locally determined by the controlled generator. It can then be learned from trajectory data via standard regression, treating diffusion noise as estimation noise that averages out over minibatches. The remaining challenge is updating V from an **instantaneous rate** q . Unlike discrete-time RL, where one can apply a backup such as $V(x) = \max_a Q(x, a)$ (or a soft analogue), this step becomes ill-posed in continuous time. We instead view the update equation as defining a **flow** over value functions. This leads to an explicit Picard-style update driven by the entropy-regularized Hamiltonian, with a step size that indexes **algorithmic progress** rather than an environment discretization. We establish convergence of this value-flow iteration under broad conditions. We further obtain a scalable actor–critic implementation through the simple critic decomposition $Q \approx V + q$, keeping the method practical while staying aligned with the continuous-time stochastic control formulation.

Contribution. Our contributions are threefold.

- (1) We propose a continuous-time RL framework that separates learning the advantage-rate signal from updating the value function, replacing martingale-coupled objectives with a simpler iterative scheme. This leads to a practical implementation compatible with standard off-policy training.
- (2) We prove rigorous convergence guarantees using a probabilistic analysis technique that avoids the heavy functional-analytic machinery typically required for generator-based operators. This approach also enables us to control the approximation error directly from sampled stochastic trajectories in continuous-time settings.
- (3) We provide an empirical study beyond fixed-step simulated SDE benchmarks, evaluating continuous-time RL on high-dimensional control tasks with irregular decision times and a minute-based trading environment. Our method achieves consistently stronger performance than existing continuous-time approaches and discrete-time baselines.

Organization. In Section 2, we introduce the continuous-time reinforcement learning formulation, together with key terminologies needed in our framework setup. In Section 3, we discuss limitations of prior martingale-based approaches and present our novel decoupled framework together with

the resulting actor–critic algorithms. In Section 4, we establish theoretical and convergence guarantees for the value function, the advantage-rate function, and the full algorithm. Finally, Section 5 evaluates our methods on continuous-control benchmarks and a real-world trading task under small and irregular time steps. Extended related work appears in Appendix A. Background material is summarized in C. Full proofs are deferred to Appendices D, E, F, G, and H. Additional experimental details and reproducibility information are provided in Appendices B and J.

2. Preliminaries

2.1. Discrete-time MDPs to continuous-time control

The usual Markov decision process (MDP) discretized with a fixed time step $\Delta > 0$ has the form:

$$X_{t+\Delta}^\Delta = X_t^\Delta + f^\Delta(X_t^\Delta, a_t), \quad a_t \sim \pi_\alpha(\cdot | X_t^\Delta) \quad (1)$$

where $t \in \{0, \Delta, 2\Delta, \dots\}$, $X_t^\Delta \in \mathbb{R}^d$, and π_α denotes an exploration policy. Through classical limit arguments, Munos (2006) shows that if the increment is approximately linear in Δ , i.e., $f^\Delta(x, a) = f(x, a) \Delta + o(\Delta)$, then, as $\Delta \rightarrow 0$, the discrete process converges to a deterministic trajectory x_t governed by the ODE:

$$\dot{x}_t = f_\alpha(x_t), \quad f_\alpha(x) := \mathbb{E}_{a \sim \pi_\alpha(\cdot | x)} [f(x, a)] \quad (2)$$

where action randomization averages into the drift. To model stochasticity beyond randomized actions, we augment the transition with a mean-zero perturbation,

$$X_{t+\Delta}^\Delta = X_t^\Delta + f^\Delta(X_t^\Delta, a_t) + \xi_t^\Delta \quad (3)$$

Under diffusion scaling (e.g., $\text{Var}(\xi_t^\Delta) = \mathcal{O}(\Delta)$), the accumulated fluctuations converge to Brownian motion (Donsker’s invariance principle; Fleming & Mete Soner, 2006), and the continuous-time limit becomes a controlled diffusion. This motivates the Itô SDE model used throughout the paper (formalized next; details in Appendix I).

2.2. Stochastic control formulation

Motivated by the diffusion limit above, we model continuous-time RL as controlled stochastic dynamics: the state process $(X_t)_{t \geq 0} \subset \mathbb{R}^d$ evolves according to Itô SDE:

$$dX_t = b(X_t, a_t) dt + \sigma(X_t, a_t) dW_t, \quad X_0 \sim \mu \quad (4)$$

where W is an n -dimensional Brownian motion, $a_t \in \mathcal{A}$ is the control (action), and $b : \mathbb{R}^d \times \mathcal{A} \rightarrow \mathbb{R}^d$, $\sigma : \mathbb{R}^d \times \mathcal{A} \rightarrow \mathbb{R}^{d \times n}$ are measurable drift/diffusion functions. We restrict to Markov feedback policies $a_t \sim \pi(\cdot | X_t)$, so exploration is implemented through randomized control.

Given discount $\beta > 0$, running reward $r : \mathbb{R}^d \times \mathcal{A} \rightarrow \mathbb{R}$, and temperature $\alpha \geq 0$, we consider the entropy-regularized objective:

$$V^{(\alpha)}(x; \pi) := \mathbb{E} \left[\int_0^\infty e^{-\beta t} \left(r(X_t, a_t) - \alpha \log \pi(a_t | X_t) \right) dt \mid X_0 = x \right] \quad (5)$$

with the optimal (entropy-regularized) value function $V^{(\alpha)}(x) := \sup_{\pi} V^{(\alpha)}(x; \pi)$.

2.3. Generators and Hamiltonians

Two standard objects from stochastic control are central to our framework: the controlled generator and the (hard/soft) Hamiltonian. For a fixed action $a \in \mathcal{A}$, define the controlled (infinitesimal) generator L^a acts on $\varphi \in C_b^2(\mathbb{R}^d)$ as:

$$(L^a \varphi)(x) := b(x, a) \cdot \nabla \varphi(x) + \frac{1}{2} \text{Tr}(\sigma(x, a) \sigma(x, a)^\top \nabla^2 \varphi(x)) \quad (6)$$

We view $L^a \varphi$ as continuous-time analogue of one-step Bellman drift. Using L^a , define the action-wise Hamiltonian:

$$H_a(V)(x) := (L^a V)(x) + r(x, a) - \beta V(x) \quad (7)$$

The corresponding hard Hamiltonian ($\alpha = 0$) is:

$$H^{(0)}(V)(x) := \sup_{a \in \mathcal{A}} H_a(V)(x) \quad (8)$$

and the soft (entropy-regularized) Hamiltonian for $\alpha > 0$ is:

$$H^{(\alpha)}(V)(x) := \alpha \log \int_{\mathcal{A}} \exp \left(\frac{1}{\alpha} H_a(V)(x) \right) da \quad (9)$$

As $\alpha \rightarrow 0$, $H^{(\alpha)}$ recovers $H^{(0)}$. We include the discount term $-\beta V(x)$ inside the Hamiltonian for a compact form. Under standard assumptions, the optimal value function $V^{(\alpha)}$ satisfies the HJB equation (Fleming & Mete Soner, 2006; Tang et al., 2021):

$$H^{(\alpha)}(V^{(\alpha)})(x) = 0, \quad x \in \mathbb{R}^d \quad (10)$$

2.4. Instantaneous q -function in continuous time

In discrete-time MDPs, the state–action value function Q provides a direct action-selection signal, e.g., through $V(x) = \max_a Q(x, a)$. In continuous time, however, the standard Q -function collapses to V as the time step shrinks to zero, i.e., $\lim_{\Delta \rightarrow 0} Q^\Delta(x, a) = V(x)$, regardless of action a . To restore action dependence, Jia & Zhou (2023) introduce the *advantage rate* (instantaneous) q -function. For a policy π with value function $V^{(\alpha)}(\cdot; \pi)$, define:

$$q^{(\alpha)}(x, a; \pi) := \lim_{u \rightarrow 0} \frac{Q_u^{(\alpha)}(x, a; \pi) - V^{(\alpha)}(x; \pi)}{u} \quad (11)$$

where $Q_u^{(\alpha)}(x, a; \pi)$ is the return obtained by executing action a for a short duration u starting from state x , and then following π afterwards. With $V = V^{(\alpha)}(\cdot; \pi)$, standard small-time expansion yields:

$$Q_u^{(\alpha)}(x, a; \pi) = V(x) + H_a(V)(x) u + o(u) \quad (12)$$

As a result, q -function can be also expressed as:

$$q_V(x, a) = q^{(\alpha)}(x, a; \pi) = H_a(V)(x) \quad (13)$$

Unlike the degenerate continuous-time limit of Q , the function $q(x, a)$ retains action dependence and provides the correct local improvement signal.

Notations. From here on, we write $V^{(\alpha)}$ for the **optimal** value function, and use V for a generic value function (e.g., under a non-optimal policy or an approximation) in place of $V^{(\alpha)}(x; \pi)$. By Equation (13), the instantaneous q -function is determined by the corresponding V , so we write $q = q_V$ instead of $q^{(\alpha)}(x, a; \pi)$ so that $q_V(x, a) = H_a(V)(x)$. In particular, the optimal q -function is denoted as $q_{V^{(\alpha)}}$.

3. Formulation

3.1. Challenges in continuous-time RL

The instantaneous q -function introduced in Section 2.4 resolves the degeneracy of the discrete-time Q -function in the infinitesimal limit. A second obstacle remains: under diffusion dynamics, the usual squared TD regression is no longer aligned with the continuous-time dynamic programming principle. Consider the TD error with step size $u > 0$,

$$\delta_u \approx e^{-\beta u} V(X_{t+u}) + u r(X_t, a_t) - V(X_t) \quad (14)$$

In a discrete-time MDP, minimizing $\mathbb{E}[\delta_u^2]$ enforces Bellman consistency. In continuous time, however, the discounted value increment contains not only a drift term but also a stochastic martingale term. In particular, with Itô lemma, rewriting δ_u in differential form as $u \rightarrow 0$ yields:

$$\begin{aligned} & d(e^{-\beta t} V(X_t)) + e^{-\beta t} r(X_t, a_t) dt \\ &= e^{-\beta t} \left((L^{a_t} V)(X_t) - \beta V(X_t) + r(X_t, a_t) \right) dt \\ & \quad + e^{-\beta t} \nabla V(X_t) \sigma(X_t, a_t) dW_t \end{aligned} \quad (15)$$

As $u \rightarrow 0$, these two terms scale differently: the drift is $O(u)$, while the stochastic increment is $O(\sqrt{u})$. Hence, δ_u^2 is dominated by martingale variation rather than the Bellman drift. To handle this mismatch, rather than simply reuse discrete-time TD updates, Jia & Zhou (2023) characterize continuous-time RL through martingales. More specifically, for V and q to be optimal, the process

$$M_t := e^{-\beta t} V(X_t) + \int_{t_0}^t e^{-\beta u} (r(X_u, a_u) - q(X_u, a_u)) du \quad (16)$$

must be a martingale for any starting time t_0 .

A direct way to enforce this is a martingale-loss objective, which leads to a nested long-horizon path functional. To avoid this complexity, [Jia & Zhou \(2023\)](#) instead propose enforcing martingality through orthogonality tests, i.e., requiring $\mathbb{E}\left[\int_0^T \omega_t dM_t\right] = 0$ for suitable filtration-adapted test processes ω_t . In theory, this condition holds for any ω_t ; in practice, [Jia & Zhou \(2023\)](#) note that numerical performance requires a careful choice of test family, and common gradient-based constructions are largely heuristic. Both martingale-loss and orthogonality enforcement then couple V and q into a single optimization problem, making them hard to reduce to standard TD-style updates. Explicit details of these approaches are given in [Appendix K](#).

Beyond these value-based martingale formulations, continuous-time policy-gradient methods such as CPPO ([Zhao et al., 2023](#)) are among the few alternatives, but they also rely on the same martingale-enforcement formulas. This leaves the current continuous-time RL approaches constrained by a common bottleneck, which is reflected in our experiments: even in settings with irregular timesteps, where continuous-time methods should be more suitable, these approaches still underperform their discrete-time counterparts (see [Section 5](#)).

3.2. Continuous-time actor–critic via Hamiltonian flow

Instead of enforcing martingale constraints through a single coupled optimization over (V, q) , we break learning into a sequence of smaller, tractable subproblems that iteratively update q and V :

$$V_0 \Rightarrow q_0 \Rightarrow V_1 \Rightarrow q_1 \Rightarrow \dots \quad (17)$$

The guiding principle is simple: *learning q is easy if V is fixed*, and the remaining difficulty is *updating V from an instantaneous rate* without degeneracy.

Step 1: Updating q from a fixed V . For a fixed value function V , from [Equation \(13\)](#), the q -function can be determined locally by the controlled diffusion generator L^a :

$$q_V(x, a) = r(x, a) + (L^a V)(x) - \beta V(x). \quad (18)$$

This characterization is exact, but it is not directly model-free since $(L^a V)(x)$ depends on unknown dynamics.

Step 2: Updating V from q is not a discrete-time max step. In discrete-time RL, one typically recovers V via a hard or soft maximization of Q :

$$\begin{aligned} V(x) &= \max_a Q(x, a), \text{ or} \\ V(x) &= \alpha \log \int_{\mathcal{A}} \exp(Q(x, a)/\alpha) da \end{aligned} \quad (19)$$

Algorithm 1 Continuous-time soft actor-critic (CT-SAC)

- 1: **Input:** discount β , temperature α , Euler step $\tau > 0$.
- 2: Initialize parameters θ and ϕ for Q_θ and policy π_ϕ .
- 3: **for** $k = 0, 1, 2, \dots$ **do**
- 4: Collect transitions (x, a, r, x', u) , where $x = X_t$, u is the time step increment, $x' = X_{t+u}$, $a = a_t$ is the action, and $r = r(X_t, a_t)$ from rollouts under current policy π_ϕ and store in an off-policy buffer. u can vary across samples.
- 5: **Update** $Q_\theta = q_\theta + V_\theta$: Fit Q_θ using mini-batch samples (x, a, r, x', u) with targets being the left hand-side of [Equation \(33\)](#).
- 6: **Update** π_ϕ : towards $\pi_\phi(a | x) \propto \exp(Q_\theta(x, a)/\alpha)$
- 7: **end for**

In continuous time, however, q is an instantaneous *rate*, not a value. If we relate a small-step return by $Q_u(x, a) \approx V(x) + u q(x, a)$ as $u \rightarrow 0$, then the soft backup degenerates:

$$\begin{aligned} V(x) &= \alpha \log \int_{\mathcal{A}} \exp((V(x) + u q(x, a))/\alpha) da \\ &= V(x) + \alpha \log \int_{\mathcal{A}} \exp(u q(x, a)/\alpha) da \end{aligned} \quad (20)$$

As $u \rightarrow 0$, this becomes a trivial update $V_{\text{new}}(x) \rightarrow V(x)$, while enforcing equality yields a meaningless normalization condition. This reflects a unit mismatch: V behaves like a displacement (a value), while q behaves like a velocity (a derivative), so direct max/softmax backups are ill-posed in the infinitesimal setting.

To extract a non-degenerate update from q in the infinitesimal setting, we propose a novel approach that interprets the update not as a discrete backup but as a *flow* indexed by an iteration parameter τ . As a first step, consider the soft backup increment at small u :

$$V_u(x) := V(x) + \alpha \log \int_{\mathcal{A}} \exp(u q(x, a)/\alpha) da \quad (21)$$

The increment vanishes as $u \rightarrow 0$. However, Jensen inequality implies an overestimation for V_u :

$$V_u(x) - V(x) \leq \alpha u \log \int_{\mathcal{A}} \exp(q(x, a)/\alpha) da \quad (22)$$

Crucially, this overestimation allows us to derive an update gradient flow by considering the ratio $[V_u(x) - V(x)]/u$:

$$\frac{d}{d\tau} V_\tau(x) = \mathcal{Q}^{(\alpha)}(q_{V_\tau})(x). \quad (23)$$

where the aggregation operator \mathcal{Q} acts on q as:

$$\begin{aligned} \mathcal{Q}^{(\alpha)}(q)(x) &:= \alpha \log \int_{\mathcal{A}} \exp(q(x, a)/\alpha) da, \\ \mathcal{Q}^{(0)}(q)(x) &:= \sup_{a \in \mathcal{A}} q(x, a). \end{aligned} \quad (24)$$

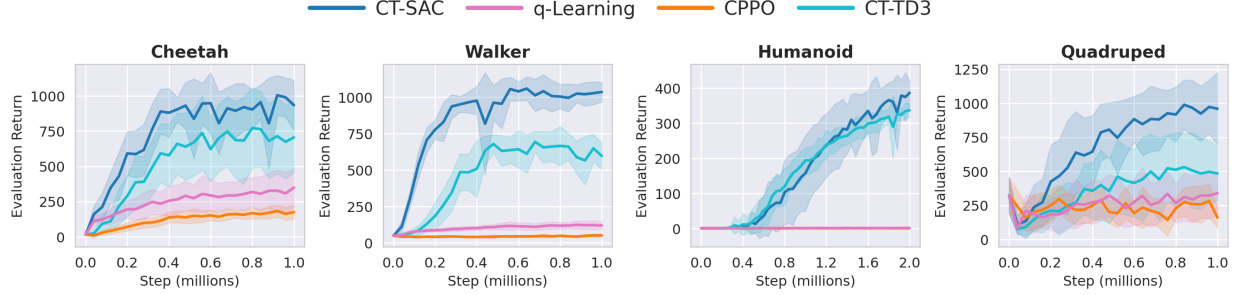


Figure 1. Evaluation returns for 4 continuous-time algorithms including our CT-SAC and CT-TD3 on control tasks over 12 seeds.

Under our decoupled scheme, $q_\tau = q_{V_\tau}$ is defined solely by V_τ , and substituting this into Equation (24) yields exactly the Hamiltonian operator:

$$\mathcal{Q}^{(\alpha)}(q_V)(x) = H^{(\alpha)}(V)(x). \quad (25)$$

Therefore the flow becomes the Hamiltonian-driven ODE:

$$\frac{d}{d\tau} V_\tau(x) = H^{(\alpha)}(V_\tau)(x), \quad (26)$$

and we have the following forward-Euler step with step size $\tau > 0$ that is called the **Picard–Hamiltonian iteration**:

$$V^{\text{new}}(x) = V(x) + \tau H^{(\alpha)}(V)(x) = T_\tau^{(\alpha)}(V)(x). \quad (27)$$

In Section 4, we establish convergence of this *ideal* iteration to $V^{(\alpha)}$ as $\tau \rightarrow 0$.

Model-free q -estimation induces discretized Hamiltonian flows. The remaining gap is that $(L^a V)(x)$ in Equation (18) is not available in model-free RL. Instead, we estimate the instantaneous rate via its small-time representation: for a holding time $u > 0$,

$$q_V(x, a) = \lim_{u \rightarrow 0} q_V^u(x, a),$$

$$q_V^u(x, a) := \frac{e^{-\beta u} \mathbb{E}[V(X_{t+u}) \mid X_t = x, a_t = a] - V(x)}{u} + r(x, a). \quad (28)$$

This replaces the generator by a short-horizon value increment and converges to q_V as $u \rightarrow 0$. To reduce discretization bias, we further apply Richardson extrapolation:

$$\tilde{q}_V^u(x, a) := 2 q_V^{u/2}(x, a) - q_V^u(x, a). \quad (29)$$

These approximations induce “discretized” Hamiltonians:

$$H_u^{(\alpha)}(V) := \mathcal{Q}^{(\alpha)}(q_V^u), \quad \tilde{H}_u^{(\alpha)}(V) := \mathcal{Q}^{(\alpha)}(\tilde{q}_V^u), \quad (30)$$

and the corresponding value iterations

$$V_{k+1} = V_k + \tau H_u^{(\alpha)}(V_k), \quad V_{k+1} = V_k + \tau \tilde{H}_u^{(\alpha)}(V_k). \quad (31)$$

In Section 4, we prove convergence of these discretized flows (including the Richardson variant) and show that \tilde{q}_V^u converges to the optimal $q_{V^{(\alpha)}}$ as $(\tau, u) \rightarrow 0$.

3.3. Final algorithm: a single critic via $Q \approx V + q$

The decoupled iteration above is conceptually clean: learn q given V , then update V via the Hamiltonian flow. However, maintaining two separate function approximators is inconvenient in practice. We therefore represent both quantities with a single critic network:

$$Q_k(x, a) := V_k(x) + q_k(x, a). \quad (32)$$

This is a numerical parameterization: while V and q have different roles, the decomposition lets one network carry both state-value and advantage-rate information. Near optimality, $q_k(x, a)$ is typically small for actions drawn from the improved policy, so $Q_k(x, a) \approx V_k(x)$ on-policy, making a single critic sufficient. With this representation, the decoupled update yields a practical sample-based critic target. By defining $\tilde{Q}_k(x, a) := Q_k(x, a) - \alpha \log \pi(a \mid x)$, the critic update takes the form:

$$Q_{k+1}(x, a) = (1 - \tau)Q_k(x, a) + \tau \mathbb{E}_a[\tilde{Q}_k(x, a)] + \tau r(x, a) + \tau \frac{\gamma \mathbb{E}_{a'}[\tilde{Q}_k(x', a')] - \mathbb{E}_a[\tilde{Q}_k(x, a)]}{u} \quad (33)$$

where discount $\gamma = e^{-\beta u}$, and u is the (possibly irregular) transition duration in the sampled tuple (x, a, r, x', u) . By the variational form of the soft Hamiltonian (Appendix I), the maximizer over $\pi(\cdot \mid x)$ is a Boltzmann policy, $\pi_V^{(\alpha)}(a \mid x) \propto \exp(q_V(x, a)/\alpha)$. Since $Q = V + q$ differs from q only by an a -independent shift, we implement the actor update equivalently as $\pi(a \mid x) \propto \exp(Q(x, a)/\alpha)$.

Combining these steps gives a continuous-time soft actor–critic method (CT-SAC; see Algorithm 1). A deterministic variant based on the hard operator gives a continuous-time analogue of TD3 (CT-TD3; see Algorithm 2).

4. Theoretical analysis

This section provides rigorous guarantees for the decoupled continuous-time learning framework in Section 3. Our analysis proceeds in three layers. We first study the *ideal* Picard–Hamiltonian iteration $V_{k+1} = T_\tau^{(\alpha)}(V_k) =$

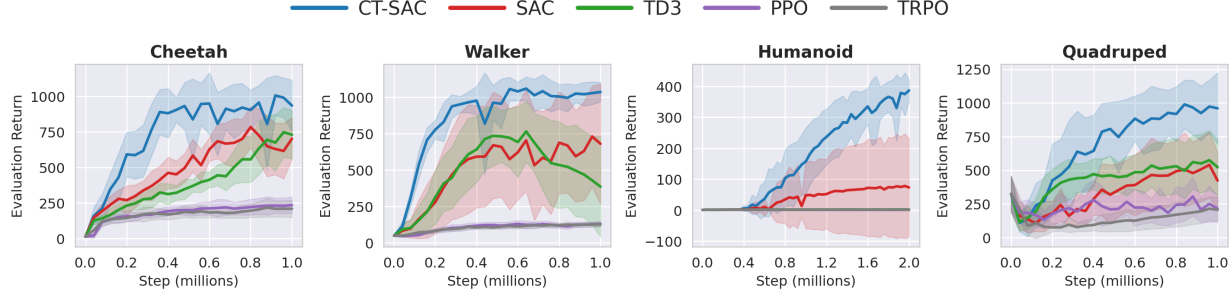


Figure 2. Evaluation returns for our CT-SAC against 4 discrete-time algorithms on control tasks over 12 seeds.

$V_k + \tau H^{(\alpha)}(V_k)$, which corresponds to the analytic rate q_V . We then analyze the *model-free discretized flows* obtained by replacing q_V with its finite-horizon approximation q_V^u , and its Richardson-corrected version \tilde{q}_V^u , yielding updates based on $H_u^{(\alpha)}$ and $\tilde{H}_u^{(\alpha)}$. Finally, we lift these results to the single-critic implementation of CT-SAC/CT-TD3.

Recall that $H^{(\alpha)}$ contains the infinitesimal generator term $L^a V$. Thus, unlike discrete-time Bellman operators, $T_\tau^{(\alpha)}$ is not a **contraction** mapping on $(C_b, \|\cdot\|_\infty)$ and purely analytic approaches often require Sobolev-type regularity with heavy analysis machinery. Instead, we compare $T_\tau^{(\alpha)}$ to a probabilistic dynamic-programming operator that is a sup-norm contraction and treat $T_\tau^{(\alpha)}$ as a controlled local approximation. We define the entropy-regularized dynamic-programming semigroup $\{\Phi_\tau^{(\alpha)}\}_{\tau \geq 0}$ by:

$$(\Phi_\tau^{(\alpha)} V)(x) := \sup_{\pi} \mathbb{E} \left[\int_0^\tau e^{-\beta t} \left(r(X_t, a_t) - \alpha \log \pi(a_t | X_t) \right) dt + e^{-\beta \tau} V(X_\tau) \mid X_0 = x \right] \quad (34)$$

The semigroup $\Phi_\tau^{(\alpha)}$ is value-only and serves as our contraction reference; it does not by itself provide the action-dependent signal needed for actor–critic updates. We begin with convergence of the ideal Picard–Hamiltonian iteration.

Theorem 4.1 (Value Function Convergence). *Fix $\alpha \geq 0$ and $\tau > 0$. Under Assumptions C.1, C.2, and C.3, let V_k being the value function after k iterations $V_{k+1} := T_\tau^{(\alpha)}(V_k)$. Then, V_k converges to $V^{(\alpha)}$ as $\tau \rightarrow 0$, and for all $k \geq 0$,*

$$\|V_k - V^{(\alpha)}\|_\infty \leq C_0 e^{-\beta \tau k} + \frac{C_1 \tau^{3/2}}{1 - e^{-\beta \tau}}. \quad (35)$$

Here C_0 and C_1 are constants independent of k .

Proof sketch. We compare the approximate update $V_{k+1} = T_\tau^{(\alpha)}(V_k)$ with the semigroup iteration

$$W_{k+1} := \Phi_\tau^{(\alpha)}(W_k), \quad C_0 := \|W_0 - V^{(\alpha)}\|_\infty. \quad (36)$$

The proof proceeds in 2 steps. In **step 1**, through a short-time Itô expansion, we prove the one-step operator error $\|\Phi_\tau^{(\alpha)}(V) - T_\tau^{(\alpha)}(V)\|_\infty \leq C_\alpha \tau^{3/2}$. Then, in **step 2**, with $E_k := V_k - W_k$, we recursively prove $\|E_k\|_\infty \leq \frac{C_\alpha \tau^{3/2}}{1 - e^{-\beta \tau}}$ through the decomposition:

$$\begin{aligned} E_{k+1} &= T_\tau^{(\alpha)}(V_k) - \Phi_\tau^{(\alpha)}(W_k) \\ &= (T_\tau^{(\alpha)}(V_k) - \Phi_\tau^{(\alpha)}(V_k)) + (\Phi_\tau^{(\alpha)}(V_k) - \Phi_\tau^{(\alpha)}(W_k)) \end{aligned}$$

Hence, $\|E_{k+1}\|_\infty \leq C_\alpha \tau^{3/2} + e^{-\beta \tau} \|E_k\|_\infty$.

Finally, Φ_τ is a contraction operator so that W_k converges exponentially to $V^{(\alpha)}$: $\|W_k - V^{(\alpha)}\|_\infty \leq e^{-\beta \tau k} C_0$. The triangle inequality then gives the desired bound (35). \square

We extend the result to the model-free estimator q_V^u (and \tilde{q}_V^u). We state the theorem for fixed u , and defer the random-increment case U to the Appendix G.

Theorem 4.2 (Convergence with q -function). *Let V_k be the resulting function defined by Richardson Picard–Hamiltonian iterations $V_{k+1} := V_k + \tau \tilde{H}_u^{(\alpha)}(V_k)$. Under Assumption E.2 and E.3, for $u > 0$, there exist constants C_1, C_2, L , and $\rho > 0$ such that for all $k \geq 0$:*

$$\|V_k - V^{(\alpha)}\|_\infty \leq e^{-\rho \tau k} \|V_0 - V^{(\alpha)}\|_\infty + \frac{C_1 (\tau^2 + \tau u^2)}{1 - e^{-\rho \tau}}. \quad (37)$$

And, for q -function estimation, we obtain the error:

$$\|\tilde{q}_{V_k}^u - q_{V^{(\alpha)}}\|_\infty \leq \frac{L}{u} \|V_k - V^{(\alpha)}\|_\infty + C_2 u^2 \quad (38)$$

In particular, if $\tau, u \rightarrow 0$ and $\tau/u \rightarrow 0$, then the value estimation V_k and the Richardson-version of q -function estimates converges to the optimal values $V^{(\alpha)}$ and $q_{V^{(\alpha)}}$.

Proof sketch. Now we need to find the error when q is estimate by finite fraction q^u . We use a similar proof as in Theorem 4.1 to bound value function with a stronger expansion for Φ_τ . The main difference now is the new error between $H^{(\alpha)}$ and $\tilde{H}_u^{(\alpha)}$. Luckily, the estimate $\|\tilde{q}_V^u - q_V\|_\infty \leq C u^2$ allows the Hamiltonian bound $\|\tilde{H}_u^{(\alpha)}(V) -$

$H^{(\alpha)}(V)\|_\infty \leq Cu^2$ so that the one-step error $\|\Phi_\tau^{(\alpha)}(V) - (V + \tau \tilde{H}_u^{(\alpha)}(V))\|_\infty$ is now bounded by $C_1(\tau^2 + \tau u^2)$.

For q -convergence, we use the Lipschitz bound $\|\tilde{q}_V^u - \tilde{q}_W^u\|_\infty \leq \frac{L}{u}\|V - W\|_\infty$, and transfer the work to V . \square

Finally, we translate these guarantees to the single-critic update $Q_k = V_k + q_k$ underlying CT-SAC/CT-TD3.

Theorem 4.3 (Theoretical Algorithm Convergence). *Consider the exact iterative update of Q_k through Equation (33) with no optimization or statistical error. Then Q_k converge to the optimal value $Q^{(\alpha)} = V^{(\alpha)} + q_{V^{(\alpha)}}$ as $k \rightarrow \infty$.*

Corollary 4.4 (Algorithm Convergence). *Suppose at each iteration k , n_k samples are used in the gradient update. Then, for any pair of $(\epsilon, \delta) > 0$, there exists an iteration L together with the sequence n_1, n_2, \dots, n_L so that with the probability of at least δ , $\mathbb{E} [|Q_L(X, A) - Q^{(\alpha)}(X, A)|^2] < \epsilon$ for random state-action pair (X, A) . Here $Q^{(\alpha)} = V^{(\alpha)} + q_{V^{(\alpha)}}$ is the optimal function, and Q_L is the learned function from Algorithm 1.*

Proof sketch. We construct the corresponding sequences (V_k, q_k) induced by the exact update and prove by induction that the decomposition (32) is preserved, i.e., $Q_k = V_k + q_k$ for all k . The convergence then follows by Theorem 4.2. For statistical part, let \hat{Q}_k denote the learned critic with finite samples of the k^{th} exact iteration of Q_k . Assume the update mapping is \mathcal{F} , then $Q_{k+1} = \mathcal{F}(Q_k)$. More importantly \hat{Q}_{k+1} is obtained by regression against $\mathcal{F}(\hat{Q}_k)$ with statistical error $\text{stat}_k := \|\hat{Q}_{k+1} - \mathcal{F}(\hat{Q}_k)\|$. For $\epsilon_k = \|\hat{Q}_k - Q_k\|$, one can obtain $\epsilon_{k+1} \leq \text{stat}_k + (1 + \frac{\tau}{u})\epsilon_k$ through the Lipschitzness of update mapping \mathcal{F} . For large enough number of samples, $\text{stat}_k \rightarrow 0$, yielding the converge of ϵ_k , and therefore, of the error w.r.t. optimal function $Q^{(\alpha)}$. \square

More refined control of sample complexity is given in Section H through a norm-transfer argument. Finally, refer to Appendices D, E, and F for the full detailed proofs of Theorems 4.1, 4.2, and 4.3 respectively.

5. Experiments

Moving beyond fixed-step simulated SDE benchmarks, we test whether continuous-time RL provides gains with irregular decision times and very small time steps on standard control benchmarks and a real trading task.

5.1. Tasks and baselines

Irregular-time setup. Across all tasks, the agent acts at event times $t_0 < t_1 < \dots$ with holding times $u_k := t_{k+1} - t_k$, where u_k **mixes between small and large timesteps** within the same rollout, so trajectories contain many short “micro-steps” interleaved with occasional larger

jumps. Concretely, we implement this by sampling u_k around the nominal control step u_{nom} . For example, for Cheetah we allow holding times as small as $\approx u_{\text{nom}}/5$ and as large as $\approx 3u_{\text{nom}}$. This setting is strictly harder than fixed-step training because trajectories are not time-aligned and learning must generalize beyond a single step size.

Legend: CT-SAC (blue), SAC (red), CPPO (orange), TD3 (green), q-Learning (magenta), PPO (purple), CT-TD3 (cyan), TRPO (grey).

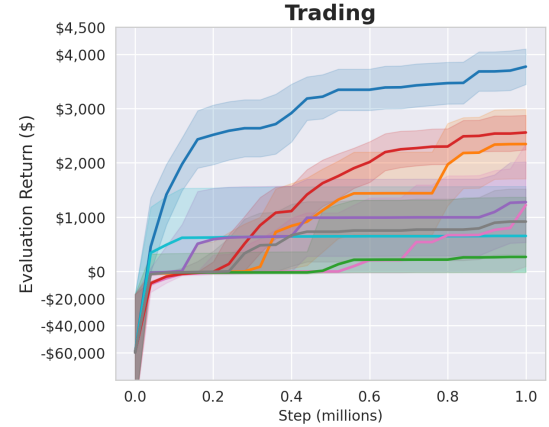


Figure 3. Two-week evaluation returns for CT-SAC and CT-TD3 (Ours) against 6 other algorithms on trading tasks.

Control tasks. We use DeepMind Control Suite (Tunyasuvunakool et al., 2020) for high-dimensional continuous control. Irregular timing is particularly important for humanoid and quadruped locomotion, where stability relies on timely corrective actions.

Real-world trading. We additionally evaluate on a trading environment constructed from minute-resolution market data (Alpaca API). The universe contains four industry sectors with five large-cap tickers each, and each episode spans two weeks of trading (390 minutes/day, 5 days/week). The agent makes decisions at irregular intervals with holding times $u \in [1, 20]$ minutes, using a state built from multi-scale historical price features (minutes to days). The action is to buy/sell a bounded quantity within an industry group, with position limits and transaction costs. The reward is the realized profit over the subsequent holding interval, so episode return equals total two-week P&L. To avoid temporal leakage, we train on Q3 2023 – Q2 2025 and evaluate on Q3 2025 using a fixed set of episodes so all methods face the same market paths. Details are provided in Appendix B.

Baselines. We benchmark against two baseline groups: continuous-time and discrete-time. For continuous-time RL, we include representative advantage-rate methods with martingale enforcement (q -Learning) (Jia & Zhou, 2023), as well as a continuous-time policy-gradient baseline (CPPO) (Zhao et al., 2023). To our knowledge, most existing continuous-time deep RL algorithms fall into these two fam-

ilies. Because these methods can be optimization-sensitive, we additionally apply stabilization techniques such as gradient clipping to improve their performance. For discrete-time RL, we compare against widely used state-of-the-art algorithms, SAC, TD3, TRPO, and PPO, implemented in Stable-Baselines3 (Raffin et al., 2021).

Evaluation. We train each method for 1M environment steps on control tasks (2M on humanoid). We tune hyperparameters over the search space (detailed in Appendix B) and select the best configuration for each method. We additionally keep the top 3 configurations for ablations, and report the best one in the main figures. Evaluation is performed periodically using 10 episodes per checkpoint for control tasks and 30 episodes for trading. We report mean learning curves and aggregate metrics over 12 random seeds.

Runtime & complexity. Details are given in Appendix B.

5.2. Results

Continuous-time baselines. Figure 1 compares CT-SAC and CT-TD3 with prior continuous-time baselines across the control suite. Our methods achieve the strongest overall performance with consistently stable learning on both high-dimensional locomotion and trading tasks. These results highlight a limitation of existing continuous-time methods, where optimizing coupled martingale objectives for V and q is challenging. Our approach instead breaks learning into simpler subproblems, improving optimization reliability.

Discrete-time baselines. Our method CT-SAC also outperforms leading discrete-time algorithms (see Figure 2 and 3). When step sizes vary across samples and between training and evaluation, standard discrete-time updates degrade, while our continuous-time-derived update remains robust to non-uniform timestamps. Across both control and trading, our method improves early, with learning curves rise within the first fraction of steps and then stabilize, while discrete-time methods typically require many more samples to accelerate. A possible explanation is that under variable step sizes, discrete-time critics may only learn an order-preserving surrogate rather than the true value function across time scales, which delays robust improvement. CT-TD3 tends to underperform CT-SAC but still improves on its discrete-time counterpart, underscoring the value of entropy regularization and the need for theory improvement.

Performance on trading. While on standard continuous-control benchmarks, CPPO is consistently weaker than its discrete-time counterparts, for trading task, CPPO becomes competitive on a similar scale to strong off-policy baselines such as SAC. This suggests that continuous-time modeling can matter more in trading under irregular decision times. Still, our method achieves the strongest overall performance. Despite using only price-derived features (no news or fun-

damentals data), our policy learns profitable strategies and attains the best evaluation returns among all baselines. Starting from \$100,000, CT-SAC achieves about \$3,500 profit every two weeks on average (see Figure 3). Across episodes of Q3 2025, it achieves a total profit of roughly \$21,000, nearly doubling the second-best method. This highlights that continuous-time RL can be effective for real-world trading when the learning objective and optimization are designed to remain stable under irregular decision intervals and noisy dynamics.

Finally, we conduct statistical testing on 12 seeds and find that improvements are significant across tasks.

Ablation study. Using the top 3 hyperparameter configurations identified during tuning for each method, we run ablations across all tasks. The results show that our tuned baselines are competitive, and that our method remains top performer even under non-optimal hyperparameter settings, indicating robustness to hyperparameter variation (Table 2).

Increment modeling. We also evaluate reward-shaping variants for discrete-time RL. These variants yield performance similar to their standard counterparts and consistently rank behind CT-SAC (Figure 4 and 5).

6. Conclusion

We introduce a continuous-time reinforcement learning framework for irregular decision times. The core idea is a simplified learning procedure: estimate an instantaneous advantage-rate signal from rollouts under a fixed value predictor, then update the value predictor via a Hamiltonian flow. This avoids the coupled martingale objectives used in prior continuous-time methods. A single-critic implementation makes the approach compatible with standard off-policy actor-critic training and stable under variable step sizes. On the theory side, we establish convergence guarantees despite the presence of infinitesimal generators, where discrete-time contraction arguments no longer apply. Our analysis uses a probabilistic technique that links the flow update to the dynamic-programming semigroup and extends naturally to the model-free setting with finite time increments. Empirically, we evaluate our method under an irregular-time setup with many short steps mixed with large jumps, on high-dimensional control benchmarks and a real-world trading task. Across these settings, our method consistently outperforms existing continuous-time baselines and strong discrete-time algorithms.

Reproducibility Statement

We provide the complete code in the codebase Github link: <https://github.com/mpnguyen2/ct-r1>. Please see Appendices B and J for further details.

Impact Statement

This paper presents work whose goal is to advance the field of Machine Learning by developing reinforcement learning methods for continuous-time settings with irregular decision intervals. The broader impacts are expected to be similar to those of many general advances in reinforcement learning: the methods may help improve robustness and reproducibility in time-irregular data and control problems, while we do not anticipate immediate or unusual ethical concerns beyond standard considerations for responsible use of learned decision-making systems.

References

Ainsworth, S., Lowrey, K., Thickstun, J., Harchaoui, Z., and Srinivasa, S. Faster policy learning with continuous-time gradients. In *Proceedings of the 3rd Conference on Learning for Dynamics and Control*, volume 144 of *Proceedings of Machine Learning Research*, pp. 1054–1067. PMLR, 07 – 08 June 2021.

Alpaca Markets. Alpaca market data api documentation. Available at <https://docs.alpaca.markets/docs/market-data-api>, 2026. Accessed: 2026-01-27.

Baird, L. Reinforcement learning in continuous time: advantage updating. In *Proceedings of 1994 IEEE International Conference on Neural Networks (ICNN'94)*, volume 4, pp. 2448–2453 vol.4, 1994.

Doya, K. Reinforcement learning in continuous time and space. *Neural Comput.*, 12(1):219–245, 2000.

Fleming, W. H. and Mete Soner, H. *Controlled Markov processes and viscosity solutions*. Springer, New York, NY, 2nd edition, 2006.

Fujimoto, S., van Hoof, H., and Meger, D. Addressing function approximation error in actor-critic methods. In *Proceedings of the 35th International Conference on Machine Learning*, volume 80 of *Proceedings of Machine Learning Research*, pp. 1587–1596. PMLR, 10–15 Jul 2018.

Haarnoja, T., Zhou, A., Abbeel, P., and Levine, S. Soft actor-critic: Off-policy maximum entropy deep reinforcement learning with a stochastic actor. In *Proceedings of the 35th International Conference on Machine Learning*, volume 80 of *Proceedings of Machine Learning Research*, pp. 1861–1870, Vienna, Austria, 10–15 Jul 2018. PMLR.

Hua, C., Gu, J., and Tang, Y. Continuous q-score matching: Diffusion guided reinforcement learning for continuous-time control. *arXiv preprint arXiv:2510.17122*, 2025.

Jia, Y. and Zhou, X. Y. Policy evaluation and temporal-difference learning in continuous time and space: A martingale approach. *Journal of Machine Learning Research*, 23(154):1–55, 2022a.

Jia, Y. and Zhou, X. Y. Policy gradient and actor-critic learning in continuous time and space: Theory and algorithms. *Journal of Machine Learning Research*, 23(275):1–50, 2022b.

Jia, Y. and Zhou, X. Y. q-learning in continuous time. *Journal of Machine Learning Research*, 24(161):1–61, 2023.

Lee, J. and Sutton, R. S. Policy iterations for reinforcement learning problems in continuous time and space — fundamental theory and methods. *Automatica*, 126:109421, 2021. ISSN 0005-1098.

Lillicrap, T. P., Hunt, J. J., Pritzel, A., Heess, N., Erez, T., Tassa, Y., Silver, D., and Wierstra, D. Continuous control with deep reinforcement learning. In *International Conference on Learning Representations (ICLR)*, 2016.

Munos, R. Policy gradient in continuous time. *Journal of Machine Learning Research*, 7(27):771–791, 2006.

Raffin, A., Hill, A., Gleave, A., Kanervisto, A., Ernestus, M., and Dormann, N. Stable-baselines3: Reliable reinforcement learning implementations. *Journal of Machine Learning Research*, 22(268):1–8, 2021.

Rebeschini, P. Algorithmic foundations of learning, 2022. URL <https://www.stats.ox.ac.uk/%7Erebeschi/teaching/AFoL/22/>.

Schulman, J., Levine, S., Abbeel, P., Jordan, M., and Moritz, P. Trust region policy optimization. In *Proceedings of the 32nd International Conference on Machine Learning*, volume 37 of *Proceedings of Machine Learning Research*, pp. 1889–1897, Lille, France, 07–09 Jul 2015. PMLR.

Schulman, J., Wolski, F., Dhariwal, P., Radford, A., and Klimov, O. Proximal policy optimization algorithms. *arXiv preprint arXiv:1707.06347*, 2017.

Sutton, R. S. and Barto, A. G. *Reinforcement Learning: An Introduction*. Bradford Books, Cambridge, MA, 2 edition, 2018.

Tallec, C., Blier, L., and Ollivier, Y. Making deep Q-learning methods robust to time discretization. In *Proceedings of the 36th International Conference on Machine Learning*, volume 97 of *Proceedings of Machine Learning Research*, pp. 6096–6104. PMLR, 09–15 Jun 2019.

Tang, W. and Zhou, X. Y. Regret of exploratory policy improvement and q-learning. *arXiv preprint arXiv:2411.01302*, 2024.

Tang, W., Zhang, P. Y., and Zhou, X. Y. Exploratory HJB equations and their convergence. *arXiv preprint arXiv:2109.10269*, 2021.

Tunyasuvunakool, S., Muldal, A., Doron, Y., Liu, S., Bohez, S., Merel, J., Erez, T., Lillicrap, T., Heess, N., and Tassa, Y. dm_control: Software and tasks for continuous control. *Software Impacts*, 6:100022, 2020. ISSN 2665-9638.

Wang, H., Zariphopoulou, T., and Zhou, X. Y. Reinforcement learning in continuous time and space: A stochastic control approach. *Journal of Machine Learning Research*, 21(198):1–34, 2020.

Wiltzer, H., Bellemare, M. G., Meger, D., Shafto, P., and Jhaveri, Y. Action gaps and advantages in continuous-time distributional reinforcement learning. In *Advances in Neural Information Processing Systems*, volume 37, pp. 47815–47848. Curran Associates, Inc., 2024.

Yıldız, C., Heinonen, M., and Lähdesmäki, H. Continuous-time model-based reinforcement learning. In *Proceedings of the 38th International Conference on Machine Learning*, volume 139 of *Proceedings of Machine Learning Research*, pp. 12009–12018. PMLR, 18–24 Jul 2021.

Zhao, H., Tang, W., and Yao, D. Policy optimization for continuous reinforcement learning. In *Advances in Neural Information Processing Systems*, volume 36, pp. 13637–13663. Curran Associates, Inc., 2023.

Zhao, H., Chen, H., Zhang, J., Yao, D., and Tang, W. Score as action: Fine tuning diffusion generative models by continuous-time reinforcement learning. In *Proceedings of the 42nd International Conference on Machine Learning*, volume 267 of *Proceedings of Machine Learning Research*, pp. 77371–77389. PMLR, 13–19 Jul 2025.

Appendix Table of Contents

A Related works	13
B Experiment details	14
B.1 Task details	14
B.2 Ablation study tables	15
B.3 Reward shaping with increment modeling	15
B.4 Performance of all algorithms	15
B.5 Runtime and time complexity	16
B.6 Hyperparameters tuning	17
B.7 Statistical testing	17
B.8 Codebase and reproducibility	17
B.9 Generalization from irregular-time training to regular-time evaluation	17
C Preliminaries for theoretical analysis	18
C.1 Notation	18
C.2 Controlled diffusion dynamics	18
C.3 Policies and value functions	19
C.4 Infinitesimal generator and q -functions	19
C.5 Dynkin’s formula and small-time moments	19
C.6 Stochastic control under relaxed (policy-averaged) dynamics	20
D Proof of value function convergence (Theorem 4.1)	21
D.1 Dynamic-programming operator and contraction	21
D.2 Picard–Hamiltonian operator	22
D.3 Small-time expansions	22
D.4 Per-step mismatch: $\Phi_\tau^{(\alpha)}$ vs. $T_\tau^{(\alpha)}$	24
D.5 Proof of Theorem 4.1	24
E Proof of q-convergence (Theorem 4.2)	25
E.1 Baseline modelling bias under standard assumptions	25
E.2 Smoothness assumptions for quantitative u -rates	26
E.3 Bias expansions for q_V^u and \tilde{q}_V^u	26
E.4 Hamiltonians and Lipschitz lemmas	27
E.5 One-step mismatch under stricter assumptions	28
E.6 Proof of Theorem 4.2	30
F Proof of convergence for CT-SAC (Theorem 4.3 and Corollary 4.4)	30

F.1	From (V_k, q_k) to a single Q_k	30
F.2	Learning-theoretic ingredients (i.i.d. regression)	33
F.3	Proof of Corollary 4.4	33
G	Random time step U	35
G.1	q -convergence	36
H	Regret bound and sample complexity	37
H.1	A norm-transfer argument from L^2 to $\ \cdot\ _\infty$	37
H.2	Main bound	38
I	Further Theoretical Details For Main Paper	39
I.1	Further explanations for the main paper	39
I.2	Discrete MDP with noise converge to SDE	40
I.3	Exact Richardson single-critic update equation.	41
I.4	Decoupled continuous-time policy evaluation	42
J	Further experiment details	43
J.1	Visualization on the trading task	43
J.2	Visualization on control tasks	43
J.3	Compute resources	43
J.4	Ablation-study hyperparameters	43
K	Benchmarking algorithms	43
K.1	Coupled-style q -learning	43
K.2	Policy gradient	44

A. Related works

Discrete-time reinforcement learning. Most effective deep reinforcement learning for continuous control can be broadly grouped into (i) off-policy actor–critic methods and (ii) on-policy policy-gradient methods (Sutton & Barto, 2018), with widely used representatives including Soft Actor–Critic (SAC) (Haarnoja et al., 2018), Twin Delayed Deep Deterministic Policy Gradient (TD3) (Fujimoto et al., 2018), Trust Region Policy Optimization (TRPO) (Schulman et al., 2015), and Proximal Policy Optimization (PPO) (Schulman et al., 2017), while many other practical algorithms can be viewed as variants, hybrids, or refinements of these cornerstones. SAC is particularly powerful due to its entropy-regularized objective, which encourages exploration while yielding stable policy improvement and strong empirical performance in high-dimensional continuous-action domains. In contrast to SAC’s stochastic policy, TD3 is a deterministic actor–critic method that can be viewed as a strengthened successor of DDPG (Lillicrap et al., 2016), mitigating overestimation bias via clipped double critics and delayed policy updates. On the policy-gradient side, TRPO is notable for its principled trust-region formulation and theoretical guarantees, whereas PPO is widely adopted as an efficient and scalable approximation that performs robustly across a wide range of tasks. Despite their success, all of these methods are fundamentally formulated on fixed-step Markov decision processes (MDPs). When the decision interval Δt becomes small or irregular, the Bellman recursion becomes increasingly sensitive to discretization (Tallec et al., 2019; Jia & Zhou, 2023). Additionally, learning signals can degenerate in the settings mentioned in Section 1, motivating new approaches that are more suitable for continuous-time problems.

Early continuous-time RL and ODE-based approaches. Continuous-time reinforcement learning has long been studied from a control-theoretic perspective, primarily through the Hamilton–Jacobi–Bellman (HJB) equation (Fleming & Mete Soner, 2006). Early work by Baird (1994), Doya (2000), and Munos (2006) explored continuous-time value learning, policy gradients, and advantage-based updates as alternatives to fixed-step MDP formulations. However, these early approaches are typically restricted to deterministic dynamical systems or require additional structure beyond standard model-free RL. For instance, they need access to the closed-form transition dynamics or their derivatives to construct path-wise or value-gradient updates. Subsequent developments (Lee & Sutton, 2021; Ainsworth et al., 2021; Yıldız et al., 2021) further refine continuous-time analogues of actor–critic or policy-gradient methods through closed-form formulae. Nonetheless, these methods also inherit similar limitations, remaining either model-based, tied to deterministic dynamics, or relying on assumptions that are difficult to meet in general stochastic environments under irregular decision times. A central limitation is that the continuous-time problem demands a stochastic-control formulation, which should be associated with stochastic differential equations (SDEs) rather than deterministic ODE, as discussed in Section 2.1. Without a framework that works well under SDEs, naïve temporal-difference (TD) learning can lead to minimizing the variance terms induced by Brownian noise rather than true dynamic-programming errors, a phenomenon highlighted in (Jia & Zhou, 2022a; 2023) and analyzed further in Section 3.1. Moreover, as the timestep shrinks, the discrete-time Q -function collapses to the value function, eliminating meaningful action ranking. This collapse is empirically suggested by Tallec et al. (2019), who demonstrate the sensitivity of Q -learning-based methods to time discretization. Nevertheless, that work still operates in a discrete setting with fixed time step, rather than a continuous-time setup under stochastic dynamics.

Stochastic-control formulations and recent continuous-time RL. A more recent novel line of work (Wang et al., 2020; Jia & Zhou, 2022a;b; 2023; Zhao et al., 2023) formulates reinforcement learning directly as stochastic control problem under diffusion dynamics. Wang et al. (2020) introduce an entropy-regularized continuous-time framework that models exploration through relaxed controls and establishes a stochastic HJB characterization. Tang et al. (2021) further prove important convergence results for the associated stochastic HJB. Building on this foundation, Jia & Zhou (2023) show that the conventional state–action value function does not survive the continuous-time limit and propose the advantage-rate (or “little- q ”) function as the correct infinitesimal analogue. This quantity is closely linked to the Hamiltonian and admits characterization via martingale conditions, enabling continuous-time analogues of policy evaluation and improvement. Crucially, such martingale conditions arise precisely to address the failure modes of naïve TD updates under diffusion noise, as discussed in Section 3.1. Within the same stochastic-control framework, (Zhao et al., 2023) further develops policy optimization methods, deriving continuous-time counterparts of TRPO and PPO based on occupation measures and performance-difference formulas. Complementary theoretical work, including regret analyses (Tang & Zhou, 2024) and the study of distributional quantities such as the action-gap (Wiltzer et al., 2024), further enriches this emerging line of work and clarifies the theoretical behavior of continuous-time learning. In terms of new algorithmic contributions, recent works include (Hua et al., 2025), which follows the martingale-based characterization in (Jia & Zhou, 2023), and (Zhao et al., 2025), which extends policy-gradient methods (Zhao et al., 2023) using diffusion-based parameterizations. These works, however, specialize the policy class through diffusion modeling or apply similar martingale objectives to other tasks, rather

than proposing a fundamentally new learning approach to address the complexity of martingale characterization. In contrast, our work focuses on developing a new decoupled learning scheme that preserves the continuous-time theoretical foundation while yielding a more practical optimization structure. As shown in Section 4 and Section 5, this decoupling leads to an efficient algorithm with theoretical guarantees and strong empirical performance on advanced control benchmarks and a real-world trading task under small and irregular time steps.

B. Experiment details

B.1. Task details

B.1.1. TRADING

Market data and episode construction. We consider a diversified equity universe consisting of four major industry sectors, each containing five liquid, large-cap tickers (20 total). We use minute-resolution OHLCV bars and define one episode as two weeks of trading, i.e., 390 minutes per day over 5 trading days per week. Decisions are made at *irregular* times: after each action, the environment samples a holding time $u \in [1, 20]$ minutes and advances the market by u minutes before the next decision.

State, action, and reward. The state summarizes recent market behavior through multi-scale historical features (e.g., rolling windows spanning minutes, hours, and days) computed from the minute bars. At each decision time, the agent chooses a bounded buy/sell quantity within a sector-specific group, subject to position limits and proportional transaction costs. Rewards are defined as realized profit over the subsequent holding interval; consequently, the episode return equals the total P&L accumulated over the two-week horizon.

Train–test split. To avoid temporal leakage, we train on a contiguous historical window from Q3 2023 through Q2 2025 and evaluate on a disjoint quarter (Q3 2025). Evaluation uses a *fixed set* of episodes spanning the full quarter, so all methods are tested on the same market-path distribution and performance differences cannot be attributed to favorable evaluation windows. Minute-level data are obtained from the Alpaca API (Alpaca Markets, 2026). For reproducibility, we provide preprocessed datasets (`train.npz` and `eval.npz`) under `data/trading/processed_data/` along with scripts and instructions to regenerate the minute-resolution features from raw data.

B.1.2. CONTROL TASKS

We evaluate on four standard continuous-control benchmarks from the DeepMind Control Suite (DMC) (Tunyasuvunakool et al., 2020): `cheetah-run`, `walker-run`, `humanoid-walk`, and `quadruped-run`. DMC provides a physics-based simulator with direct control over integration and control rates, which makes it well-suited for our irregular-time setting. In DMC, rewards are normalized to $[0, 1]$; thus the maximum achievable return is approximately proportional to the episode duration.

B.1.3. IRREGULAR-TIME CONFIGURATION

A central goal of this work is to evaluate learning under *intertwined* time scales, where trajectories contain a mixture of very small and very large time steps within the same episode. For each task, we report the finest time scale $\Delta t_{\text{physics}}$, the minimum and maximum decision increments (Δt_{\min} , Δt_{\max}), and the maximum episode duration T_{\max} , along with the fractions of *small*, *large*, and *average* steps and the range of number of decision steps per episode. Control-task time is measured in seconds, while trading time is measured in minutes (See Table 1).

Table 1. Irregular-time sampling configuration per task: finest time scale $\Delta t_{\text{physics}}$, decision-step bounds (Δt_{\min} , Δt_{\max}), maximum episode duration T_{\max} , step-type proportions (small/large/average), and the step range per episode.

Task	$\Delta t_{\text{physics}}$	Δt_{\min}	Δt_{\max}	% small	% large	% avg	T_{\max}	# of steps range
Cheetah	0.0020	0.002	0.030	89.1%	9.9%	1.0%	10	1200-2000
Walker	0.0025	0.005	0.075	89.1%	9.9%	1.0%	25	1200-2000
Humanoid	0.0050	0.010	0.040	40.0%	40.0%	20.0%	25	800-1000
Quadruped	0.0050	0.005	0.050	89.1%	9.9%	1.0%	20	1200-2000
Trading	1	1	11	89.1%	9.9%	1.0%	4000	1600-2100

B.2. Ablation study tables

We report hyperparameter ablations in Table 2. Across all environments, **CT-SAC is consistently the best-performing method among the tested configurations**, and the same trend holds for **CT-TD3 vs. TD3**. To keep the main ablation table compact, we show the **top/second/third** configurations per algorithm and task; the exact hyperparameter settings corresponding to these entries are provided in the hyperparameter dictionary in Section J.

Table 2. Hyperparameter ablations across all tasks. For each algorithm and task, we report the returns of the **top**, **second**, and **third** configurations from the hyperparameter tuning process.

(a) CT-SAC versus discrete-time algorithms SAC and TD3

Task	CT-SAC			SAC			TD3		
	top	second	third	top	second	third	top	second	third
Cheetah	934.76	863.45	807.19	701.88	680.30	605.63	730.12	694.15	692.81
Walker	1035.52	928.26	817.28	680.08	560.98	522.85	385.73	286.09	191.74
Humanoid	386.75	379.75	371.75	73.39	39.28	2.12	2.28	2.24	2.11
Quadruped	959.75	958.44	829.41	423.33	314.77	284.00	522.63	518.37	464.95
Trading	37.72	33.09	31.98	25.59	21.04	13.77	2.67	-5.46	-9.46

(b) CT-SAC versus discrete-time algorithms TRPO and PPO

Task	CT-SAC			TRPO			PPO		
	top	second	third	top	second	third	top	second	third
Cheetah	934.76	863.45	807.19	210.10	190.51	170.73	235.61	208.42	206.70
Walker	1035.52	928.26	817.28	126.73	119.95	114.90	129.94	120.28	118.08
Humanoid	386.75	379.75	371.75	1.39	1.33	1.30	1.18	1.17	1.11
Quadruped	959.75	958.44	829.41	206.24	178.01	135.29	214.13	208.47	202.72
Trading	37.72	33.09	31.98	9.17	-3.36	-4.77	12.76	11.94	4.19

(c) CT-SAC versus continuous-time algorithms CPPO, q-Learning, and CT-TD3

Task	CT-SAC			CPPO			q-Learning			CT-TD3		
	top	second	third	top	second	third	top	second	third	top	second	third
Cheetah	934.76	863.45	807.19	174.50	168.64	145.92	348.61	328.69	272.00	705.86	457.24	268.61
Walker	1035.52	928.26	817.28	51.77	44.24	42.04	119.78	94.79	74.67	596.50	578.19	567.22
Humanoid	386.75	379.75	371.75	1.16	1.08	1.04	1.81	1.59	1.28	337.23	326.61	295.94
Quadruped	959.75	958.44	829.41	160.19	159.80	159.05	339.49	299.32	216.92	484.25	455.86	345.87
Trading	37.72	33.09	31.98	23.46	23.37	22.32	12.22	2.37	-39.94	6.53	-0.11	-6.22

B.3. Reward shaping with increment modeling

We also evaluate a reward-shaping variant (*increment modeling*) defined as $r_t^{\text{new}} = \Delta_t r_t$, to test whether scaling rewards by the observed time increment improves learning under non-uniform time steps. Across control tasks and the trading task, this modification does not improve performance. In most cases, it is worse or statistically indistinguishable from the unshaped baseline, suggesting that naive time-scaling can distort the learning signal and increase variance rather than stabilizing training (See Figures 4 and 5).

B.4. Performance of all algorithms

To facilitate comparison across all eight algorithms, Figure 6 reports the **mean evaluation return only** (without variance bands). This view highlights the overall ranking and learning dynamics without clutter; variance plots and full per-seed statistics are already provided in the main paper and in the appendix.

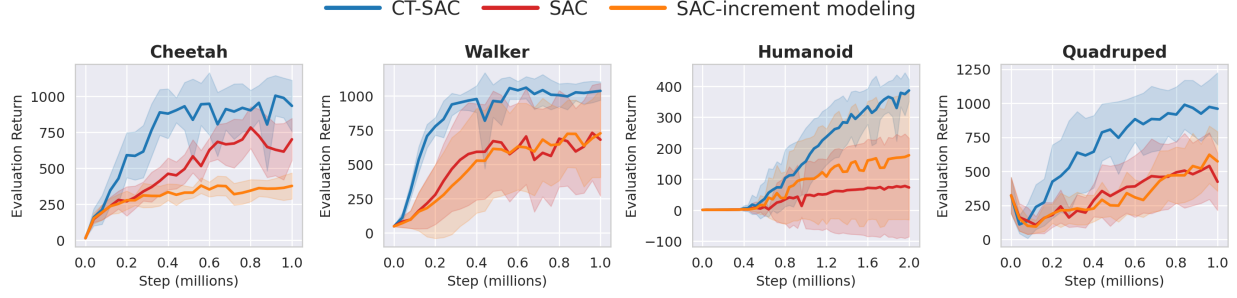


Figure 4. Evaluation returns for CT-SAC against SAC and its reward-shaping version on control tasks over 12 seeds.

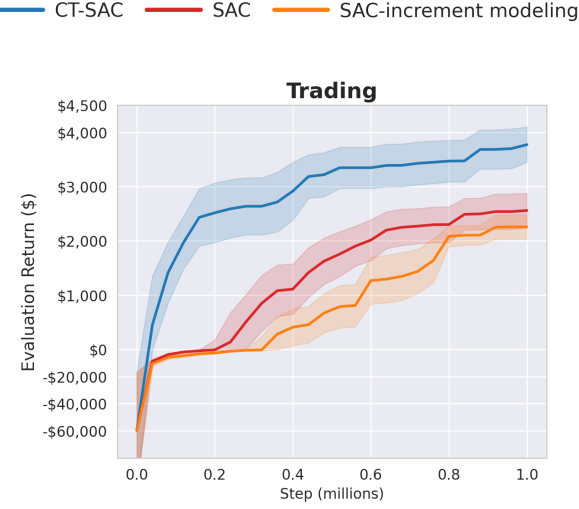


Figure 5. Evaluation returns for CT-SAC against SAC and its reward-shaping version on trading task over 12 seeds.

B.5. Runtime and time complexity

Runtime. We summarize the runtime in Table 3, reported as mean \pm std over 12 seeds for the **top** configuration of each algorithm. Overall, **CT-SAC has runtime comparable to SAC**, and **CT-TD3 is comparable to TD3**, indicating that our continuous-time modifications do not materially increase training cost relative to their discrete-time counterparts.

Time complexity. CT-SAC follows the same training structure as SAC: sampling rollouts and performing batched critic/actor updates at a fixed update schedule. Let N denote the number of environment interaction steps (or sampled decision times), f the update frequency (updates every f steps), and d the number of gradient updates per update event. Then the total number of update steps scales as $\mathcal{O}(Nd/f)$. Per update, CT-SAC and SAC share the same dominant costs (forward/backward passes through the actor/critic networks). CT-SAC additionally includes time operations (e.g., dividing by Δ_t or using Δ_t in targets), which may increase constants slightly but does not change asymptotic complexity.

Table 3. Training runtime (hours) for each algorithm on each task, reported as mean \pm std over $n=12$ seeds.

Task	CT-SAC	SAC	TD3	TRPO	PPO	CPPO	q-Learning	CT-TD3
Cheetah	10.62 ± 0.53	6.29 ± 0.04	3.98 ± 0.05	0.44 ± 0.07	0.29 ± 0.07	0.57 ± 0.06	9.12 ± 0.17	4.60 ± 0.04
Walker	9.69 ± 0.83	8.90 ± 0.54	4.57 ± 0.24	0.40 ± 0.00	0.41 ± 0.07	0.61 ± 0.04	5.59 ± 0.08	4.68 ± 0.09
Humanoid	8.30 ± 0.50	6.02 ± 0.09	3.87 ± 0.06	0.82 ± 0.01	0.48 ± 0.02	1.01 ± 0.02	5.07 ± 0.14	5.32 ± 0.16
Quadruped	8.21 ± 0.41	6.49 ± 0.04	4.66 ± 0.04	0.40 ± 0.02	0.41 ± 0.01	0.36 ± 0.01	6.87 ± 0.32	2.65 ± 1.91
Trading	8.42 ± 0.11	7.42 ± 0.07	4.90 ± 0.08	0.81 ± 0.00	0.52 ± 0.01	0.89 ± 0.17	6.38 ± 0.10	5.44 ± 0.08

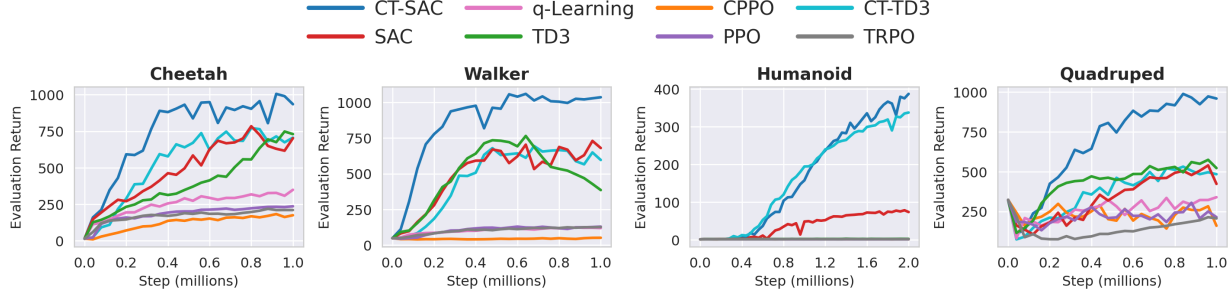


Figure 6. Evaluation returns for all algorithms on the control task over 12 seeds.

B.6. Hyperparameters tuning

We perform hyperparameter search to select the best configuration for each algorithm–task pair. Because the full sweep spans 8 algorithms \times 5 tasks with distinct search spaces (in total roughly 40 algorithm–task search families), we place the complete search ranges and the selected **top/second/third** settings in the codebase under the `out/final_reports/hyperparam_spaces` folder.

B.7. Statistical testing

We report statistical comparisons across 12 independent seeds. We use the same seeds across all algorithms and tasks. We run two complementary tests using `scipy.stats`: Welch’s t-test and a paired test. Across tasks, these tests support that **CT-SAC outperforms the baselines** with statistically significant differences in the majority of settings. The full set of p -values and other details are included in `out/final_reports/significant_testing.csv` (available in the codebase repository).

B.8. Codebase and reproducibility

Our codebase is available at the GitHub link: <https://github.com/mpnguyen2/ct-rl>. Additional plots/media/tables are under `out/final_reports` folder.

Because training logs and saved checkpoints are large (\sim 6 GB), we provide them via the SwissTransfer links, given in the codebase: <https://github.com/mpnguyen2/ct-rl>. A step-by-step reproduction guide (exact commands, dependencies, seeds, and evaluation protocol) is documented in `README.md`, including how to regenerate the tables and figures from raw logs.

B.9. Generalization from irregular-time training to regular-time evaluation

We further evaluate whether policies trained under *irregular* decision times transfer to the standard *regular*-time evaluation setting. This test checks whether the learned policies capture the underlying control structure rather than overfitting to a particular irregular sampling pattern. Table 4 reports mean evaluation return over 12 seeds on the control tasks. CT-SAC achieve the best performance on all tasks, followed closely by CT-TD3. This indicates strong generalization from complex, noisy, intertwined irregular-time trajectories to the regular-time setting.

Table 4. Regular-time evaluation of policies trained under irregular time steps. We report mean return over 12 seeds on control tasks.

Task	CT-SAC	SAC	TD3	PPO	TRPO	q-Learning	CPPO	CT-TD3
Cheetah	605.05	455.74	404.18	124.45	104.46	208.04	102.03	513.39
Walker	610.03	403.44	509.23	73.06	64.55	70.94	25.04	512.30
Humanoid	404.64	77.14	2.27	1.34	1.35	1.90	1.42	356.90
Quadruped	530.13	328.30	325.87	159.52	121.84	192.86	125.30	284.23

Finally, we provide additional visualization for the trading task (Figure 7) and for control tasks under both the irregular setting (Figures 8 and 9) and the regular setting (Figures 10 and 11). Further implementation and evaluation details are

provided in Section J.

C. Preliminaries for theoretical analysis

State, action, and function space. Let $\mathcal{S} \subseteq \mathbb{R}^d$ be the state space and let \mathcal{A} be a compact metric action space. For value functions, we work on the Banach space $\mathcal{D} := C_b(\mathbb{R}^d)$ of bounded continuous functions equipped with the sup-norm $\|V\|_\infty := \sup_{x \in \mathbb{R}^d} |V(x)|$.

For convenience, we recall all notations and definitions introduced in Section 2, Section 3, and Section 4 in the main paper.

C.1. Notation

Table 5. Notations used throughout the paper.

Symbol	Meaning
$V^{(\alpha)}(x)$	Optimal value function with temperature α .
$V(x)$	Generic value function (not necessarily optimal).
$q_V(x, a)$	Advantage-rate q -function associated with V at state–action (x, a) .
$q_V^u(x, a)$	Finite-time approximation of $q_V(x, a)$ using time increment u .
$\tilde{q}_V^u(x, a)$	Richardson-interpolated version of $q_V^u(x, a)$.
L^a	Infinitesimal generator under fixed action a .
$H_a(V)$	Action-wise Hamiltonian at a , defined via $L^a V$.
$H^{(0)}(V)$	Hard Hamiltonian (standard max aggregation over actions).
$H^{(\alpha)}(V)$	Soft Hamiltonian with temperature α .
$H_u^{(\alpha)}(V)$	Soft Hamiltonian using the finite-time approximation q_V^u .
$\tilde{H}_u^{(\alpha)}(V)$	Soft Hamiltonian using the Richardson approximation \tilde{q}_V^u .
$\mathcal{Q}^{(\alpha)}$	Soft aggregation operator acting on q -functions (temperature α).
$Q(x, a)$	Numerical Q -function defined by $Q := V + q_V$.
$T_\tau^{(\alpha)}(V)$	Picard–Hamiltonian operator: $T_\tau^{(\alpha)}(V) := V + \tau H^{(\alpha)}(V)$.
$\Phi_\tau^{(\alpha)}$	Probabilistic dynamic-programming semigroup (step size τ , temperature α).
X_t	State process at time t .
a_t	Action at time t .
W_t	Brownian motion at time t .
b, σ	Drift and diffusion coefficients of the controlled SDE.
$\tilde{b}, \tilde{\sigma}, \tilde{X}_t$	Policy-averaged drift/diffusion and the induced averaged state process.
L^π	Policy-averaged generator: $L^\pi = \mathbb{E}_{a \sim \pi(\cdot x)}[L^a]$.
P_t^a	Markov semigroup of the diffusion under fixed action a .
$\mathcal{F}_{\tau, u}$	Single-critic update operator for the Q -function (step size τ , increment u).
$\mathcal{F}_{\tau, u}^{\text{Rich}}$	Richardson version of the single-critic update operator $\mathcal{F}_{\tau, u}$.
$\bar{H}_U^{(\alpha)}(V)$	Random-increment Hamiltonian: $\bar{H}_U^{(\alpha)}(V) = \mathbb{E}[H_U^{(\alpha)}(V)]$ for random U .
$\tilde{T}_\tau^{(\alpha)}(V)$	Random-time Picard–Hamiltonian operator corresponding to $\bar{H}_U^{(\alpha)}(V)$.

C.2. Controlled diffusion dynamics

Given a progressively measurable control process $(a_t)_{t \geq 0}$ taking values in \mathcal{A} , we consider the controlled stochastic differential equation (SDE)

$$dX_t = b(X_t, a_t) dt + \sigma(X_t, a_t) dW_t, \quad X_0 = x \in \mathbb{R}^d, \quad (39)$$

where W_t is a d -dimensional Brownian motion and $b : \mathbb{R}^d \times \mathcal{A} \rightarrow \mathbb{R}^d$ and $\sigma : \mathbb{R}^d \times \mathcal{A} \rightarrow \mathbb{R}^{d \times d}$ are measurable.

Assumption C.1 (Dynamics regularity). The drift b and diffusion σ satisfy:

1. **Global Lipschitz and linear growth.** There exists $C > 0$ such that for all $x, y \in \mathbb{R}^d$ and $a \in \mathcal{A}$,

$$\|b(x, a) - b(y, a)\| + \|\sigma(x, a) - \sigma(y, a)\| \leq C\|x - y\|, \quad \|b(x, a)\| + \|\sigma(x, a)\| \leq C(1 + \|x\|).$$

2. **Uniform nondegeneracy and boundedness.** There exist $0 < \underline{\sigma} \leq \bar{\sigma} < \infty$ such that

$$\underline{\sigma}^2 I \preceq \sigma(x, a)\sigma(x, a)^\top \preceq \bar{\sigma}^2 I \quad \forall x \in \mathbb{R}^d, \forall a \in \mathcal{A}.$$

Assumption C.2 (Reward and policy regularity). The running reward $r : \mathbb{R}^d \times \mathcal{A} \rightarrow \mathbb{R}$ satisfies:

1. $r(\cdot, a)$ is bounded and is globally Lipschitz uniformly in a , i.e., there exist $R_{\max} < \infty$ and $L_r < \infty$ such that for all x, y and all a ,

$$|r(x, a)| \leq R_{\max}, \quad |r(x, a) - r(y, a)| \leq L_r \|x - y\|$$

2. For the entropy term, admissible Markov policies $\pi(\cdot | x)$ satisfy that $\log \pi(a | x)$ is well-defined and uniformly integrable under the induced state-action distribution.

Assumption C.3 (Regularity of value functions). There exists a class $\mathcal{D} \subset C_b^2(\mathbb{R}^d)$ of value functions such that for every $V \in \mathcal{D}$:

1. For each fixed $a \in \mathcal{A}$, the generator $L^a V$ is globally Lipschitz in x , uniformly in a .
2. For $\alpha > 0$, we restrict to policies π for which $x \mapsto \log \pi(a | x)$ is globally Lipschitz uniformly in a .

Throughout this work, \mathcal{D} refers to the domain of all value functions. Under Assumptions C.1–C.3, the SDE (39) admits a unique strong solution for any admissible control, and the entropy-regularized HJB equation admits a unique bounded viscosity solution $V^{(\alpha)} \in \mathcal{D}$ (Fleming & Mete Soner, 2006; Wang et al., 2020).

C.3. Policies and value functions

Fix a discount $\beta > 0$ and an entropy coefficient $\alpha \geq 0$. A Markov policy π maps each state x to a probability distribution $\pi(\cdot | x)$ on \mathcal{A} , and we write $\mathbb{E}_x^\pi[\cdot]$ for expectation under (39) when $a_t \sim \pi(\cdot | X_t)$.

Recall that the entropy-regularized objective of policy π is:

$$V^{(\alpha)}(x; \pi) := \mathbb{E}_x^\pi \left[\int_0^\infty e^{-\beta t} \left(r(X_t, a_t) - \alpha \log \pi(a_t | X_t) \right) dt \right], \quad (40)$$

and the optimal value function is $V^{(\alpha)}(x) := \sup_\pi V^{(\alpha)}(x; \pi)$. The case $\alpha = 0$ recovers the standard (non-regularized) value function. Additionally, for notational convenience, if π and x is clear from the context, we simply use $\mathbb{E}[\cdot]$.

C.4. Infinitesimal generator and q -functions

Recall the following notations from Section 2 and Section 3. For a fixed action $a \in \mathcal{A}$, the controlled infinitesimal generator L^a acting on $\varphi \in C_b^2(\mathbb{R}^d)$ is:

$$(L^a \varphi)(x) := b(x, a) \cdot \nabla \varphi(x) + \frac{1}{2} \text{Tr}(\sigma(x, a) \sigma(x, a)^\top \nabla^2 \varphi(x)). \quad (41)$$

Given $V \in \mathcal{D}$, the q -function has the form:

$$q_V(x, a) := r(x, a) + (L^a V)(x) - \beta V(x). \quad (42)$$

For a short horizon $u > 0$, the finite time estimation for q under constant action a is:

$$q_V^u(x, a) := \frac{e^{-\beta u} \mathbb{E}_x^a[V(X_u)] - V(x)}{u} + r(x, a), \quad (43)$$

where $\mathbb{E}_x^a[\cdot]$ denotes expectation for the SDE (39) with constant control $a_t \equiv a$.

C.5. Dynkin's formula and small-time moments

Lemma C.4 (Dynkin's formula for controlled diffusions). *Let $(X_t)_{t \geq 0}$ solve (39) under a progressively measurable control $(a_t)_{t \geq 0}$ and let τ be a bounded stopping time. Then for any $f \in C_b^2(\mathbb{R}^d)$,*

$$\mathbb{E}[f(X_\tau)] = f(x) + \mathbb{E} \left[\int_0^\tau (L^{a_t} f)(X_t) dt \right], \quad (44)$$

where $(L^{a_t} f)(X_t)$ is understood pointwise using (41). Additionally, under the diffusion without control: $dX_t = b(X_t) dt + \sigma(X_t) dW_t$, Equation (44) also holds with the (uncontrolled) infinitesimal generator $L\varphi(x) := b(x) \cdot \nabla \varphi(x) + \frac{1}{2} \text{Tr}(\sigma(x) \sigma(x)^\top \nabla^2 \varphi(x))$. This can easily be seen by treating drift $b(x)$ as $b(x, a_0)$, and diffusion $\sigma(x)$ as $\sigma(x, a_0)$ for a fixed constant action a_0 .

Proof. This is a direct consequence of Itô's formula applied to $f(X_t)$ and taking expectations (Fleming & Mete Soner, 2006). \square

We now recall a standard result in stochastic processes.

Lemma C.5 (Small-time moment bounds). *Under Assumption C.1, for X_t in Equation (39), there exists a constant $C > 0$ such that for all $t \in (0, 1]$ and for any admissible control process $(a_s)_{0 \leq s \leq t}$,*

$$\mathbb{E}_x [\|X_t - x\|] \leq C\sqrt{t}, \quad (45)$$

and moreover

$$\mathbb{E}_x \left[\sup_{0 \leq s \leq t} \|X_s - x\|^2 \right] \leq Ct, \quad \mathbb{E}_x \left[\sup_{0 \leq s \leq t} \|X_s - x\| \right] \leq C\sqrt{t}. \quad (46)$$

The constant C depends only on the constants in Assumption C.1 and d , and is independent of the choice of control.

Proof sketch. We have $X_t - x = \int_0^t b(X_s, a_s) ds + \int_0^t \sigma(X_s, a_s) dW_s$. Because of the linear growth, we get $\|b(x, a)\|^2 \leq K(1 + \|x\|^2)$ and $\|\sigma(x, a)\|_F^2 \leq K(1 + \|x\|^2)$ for some constant K . From here, we bound the second moment through Itô isometry and Cauchy-Schwarz inequalities:

$$\begin{aligned} \mathbb{E}\|X_t - x\|^2 &\leq 2\mathbb{E} \left\| \int_0^t b(X_s, a_s) ds \right\|^2 + 2\mathbb{E} \left\| \int_0^t \sigma(X_s, a_s) dW_s \right\|^2 \\ &\leq 2t \int_0^t \mathbb{E}\|b(X_s, a_s)\|^2 ds + 2 \int_0^t \mathbb{E}\|\sigma(X_s, a_s)\|_F^2 ds \\ &\leq 2t \int_0^t K(1 + \|X_s\|^2) ds + 2 \int_0^t K(1 + \|X_s\|^2) ds \leq C_1 t, \end{aligned}$$

as we can bound $\|X_s\|^2$ easily through an argument using Gronwall's lemma. Hence, by Cauchy-Schwarz again, we obtain the desired bound. For the supremum, note that with $A_s := \int_0^s b(X_u, a_u) du$ and $M_s := \int_0^s \sigma(X_u, a_u) dW_u$, we have

$$\sup_{0 \leq s \leq t} \|X_s - x\|^2 \leq 2 \sup_{s \leq t} \|A_s\|^2 + 2 \sup_{s \leq t} \|M_s\|^2,$$

We can then apply the Burkholder–Davis–Gundy inequality to the martingale part M_t and use similar estimates to obtain desired bound. \square

C.6. Stochastic control under relaxed (policy-averaged) dynamics

When the action is sampled from a Markov policy $\pi(\cdot | X_t)$, it is convenient to use an equivalent diffusion with drift and covariance averaged under π . For a fixed Markov policy π , define:

$$\tilde{b}(x; \pi) := \int_{\mathcal{A}} b(x, a) \pi(da | x), \quad (47)$$

Here $\pi(da | x)$ is the measured induced by the policy $\pi(\cdot | x)$ on \mathcal{A} . We will use this notation rather than $\int_{a \in \pi(\cdot | x)} b(x, a) da$ from now on, as it is more aligned with the measure-theoretic nature of the theoretical details. We also define $\tilde{\sigma}(x; \pi)$ via the covariance identity

$$\tilde{\sigma}(x; \pi) \tilde{\sigma}(x; \pi)^\top := \int_{\mathcal{A}} \sigma(x, a) \sigma(x, a)^\top \pi(da | x). \quad (48)$$

Under Assumption C.1 and the mild Lipschitz regularity of π in Assumption C.3, there exists a filtered probability space supporting a Brownian motion \tilde{W} and a process $(\tilde{X}_t)_{t \geq 0}$ solving

$$d\tilde{X}_t = \tilde{b}(\tilde{X}_t; \pi) dt + \tilde{\sigma}(\tilde{X}_t; \pi) d\tilde{W}_t, \quad \tilde{X}_0 = x, \quad (49)$$

such that, for each $t \geq 0$, the law of \tilde{X}_t coincides with the law of X_t under the original controlled system (39) with $a_t \sim \pi(\cdot | X_t)$ (Wang et al., 2020; Tang et al., 2021). Hence distributional quantities (value functions, occupancy measures, etc.) can be computed using (49).

For $\varphi \in C_b^2(\mathbb{R}^d)$, we also define the relaxed infinitesimal generator with two equivalent representations:

$$(L^\pi \varphi)(x) := \int_{\mathcal{A}} (L^a \varphi)(x) \pi(da | x) = \tilde{b}(x; \pi) \cdot \nabla \varphi(x) + \frac{1}{2} \text{Tr}(\tilde{\sigma}(x; \pi) \tilde{\sigma}(x; \pi)^\top \nabla^2 \varphi(x)). \quad (50)$$

Finally, we may write the policy value (40) equivalently as

$$V^{(\alpha)}(x; \pi) = \mathbb{E} \left[\int_0^\infty e^{-\beta t} \tilde{r}^{(\alpha)}(\tilde{X}_t; \pi) dt \mid \tilde{X}_0 = x \right], \quad (51)$$

where the relaxed running reward is

$$\tilde{r}^{(\alpha)}(x; \pi) := \int_{\mathcal{A}} \left(r(x, a) - \alpha \log \pi(a | x) \right) \pi(da | x). \quad (52)$$

Note that the drift function \tilde{b} defined by averaging over policy randomness is similar to the result obtained by (Munos, 2006) that we mentioned in Section 2.1. Here we also have the diffusion (Brownian motion) part. See (Wang et al., 2020; Tang et al., 2021; Jia & Zhou, 2023) for more details on the policy-averaged SDE.

Lastly, we would like to state an useful lemma that will be used throughout Appendices D, E, and F.

Lemma C.6 (Entropy-regularized expectation via a KL shift). *Fix $\alpha > 0$ and let $q : \mathcal{X} \times \mathcal{A} \rightarrow \mathbb{R}$ be any measurable function. For each $x \in \mathcal{X}$ recall the functional \mathcal{Q} on q (see Section 3.2) that:*

$$\mathcal{Q}^{(\alpha)}(q)(x) = \alpha \log \left(\int_{\mathcal{A}} \exp(q(x, a)/\alpha) da \right) = \alpha \log Z_q(x),$$

with partition function Z_q , and the Boltzmann distribution π_q :

$$\pi_q(a | x) := \frac{\exp(q(x, a)/\alpha)}{Z_q(x)}, \quad Z_q(x) := \int_{\mathcal{A}} \exp(q(x, a)/\alpha) da.$$

Then for any policy $\pi(\cdot | x)$,

$$\alpha \log Z_q(x) - \alpha \text{KL}(\pi(\cdot | x) \| \pi_q(\cdot | x)) = \mathbb{E}_{a \sim \pi(\cdot | x)} [q(x, a) - \alpha \log \pi(a | x)]. \quad (53)$$

In particular,

$$\mathcal{Q}^{(\alpha)}(q)(x) = \alpha \log Z_q(x) = \sup_{\pi(\cdot | x)} \mathbb{E}_{a \sim \pi(\cdot | x)} [q(x, a) - \alpha \log \pi(a | x)], \quad (54)$$

and the supremum is achieved uniquely by $\pi = \pi_q$.

Proof. By definition,

$$\text{KL}(\pi \| \pi_q) = \int_{\mathcal{A}} \pi(a | x) \log \frac{\pi(a | x)}{\pi_q(a | x)} da = \int_{\mathcal{A}} \pi(a | x) \log \pi(a | x) da - \int_{\mathcal{A}} \pi(a | x) \log \pi_q(a | x) da.$$

Since $\log \pi_q(a | x) = \frac{1}{\alpha} q(x, a) - \log Z_q(x)$, we obtain

$$\text{KL}(\pi \| \pi_q) = \int_{\mathcal{A}} \pi(a | x) \log \pi(a | x) da - \frac{1}{\alpha} \mathbb{E}_{\pi} [q(x, a)] + \log Z_q(x).$$

Rearranging terms gives us the equation (53). Finally, (54) follows because $\text{KL}(\pi \| \pi_q) \geq 0$ with equality iff $\pi = \pi_q$. \square

D. Proof of value function convergence (Theorem 4.1)

This appendix proves the convergence result for the **ideal** Picard–Hamiltonian value iteration $V_{k+1} = T_{\tau}^{(\alpha)}(V_k)$ in Theorem 4.1. The key idea is to compare the Picard update to the short-horizon dynamic-programming operator $\Phi_{\tau}^{(\alpha)}$, which is a strict contraction in the sup-norm.

D.1. Dynamic-programming operator and contraction

For $\tau > 0$ and $\alpha \geq 0$, recall the entropy-regularized dynamic-programming operator $\Phi_{\tau}^{(\alpha)} : \mathcal{D} \rightarrow \mathcal{D}$ defined earlier:

$$(\Phi_{\tau}^{(\alpha)} V)(x) := \sup_{\pi} \mathbb{E}_x \left[\int_0^{\tau} e^{-\beta t} \left(r(X_t, a_t) - \alpha \log \pi(a_t | X_t) \right) dt + e^{-\beta \tau} V(X_{\tau}) \right], \quad (55)$$

where X follows the controlled SDE (39) and $a_t \sim \pi(\cdot | X_t)$.

Lemma D.1 (Contraction of $\Phi_{\tau}^{(\alpha)}$). *Assume Assumption C.1. Then for all $\tau > 0$ and $\alpha \geq 0$,*

$$\|\Phi_{\tau}^{(\alpha)}(V) - \Phi_{\tau}^{(\alpha)}(W)\|_{\infty} \leq e^{-\beta \tau} \|V - W\|_{\infty}, \quad \forall V, W \in \mathcal{X}. \quad (56)$$

Consequently, $\Phi_{\tau}^{(\alpha)}$ admits a unique fixed point $V^{(\alpha)} \in \mathcal{X}$ and

$$\|(\Phi_{\tau}^{(\alpha)})^{(k)}(V_0) - V^{(\alpha)}\|_{\infty} \leq e^{-\beta \tau k} \|V_0 - V^{(\alpha)}\|_{\infty}, \quad \forall k \geq 0. \quad (57)$$

Proof. Fix $x \in \mathbb{R}^d$ and any policy π . Since the running reward terms cancel,

$$\begin{aligned} & \left| \mathbb{E}_x^\pi \left[\int_0^\tau e^{-\beta t} (r - \alpha \log \pi) dt + e^{-\beta \tau} V(X_\tau) \right] - \mathbb{E}_x^\pi \left[\int_0^\tau e^{-\beta t} (r - \alpha \log \pi) dt + e^{-\beta \tau} W(X_\tau) \right] \right| \\ &= e^{-\beta \tau} \left| \mathbb{E}_x^\pi [V(X_\tau) - W(X_\tau)] \right| \leq e^{-\beta \tau} \|V - W\|_\infty. \end{aligned}$$

so $\Phi_\tau^{(\alpha)}$ is a contraction on bounded functions with modulus $e^{-\beta \tau} < 1$. By the Banach fixed-point theorem, it admits a unique fixed point V^* , and $(\Phi_\tau^{(\alpha)})^{(k)}(V_0)$ converge to V^* at a geometric rate. Finally, the entropy-regularized value function $V^{(\alpha)}$ satisfies the dynamic programming principle, hence $V^{(\alpha)}$ is a fixed point of $\Phi_\tau^{(\alpha)}$. By uniqueness of the fixed point, $V^* = V^{(\alpha)}$, and Equation (57) follows trivially. \square

D.2. Picard–Hamiltonian operator

Recall the infinitesimal rate q_V from (42):

$$q_V(x, a) = r(x, a) + (L^a V)(x) - \beta V(x),$$

and the (soft/hard) Hamiltonian $H^{(\alpha)}(V) : \mathbb{R}^d \rightarrow \mathbb{R}$:

$$H^{(\alpha)}(V)(x) := \begin{cases} \alpha \log \int_{\mathcal{A}} \exp\left(\frac{q_V(x, a)}{\alpha}\right) da, & \alpha > 0, \\ \sup_{a \in \mathcal{A}} q_V(x, a), & \alpha = 0, \end{cases} \quad (58)$$

The **ideal** Picard–Hamiltonian operator has the form:

$$(T_\tau^{(\alpha)} V)(x) := V(x) + \tau H^{(\alpha)}(V)(x). \quad (59)$$

D.3. Small-time expansions

We first give a small-time expansion for a *fixed action* a and then for a *fixed policy* π . The policy expansion is the missing ingredient needed to justify the per-step mismatch bound for $\alpha > 0$.

Lemma D.2 (Small-time expansion, fixed action). *Assume Assumptions C.1, C.2, and C.3. Fix $a \in \mathcal{A}$ and $V \in \mathcal{D}$. Define*

$$(\Phi_\tau^a V)(x) := \mathbb{E}_x^a \left[\int_0^\tau e^{-\beta t} r(X_t, a) dt + e^{-\beta \tau} V(X_\tau) \right], \quad (60)$$

where X_t follows (39) with constant control $a_t \equiv a$. Then for all sufficiently small $\tau \in (0, 1]$,

$$(\Phi_\tau^a V)(x) = V(x) + \tau q_V(x, a) + R_\tau^a(V)(x), \quad (61)$$

and the remainder satisfies

$$\sup_{x \in \mathbb{R}^d, a \in \mathcal{A}} |R_\tau^a(V)(x)| \leq C \tau^{3/2}, \quad (62)$$

where C depends on bounds/Lipschitz constants of $b, \sigma, r, L^a V$ and $\|V\|_{C^2}$ but is independent of τ .

Proof. We treat the terminal and running reward parts separately.

Terminal term. By Dynkin's formula (Lemma C.4) under constant action a ,

$$\mathbb{E}_x^a[V(X_\tau)] - V(x) = \int_0^\tau \mathbb{E}_x^a[(L^a V)(X_t)] dt.$$

Add and then subtract $(L^a V)(x)$ inside the integral gives:

$$\mathbb{E}_x^a[V(X_\tau)] = V(x) + \tau (L^a V)(x) + \int_0^\tau \mathbb{E}_x^a[(L^a V)(X_t) - (L^a V)(x)] dt.$$

Since $L^a V$ is globally Lipschitz in x (Assumption C.3), Lemma C.5 then implies that:

$$\left| \int_0^\tau \mathbb{E}_x^a[(L^a V)(X_t) - (L^a V)(x)] dt \right| \leq C \int_0^\tau \sqrt{t} dt = \mathcal{O}(\tau^{3/2}).$$

Therefore,

$$\mathbb{E}_x^a[e^{-\beta\tau}V(X_\tau)] = V(x) + \tau((L^aV)(x) - \beta V(x)) + \mathcal{O}(\tau^{3/2}),$$

using $e^{-\beta\tau} = 1 - \beta\tau + \mathcal{O}(\tau^2)$ and absorbing $\mathcal{O}(\tau^2)$ into $\mathcal{O}(\tau^{3/2})$.

Running reward term. Using Lipschitz continuity of $r(\cdot, a)$ and Lemma C.5,

$$\begin{aligned} \left| \mathbb{E}_x^a \left[\int_0^\tau e^{-\beta t} r(X_t, a) dt \right] - r(x, a) \int_0^\tau e^{-\beta t} dt \right| &\leq \int_0^\tau e^{-\beta t} L_r \mathbb{E}_x^a \|X_t - x\| dt \\ &\leq C \int_0^\tau \sqrt{t} dt = \mathcal{O}(\tau^{3/2}). \end{aligned}$$

Since $\int_0^\tau e^{-\beta t} dt = \tau + \mathcal{O}(\tau^2)$, we conclude

$$\mathbb{E}_x^a \left[\int_0^\tau e^{-\beta t} r(X_t, a) dt \right] = \tau r(x, a) + \mathcal{O}(\tau^{3/2}).$$

Combining the two expansions and the definition of q -function ($q_V(x, a) = r(x, a) + (L^a V)(x) - \beta V(x)$) yields (61) and the remainder bound (62). \square

Lemma D.3 (Small-time expansion, fixed policy via relaxed dynamics). *Assume Assumptions C.1, C.2, and C.3. Fix a Markov policy π and $V \in \mathcal{D}$. Let $(\tilde{X}_t)_{t \geq 0}$ follow the relaxed SDE (49) and define the relaxed reward $\tilde{r}^{(\alpha)}(\cdot; \pi)$ as in (52). Define the fixed-policy short-horizon operator*

$$(\Phi_\tau^{\pi, (\alpha)} V)(x) := \mathbb{E} \left[\int_0^\tau e^{-\beta t} \tilde{r}^{(\alpha)}(\tilde{X}_t; \pi) dt + e^{-\beta\tau} V(\tilde{X}_\tau) \mid \tilde{X}_0 = x \right]. \quad (63)$$

Then for all sufficiently small $\tau \in (0, 1]$,

$$(\Phi_\tau^{\pi, (\alpha)} V)(x) = V(x) + \tau \left(\tilde{r}^{(\alpha)}(x; \pi) + (L^\pi V)(x) - \beta V(x) \right) + R_\tau^{\pi, (\alpha)}(V)(x), \quad (64)$$

where L^π is the relaxed generator in Equation (50), and

$$\sup_{x \in \mathbb{R}^d} |R_\tau^{\pi, (\alpha)}(V)(x)| \leq C_\alpha \tau^{3/2}, \quad (65)$$

with C_α independent of τ and uniform over π in the admissible class.

Proof. We again treat the terminal and running terms separately.

Terminal term. Applying Dynkin's formula (Lemma C.4) to $V(\tilde{X}_t)$ under the relaxed generator L^π ,

$$\mathbb{E}[V(\tilde{X}_\tau)] - V(x) = \int_0^\tau \mathbb{E}[(L^\pi V)(\tilde{X}_t)] dt.$$

Add and subtract $(L^\pi V)(x)$:

$$\mathbb{E}[V(\tilde{X}_\tau)] = V(x) + \tau(L^\pi V)(x) + \int_0^\tau \mathbb{E}[(L^\pi V)(\tilde{X}_t) - (L^\pi V)(x)] dt.$$

By Assumption C.3, $L^\pi V$ is globally Lipschitz in x (uniformly over admissible π). In addition, Lemma C.5 applies to \tilde{X} as well, and hence the last integral is $\mathcal{O}(\tau^{3/2})$ uniformly in π . Multiplying by $e^{-\beta\tau} = 1 - \beta\tau + \mathcal{O}(\tau^2)$ yields:

$$\mathbb{E}[e^{-\beta\tau} V(\tilde{X}_\tau)] = V(x) + \tau((L^\pi V)(x) - \beta V(x)) + \mathcal{O}(\tau^{3/2}).$$

Running term. Using Lipschitz continuity of $\tilde{r}^{(\alpha)}(\cdot; \pi)$ in x over the admissible class, together with Lemma C.5,

$$\begin{aligned} \left| \mathbb{E} \left[\int_0^\tau e^{-\beta t} \tilde{r}^{(\alpha)}(\tilde{X}_t; \pi) dt \right] - \tilde{r}^{(\alpha)}(x; \pi) \int_0^\tau e^{-\beta t} dt \right| &\leq \int_0^\tau e^{-\beta t} C \mathbb{E} \|\tilde{X}_t - x\| dt \\ &\leq C \int_0^\tau \sqrt{t} dt = \mathcal{O}(\tau^{3/2}), \end{aligned}$$

uniformly in π . Again, because $\int_0^\tau e^{-\beta t} dt = \tau + \mathcal{O}(\tau^2)$, we obtain:

$$\mathbb{E} \left[\int_0^\tau e^{-\beta t} \tilde{r}^{(\alpha)}(\tilde{X}_t; \pi) dt \right] = \tau \tilde{r}^{(\alpha)}(x; \pi) + \mathcal{O}(\tau^{3/2}).$$

Combining both parts gives (64) and (65). \square

D.4. Per-step mismatch: $\Phi_\tau^{(\alpha)}$ vs. $T_\tau^{(\alpha)}$

Lemma D.4 (Per-step mismatch bound). *Assume Assumptions C.1, C.2, and C.3. Let $V \in \mathcal{D}$ and $\alpha \geq 0$. Then for all sufficiently small $\tau \in (0, 1]$,*

$$\Phi_\tau^{(\alpha)}(V)(x) = V(x) + \tau H^{(\alpha)}(V)(x) + R_\tau^{(\alpha)}(V)(x), \quad (66)$$

with

$$\|R_\tau^{(\alpha)}(V)\|_\infty \leq C_\alpha \tau^{3/2}, \quad (67)$$

where C_α is independent of τ . Consequently,

$$\|T_\tau^{(\alpha)}(V) - \Phi_\tau^{(\alpha)}(V)\|_\infty \leq C_\alpha \tau^{3/2}. \quad (68)$$

Proof. We treat $\alpha = 0$ and $\alpha > 0$ separately.

Case 1: $\alpha = 0$ (hard-max). For fixed a , Lemma D.2 yields

$$\Phi_\tau^a V(x) = V(x) + \tau q_V(x, a) + R_\tau^a(V)(x), \quad \sup_{x, a} |R_\tau^a(V)(x)| \leq C \tau^{3/2}.$$

Since $\Phi_\tau^{(0)} V(x) = \sup_{a \in \mathcal{A}} \Phi_\tau^a V(x)$,

$$\begin{aligned} \Phi_\tau^{(0)} V(x) &= V(x) + \tau \sup_{a \in \mathcal{A}} q_V(x, a) + \sup_{a \in \mathcal{A}} R_\tau^a(V)(x) \\ &= V(x) + \tau H^{(0)}(V)(x) + R_\tau^{(0)}(V)(x), \end{aligned}$$

and $\|R_\tau^{(0)}(V)\|_\infty \leq C \tau^{3/2}$.

Case 2: $\alpha > 0$ (soft-max). For any fixed Markov policy π , Lemma D.3 gives

$$\Phi_\tau^{\pi, (\alpha)} V(x) = V(x) + \tau \left(\tilde{r}^{(\alpha)}(x; \pi) + (L^\pi V)(x) - \beta V(x) \right) + R_\tau^{\pi, (\alpha)}(V)(x),$$

with $\sup_x |R_\tau^{\pi, (\alpha)}(V)(x)| \leq C_\alpha \tau^{3/2}$ uniformly in π . Taking supremum over π and using $\Phi_\tau^{(\alpha)} V = \sup_\pi \Phi_\tau^{\pi, (\alpha)} V$ yields

$$\Phi_\tau^{(\alpha)} V(x) = V(x) + \tau \sup_\pi \left(\tilde{r}^{(\alpha)}(x; \pi) + (L^\pi V)(x) - \beta V(x) \right) + R_\tau^{(\alpha)}(V)(x),$$

where $\|R_\tau^{(\alpha)}(V)\|_\infty \leq C_\alpha \tau^{3/2}$.

It remains to identify the second supremum term as $H^{(\alpha)}(V)(x)$. Using the definitions of $\tilde{r}^{(\alpha)}$ and L^π ,

$$\begin{aligned} \tilde{r}^{(\alpha)}(x; \pi) + (L^\pi V)(x) - \beta V(x) &= \int_{\mathcal{A}} \left(r(x, a) + (L^a V)(x) - \beta V(x) \right) \pi(da | x) - \alpha \int_{\mathcal{A}} \log \pi(a | x) \pi(da | x) \\ &= \int_{\mathcal{A}} q_V(x, a) \pi(da | x) - \alpha \int_{\mathcal{A}} \log \pi(a | x) \pi(da | x). \end{aligned}$$

Through Lemma C.6, for each fixed x ,

$$\begin{aligned} \sup_{\pi(\cdot | x)} \left\{ \int_{\mathcal{A}} q_V(x, a) \pi(da | x) - \alpha \int_{\mathcal{A}} \log \pi(a | x) \pi(da | x) \right\} &= \sup_{\pi(\cdot | x)} \mathbb{E}_{a \sim \pi(\cdot | x)} [q_V(x, a) - \alpha \log \pi(a | x)] \\ &= \mathcal{Q}^{(\alpha)}(q_V)(x) = \alpha \log \int_{\mathcal{A}} \exp\left(\frac{q_V(x, a)}{\alpha}\right) da \end{aligned}$$

which is exactly $H^{(\alpha)}(V)(x)$ by (58). Substituting gives (66)–(67). Finally, (68) follows immediately from the definition $T_\tau^{(\alpha)}(V) = V + \tau H^{(\alpha)}(V)$. \square

D.5. Proof of Theorem 4.1

Theorem 4.1 (Value Function Convergence). *Fix $\alpha \geq 0$ and $\tau > 0$. Under Assumptions C.1, C.2, and C.3, let V_k being the value function after k iterations $V_{k+1} := T_\tau^{(\alpha)}(V_k)$. Then, V_k converges to $V^{(\alpha)}$ as $\tau \rightarrow 0$, and for all $k \geq 0$,*

$$\|V_k - V^{(\alpha)}\|_\infty \leq C_0 e^{-\beta \tau k} + \frac{C_1 \tau^{3/2}}{1 - e^{-\beta \tau}}. \quad (35)$$

Here C_0 and C_1 are constants independent of k .

Proof. Let $W_{k+1} := \Phi_\tau^{(\alpha)}(W_k)$ be the exact dynamic-programming iterations initialized at the same $W_0 := V_0$. Define $\Delta_k := V_k - W_k$. Then

$$\begin{aligned}\Delta_{k+1} &= T_\tau^{(\alpha)}(V_k) - \Phi_\tau^{(\alpha)}(W_k) \\ &= \left(T_\tau^{(\alpha)}(V_k) - \Phi_\tau^{(\alpha)}(V_k) \right) + \left(\Phi_\tau^{(\alpha)}(V_k) - \Phi_\tau^{(\alpha)}(W_k) \right).\end{aligned}$$

Taking sup norms and using Lemma D.4 and Lemma D.1, we get:

$$\|\Delta_{k+1}\|_\infty \leq C_\alpha \tau^{3/2} + e^{-\beta\tau} \|\Delta_k\|_\infty.$$

Since $\Delta_0 = 0$, unrolling the recursion gives

$$\|\Delta_k\|_\infty \leq \frac{C_\alpha \tau^{3/2}}{1 - e^{-\beta\tau}} \quad \forall k \geq 0.$$

Finally, by the triangle inequality and Lemma D.1,

$$\begin{aligned}\|V_k - V^{(\alpha)}\|_\infty &\leq \|V_k - W_k\|_\infty + \|W_k - V^{(\alpha)}\|_\infty \\ &\leq \frac{C_\alpha \tau^{3/2}}{1 - e^{-\beta\tau}} + e^{-\beta\tau k} \|W_0 - V^{(\alpha)}\|_\infty,\end{aligned}$$

which is the claimed bound. \square

Note that, since $1 - e^{-\beta\tau} = \beta\tau + \mathcal{O}(\tau^2)$, the error estimate implies that $\|V_k - V^{(\alpha)}\| \leq C_0 e^{-\beta\tau k} + C_1 \tau^{1/2}$, and as $k, \tau \rightarrow 0$, this error also goes to 0.

E. Proof of q -convergence (Theorem 4.2)

This appendix proves the model-free convergence guarantee in Theorem 4.2. The key challenge is that the infinitesimal generator term $L^a V$ is unavailable in model-free learning, so we replace the infinitesimal advantage-rate q_V by a short-horizon estimator q_V^u computed from rollouts of length u (See Section 3.2). This introduces a *modelling bias* $q_V^u - q_V$ and an additional stability issue because q_V^u is $\mathcal{O}(1/u)$ -Lipschitz in V . Richardson extrapolation removes the leading $\mathcal{O}(u)$ bias term and improves the approximation accuracy of the learning signal while preserving the same stability structure.

E.1. Baseline modelling bias under standard assumptions

Before imposing higher-order smoothness (which yields $\mathcal{O}(u)$ and Richardson $\mathcal{O}(u^2)$), we record the baseline modelling-bias rate available under the standard diffusion assumptions. In this setting, one only obtains $\|q_V^u - q_V\|_\infty = \mathcal{O}(\sqrt{u})$.

Lemma E.1 (Baseline bias for q_V^u : $\|q_V^u - q_V\|_\infty = \mathcal{O}(\sqrt{u})$). *Assume Assumptions C.1 and C.2. Suppose $V \in C_b^2(\mathbb{R}^d)$ and $L^a V$ is globally Lipschitz in x uniformly over $a \in \mathcal{A}$. Then there exist $u_0 > 0$ and $C < \infty$ such that for all $u \in (0, u_0]$,*

$$\|q_V^u - q_V\|_\infty \leq C\sqrt{u}. \quad (69)$$

Consequently, for any $\alpha > 0$,

$$\|H_u^{(\alpha)}(V) - H^{(\alpha)}(V)\|_\infty \leq C\sqrt{u}. \quad (70)$$

Proof sketch. By Dynkin's formula,

$$\mathbb{E}_x^a[V(X_u^a)] - V(x) = \int_0^u \mathbb{E}_x^a[(L^a V)(X_t^a)] dt.$$

Subtract $u(L^a V)(x)$ and use the Lipschitz property of $L^a V$ gives:

$$\left| \mathbb{E}_x^a[V(X_u^a)] - V(x) - u(L^a V)(x) \right| \leq \int_0^u \mathbb{E}_x^a[|(L^a V)(X_t^a) - (L^a V)(x)|] dt \leq C \int_0^u \mathbb{E}_x^a[\|X_t^a - x\|] dt.$$

Lemma C.5 give $\mathbb{E}_x^a[\|X_t^a - x\|] \leq C\sqrt{t}$ uniformly in (x, a) , and hence the right-hand side is $\mathcal{O}(u^{3/2})$. Through definitions of q_V^u and q_V , dividing by u and accounting for the discount factor $e^{-\beta u} = 1 - \beta u + \mathcal{O}(u^2)$ yields $q_V^u(x, a) = q_V(x, a) + \mathcal{O}(\sqrt{u})$ uniformly in (x, a) , proving (69). The Hamiltonian bound (70) follows from a similar Lipschitz argument as in Lemma E.7. \square

E.2. Smoothness assumptions for quantitative u -rates

Assumption E.2 (Smooth C^2 assumptions). In addition to Assumption C.1, assume:

1. For each $a \in \mathcal{A}$, the drift and diffusion maps $x \mapsto b(x, a)$ and $x \mapsto \sigma(x, a)$ are C^2 with bounded derivatives up to order 2, uniformly in a , and globally Lipschitz in x uniformly in a .
2. For each $a \in \mathcal{A}$, the reward map $x \mapsto r(x, a)$ is C^2 with bounded derivatives up to order 2, uniformly in a , and globally Lipschitz in x .

Assumption E.3 (Value function smoothness). In addition to standard assumptions C.2 and C.3, assume that the value function domain $\mathcal{D} \subseteq C_b^4(\mathbb{R}^d)$ so that for value function V , and for each $a \in \mathcal{A}$, both $L^a V$ and $(L^a)^2 V$ are bounded and continuous.

Notation. Fix $a \in \mathcal{A}$. Let $(X_t^a)_{t \geq 0}$ solve the controlled SDE

$$dX_t^a = b(X_t^a, a) dt + \sigma(X_t^a, a) dW_t, \quad X_0^a = x,$$

Recall the fixed action controlled generator L^a is:

$$(L^a f)(x) := b(x, a) \cdot \nabla f(x) + \frac{1}{2} \text{Tr}(\sigma(x, a) \sigma(x, a)^\top \nabla^2 f(x)).$$

We additionally define the Markov semigroup

$$(P_t^a f)(x) := \mathbb{E}_x^a[f(X_t^a)]. \quad (71)$$

For $V \in C_b^2(\mathbb{R}^d)$, recall the q -function:

$$q_V(x, a) := r(x, a) + (L^a V)(x) - \beta V(x). \quad (72)$$

Together with its finite-step estimator q_V^u with time step $u > 0$:

$$q_V^u(x, a) := \frac{e^{-\beta u} \mathbb{E}_x^a[V(X_u^a)] - V(x)}{u} + r(x, a). \quad (73)$$

And the Richardson version \tilde{q}_V^u :

$$\tilde{q}_V^u(x, a) := 2 q_V^{u/2}(x, a) - q_V^u(x, a). \quad (74)$$

We now start with a series of lemmas that serve as the main ingredients for the proof of Theorem 4.2.

E.3. Bias expansions for q_V^u and \tilde{q}_V^u

We begin with a quantitative small-time expansion of the semigroup P_t^a .

Lemma E.4 (Second-order semigroup expansion). *Under assumptions E.2 and E.3, for $a \in \mathcal{A}$, $V \in C_b^4(\mathbb{R}^d)$, and for all $t \in [0, 1]$, we have*

$$(P_t^a V)(x) = V(x) + t(L^a V)(x) + R_V(t; x, a), \quad (75)$$

where the remainder satisfies

$$\sup_{x \in \mathbb{R}^d, a \in \mathcal{A}} |R_V(t; x, a)| \leq \frac{t^2}{2} \sup_{a \in \mathcal{A}} \|(L^a)^2 V\|_\infty \leq C_V t^2, \quad (76)$$

for a constant $C_V < \infty$ depending only on V and the coefficients.

Proof. Fix a and write $P_t := P_t^a$ and $L := L^a$ for notation convenience. Dynkin's formula (Lemma C.4) gives

$$(P_t V)(x) = V(x) + \int_0^t (P_s L V)(x) ds.$$

Applying the same identity to LV one more time yields:

$$(P_s L V)(x) = (LV)(x) + \int_0^s (P_r L^2 V)(x) dr.$$

Substitute into the first identity and use Fubini theorem, we have:

$$(P_t V)(x) = V(x) + t(LV)(x) + \int_0^t (t-r)(P_r L^2 V)(x) dr.$$

Define $R_V(t; x, a) := \int_0^t (t-r)(P_r^a(L^a)^2 V)(x) dr$. Then

$$|R_V(t; x, a)| \leq \|(L^a)^2 V\|_\infty \int_0^t (t-r) dr = \frac{t^2}{2} \|(L^a)^2 V\|_\infty,$$

which gives (76). \square

Lemma E.5 (First-order bias for q_V^u : $\|q_V^u - q_V\|_\infty = \mathcal{O}(u)$). *Under Assumptions E.2 and E.3, there exist $u_0 > 0$ and $C_q < \infty$ such that for all $u \in (0, u_0]$,*

$$\|q_V^u - q_V\|_\infty \leq C_q u. \quad (77)$$

Proof. Fix (x, a) . By Lemma E.4,

$$\mathbb{E}_x^a[V(X_u^a)] = V(x) + u(L^a V)(x) + \mathcal{O}(u^2),$$

uniformly in (x, a) . Also $e^{-\beta u} = 1 - \beta u + \mathcal{O}(u^2)$, hence

$$\begin{aligned} e^{-\beta u} \mathbb{E}_x^a[V(X_u^a)] - V(x) &= (1 - \beta u + \mathcal{O}(u^2))(V(x) + u(L^a V)(x) + \mathcal{O}(u^2)) - V(x) \\ &= u((L^a V)(x) - \beta V(x)) + \mathcal{O}(u^2), \end{aligned}$$

uniformly in (x, a) . Divide by u and add $r(x, a)$, we obtain

$$q_V^u(x, a) = r(x, a) + (L^a V)(x) - \beta V(x) + \mathcal{O}(u) = q_V(x, a) + \mathcal{O}(u),$$

uniformly in (x, a) , proving (77). \square

Lemma E.6 (Richardson bias for \tilde{q}_V^u : $\|\tilde{q}_V^u - q_V\|_\infty = \mathcal{O}(u^2)$). *Under Assumptions E.2 and E.3, there exist $u_0 > 0$ and $\tilde{C}_q < \infty$ such that for all $u \in (0, u_0]$,*

$$\|\tilde{q}_V^u - q_V\|_\infty \leq \tilde{C}_q u^2. \quad (78)$$

Proof. Proof of Lemma E.5 implies the expansion of $q_V^u(x, a)$ contains only u and u^2 terms with no u^h , $h \in (1, 2)$ in between:

$$q_V^u(x, a) = q_V(x, a) + u c_1(x, a) + u^2 c_2(u; x, a),$$

where c_1 is bounded and c_2 is uniformly bounded for u small. Evaluating at $u/2$ and forming $\tilde{q}_V^u = 2q_V^{u/2} - q_V^u$ cancels the linear term:

$$\tilde{q}_V^u(x, a) = q_V(x, a) + u^2 \left(\frac{1}{2} c_2(u/2; x, a) - c_2(u; x, a) \right),$$

which is $\mathcal{O}(u^2)$ uniformly in (x, a) . \square

E.4. Hamiltonians and Lipschitz lemmas

Recall the (soft) Hamiltonian for $\alpha > 0$,

$$H^{(\alpha)}(V)(x) := \alpha \log \int_{\mathcal{A}} \exp\left(\frac{q_V(x, a)}{\alpha}\right) da, \quad (79)$$

and its finite-horizon analogues on approximations q_V^u and \tilde{q}_V^u of q -function:

$$H_u^{(\alpha)}(V)(x) := \alpha \log \int_{\mathcal{A}} \exp\left(\frac{q_V^u(x, a)}{\alpha}\right) da, \quad (80)$$

$$\tilde{H}_u^{(\alpha)}(V)(x) := \alpha \log \int_{\mathcal{A}} \exp\left(\frac{\tilde{q}_V^u(x, a)}{\alpha}\right) da. \quad (81)$$

Lemma E.7 (Lipschitz Hamiltonian bias). *Fix $\alpha > 0$ and let $z, \bar{z} : \mathcal{A} \rightarrow \mathbb{R}$ be bounded. Then*

$$\left| \alpha \log \int_{\mathcal{A}} e^{z(a)/\alpha} da - \alpha \log \int_{\mathcal{A}} e^{\bar{z}(a)/\alpha} da \right| \leq \|z - \bar{z}\|_\infty. \quad (82)$$

Consequently, for any bounded V ,

$$\|H_u^{(\alpha)}(V) - H^{(\alpha)}(V)\|_\infty \leq \|q_V^u - q_V\|_\infty, \quad (83)$$

$$\|\tilde{H}_u^{(\alpha)}(V) - H^{(\alpha)}(V)\|_\infty \leq \|\tilde{q}_V^u - q_V\|_\infty. \quad (84)$$

Proof. For all a , $z(a) \leq \bar{z}(a) + \|z - \bar{z}\|_\infty$, hence $e^{z(a)/\alpha} \leq e^{\|z - \bar{z}\|_\infty/\alpha} e^{\bar{z}(a)/\alpha}$. Integrate and take logs to get

$$\log \int e^{z/\alpha} \leq \frac{\|z - \bar{z}\|_\infty}{\alpha} + \log \int e^{\bar{z}/\alpha}.$$

Reverse the roles of z, \bar{z} to obtain the other inequality, we can deduce (82). Apply this pointwise in x with $(z, \bar{z}) = (q_V^u(x, \cdot), q_V(x, \cdot))$ and $(z, \bar{z}) = (\tilde{q}_V^u(x, \cdot), q_V(x, \cdot))$, and then take the supremum over x , we obtain (83)–(84). \square

Now we show that q_V^u is $\mathcal{O}(1/u)$ -Lipschitz in V

Lemma E.8 (Lipschitz dependence of q_V^u on V). *For any bounded functions V, W and any $u > 0$,*

$$\|q_V^u - q_W^u\|_\infty \leq \frac{2}{u} \|V - W\|_\infty. \quad (85)$$

Consequently, for the Richardson rate,

$$\|\tilde{q}_V^u - \tilde{q}_W^u\|_\infty \leq \frac{6}{u} \|V - W\|_\infty. \quad (86)$$

Proof. From (73), the $r(x, a)$ term cancels, so

$$q_V^u(x, a) - q_W^u(x, a) = \frac{e^{-\beta u} \mathbb{E}_x^a[(V - W)(X_u^a)] - (V - W)(x)}{u}.$$

Taking absolute values and using $|\mathbb{E}[(V - W)(X_u^a)]| \leq \|V - W\|_\infty$ and $|(V - W)(x)| \leq \|V - W\|_\infty$ gives (85). For Richardson, use $\tilde{q}_V^u = 2q_V^{u/2} - q_V^u$ and apply the first bound twice:

$$\|\tilde{q}_V^u - \tilde{q}_W^u\|_\infty \leq 2\|q_V^{u/2} - q_W^{u/2}\|_\infty + \|q_V^u - q_W^u\|_\infty \leq 2 \cdot \frac{2}{u/2} \|V - W\|_\infty + \frac{2}{u} \|V - W\|_\infty = \frac{6}{u} \|V - W\|_\infty.$$

\square

E.5. One-step mismatch under stricter assumptions

Compared to Lemma D.4 (which gives an $\mathcal{O}(\tau^{3/2})$ remainder under standard assumptions), with stricter smooth assumptions, we can upgrade the local mismatch to $\mathcal{O}(\tau^2)$. This allows the τ^2 term in Theorem 4.2.

Lemma E.9 (Smooth local expansion of $\Phi_\tau^{(\alpha)}$). *Under Assumptions E.2, and E.3, fix $\alpha \geq 0$ and $V \in C_b^4(\mathbb{R}^d)$. Then there exist $\tau_0 > 0$ and $C_\Phi < \infty$ such that for all $\tau \in (0, \tau_0]$,*

$$\Phi_\tau^{(\alpha)}(V) = V + \tau H^{(\alpha)}(V) + R_\tau^{(\alpha)}(V), \quad \|R_\tau^{(\alpha)}(V)\|_\infty \leq C_\Phi \tau^2. \quad (87)$$

Equivalently,

$$\|\Phi_\tau^{(\alpha)}(V) - T_\tau^{(\alpha)}(V)\|_\infty \leq C_\Phi \tau^2. \quad (88)$$

Proof. We follow similar steps as in the proof of Lemma D.4. First we consider a fixed policy π , and recall from Lemma D.4 the policy-wise operator $\Phi_\tau^{\pi, (\alpha)}$:

$$(\Phi_\tau^{\pi, (\alpha)} V)(x) := \mathbb{E}_x^\pi \left[\int_0^\tau e^{-\beta t} \left(r(X_t, a_t) - \alpha \log \pi(a_t | X_t) \right) dt + e^{-\beta \tau} V(X_\tau) \right]. \quad (89)$$

We will show that, uniformly in x and uniformly over admissible π ,

$$\Phi_\tau^{\pi, (\alpha)} V(x) = V(x) + \tau G_\alpha(V)(x, \pi) + \mathcal{O}(\tau^2), \quad (90)$$

where

$$G_\alpha(V)(x, \pi) := \int_{\mathcal{A}} q_V(x, a) \pi(da | x) - \alpha \int_{\mathcal{A}} \log \pi(a | x) \pi(da | x). \quad (91)$$

To see this, we again treat separately the terminal term and the running term.

Terminal term. Under Assumptions E.2 and C.2, the relaxed coefficients $(\tilde{b}(\cdot; \pi), \tilde{\sigma}(\cdot; \pi))$ are Lipschitz, and the relaxed generator L^π is well-defined and has bounded coefficients. Moreover $V \in C_b^4$ implies $L^\pi V$ and $(L^\pi)^2 V$ are bounded. Hence the same Dynkin-iteration argument as in Lemma E.4 (with L^a replaced by L^π) yields the second-order expansion

$$\mathbb{E}_x^\pi[V(X_\tau)] = V(x) + \tau(L^\pi V)(x) + \mathcal{O}(\tau^2), \quad (92)$$

uniformly in x and uniformly over admissible π . Multiplying by $e^{-\beta\tau} = 1 - \beta\tau + \mathcal{O}(\tau^2)$ gives

$$\mathbb{E}_x^\pi[e^{-\beta\tau}V(X_\tau)] = V(x) + \tau((L^\pi V)(x) - \beta V(x)) + \mathcal{O}(\tau^2). \quad (93)$$

Running term. Define the relaxed one-step reward-with-entropy

$$\tilde{r}^{(\alpha)}(x; \pi) := \int_{\mathcal{A}} (r(x, a) - \alpha \log \pi(a | x)) \pi(da | x).$$

Under Assumptions E.2 and C.2 and the policy regularity in Assumption C.2, the function $x \mapsto \tilde{r}^{(\alpha)}(x; \pi)$ is bounded and C^2 with bounded derivatives, uniformly over admissible π . Applying the same second-order semigroup expansion (again with generator L^π) to $\tilde{r}^{(\alpha)}(\cdot; \pi)$ implies

$$\mathbb{E}_x^\pi[\tilde{r}^{(\alpha)}(X_t; \pi)] = \tilde{r}^{(\alpha)}(x; \pi) + \mathcal{O}(t), \quad t \in [0, 1], \quad (94)$$

uniformly in x and uniformly over π . Therefore,

$$\mathbb{E}_x^\pi \left[\int_0^\tau e^{-\beta t} \tilde{r}^{(\alpha)}(X_t; \pi) dt \right] = \int_0^\tau (1 + \mathcal{O}(t)) (\tilde{r}^{(\alpha)}(x; \pi) + \mathcal{O}(t)) dt = \tau \tilde{r}^{(\alpha)}(x; \pi) + \mathcal{O}(\tau^2) \quad (95)$$

uniformly in x and uniformly over π .

Combining (93) and (95) in (89) gives (90). Finally, note that the bracketed term in (90) equals

$$\tilde{r}^{(\alpha)}(x; \pi) + (L^\pi V)(x) - \beta V(x) = \int_{\mathcal{A}} q_V(x, a) \pi(da | x) - \alpha \int_{\mathcal{A}} \log \pi(a | x) \pi(da | x),$$

which is exactly $G_\alpha(V)(x, \pi)$ in (91).

Now we optimize over policies π to obtain the term $H^{(\alpha)}(V)$. By definition, $\Phi_\tau^{(\alpha)}(V)(x) = \sup_\pi \Phi_\tau^{\pi, (\alpha)}(V)(x)$. Hence, taking the supremum in (90) yields

$$\Phi_\tau^{(\alpha)}(V)(x) = V(x) + \tau \sup_\pi G_\alpha(V)(x, \pi) + \mathcal{O}(\tau^2).$$

Again, through a similar argument as in Lemma D.4 that invokes Lemma C.6, we have:

$$\sup_{\pi(\cdot | x)} \left\{ \int q_V(x, a) \pi(da | x) - \alpha \int \log \pi(a | x) \pi(da | x) \right\} = \alpha \log \int_{\mathcal{A}} \exp\left(\frac{q_V(x, a)}{\alpha}\right) da = H^{(\alpha)}(V)(x).$$

For $\alpha = 0$ the same optimization reduces to $\sup_a q_V(x, a) = H^{(0)}(V)(x)$. Thus

$$\Phi_\tau^{(\alpha)}(V)(x) = V(x) + \tau H^{(\alpha)}(V)(x) + \mathcal{O}(\tau^2),$$

uniformly in x , which proves (87). The equivalent form (88) follows from the definition $T_\tau^{(\alpha)}(V) = V + \tau H^{(\alpha)}(V)$. \square

Now define the finite-horizon Picard operator and its Richardson variant:

$$(T_{\tau, u}^{(\alpha)} V)(x) := V(x) + \tau H_u^{(\alpha)}(V)(x), \quad (96)$$

$$(T_{\tau, u}^{R, (\alpha)} V)(x) := V(x) + \tau \tilde{H}_u^{(\alpha)}(V)(x). \quad (97)$$

Here we have similar one-step mismatch as in Lemma D.4, but with better errors.

Lemma E.10 (One-step mismatch: finite-horizon and Richardson). *Assume Assumptions E.2 and E.3, and fix $\alpha > 0$. Then there exist $\tau_0, u_0 > 0$ and $C < \infty$ such that for all $\tau \in (0, \tau_0]$, $u \in (0, u_0]$, and all $V \in C_b^4(\mathbb{R}^d)$,*

$$\|\Phi_\tau^{(\alpha)}(V) - T_{\tau, u}^{(\alpha)}(V)\|_\infty \leq C(\tau^2 + \tau u), \quad (98)$$

$$\|\Phi_\tau^{(\alpha)}(V) - T_{\tau, u}^{R, (\alpha)}(V)\|_\infty \leq C(\tau^2 + \tau u^2). \quad (99)$$

Proof. By Lemma E.9,

$$\|\Phi_\tau^{(\alpha)}(V) - T_\tau^{(\alpha)}(V)\|_\infty \leq C_\Phi \tau^2.$$

For the finite-horizon Picard operator,

$$\|T_\tau^{(\alpha)}(V) - T_{\tau, u}^{(\alpha)}(V)\|_\infty = \tau \|H^{(\alpha)}(V) - H_u^{(\alpha)}(V)\|_\infty \leq \tau \|q_V - q_V^u\|_\infty,$$

using Lemma E.7. Then Lemma E.5 yields $\|q_V - q_V^u\|_\infty \leq C_q u$, hence

$$\|\Phi_\tau^{(\alpha)}(V) - T_{\tau, u}^{(\alpha)}(V)\|_\infty \leq C_\Phi \tau^2 + \tau C_q u \leq C(\tau^2 + \tau u).$$

The Richardson bound's proof is identical through using the following inequality from Lemmas E.6 and E.7:

$$\|H^{(\alpha)}(V) - \tilde{H}_u^{(\alpha)}(V)\|_\infty \leq \|\tilde{q}_V^u - q_V\|_\infty \leq \tilde{C}_q u^2$$

\square

E.6. Proof of Theorem 4.2

Theorem 4.2 (Convergence with q -function). *Let V_k be the resulting function defined by Richardson Picard-Hamiltonian iterations $V_{k+1} := V_k + \tau \tilde{H}_u^{(\alpha)}(V_k)$. Under Assumption E.2 and E.3, for $u > 0$, there exist constants C_1, C_2, L , and $\rho > 0$ such that for all $k \geq 0$:*

$$\|V_k - V^{(\alpha)}\|_\infty \leq e^{-\rho\tau k} \|V_0 - V^{(\alpha)}\|_\infty + \frac{C_1(\tau^2 + \tau u^2)}{1 - e^{-\rho\tau}}. \quad (37)$$

And, for q -function estimation, we obtain the error:

$$\|\tilde{q}_{V_k}^u - q_{V^{(\alpha)}}\|_\infty \leq \frac{L}{u} \|V_k - V^{(\alpha)}\|_\infty + C_2 u^2 \quad (38)$$

Proof. We present the Richardson-based statement; the non-Richardson bound follows by replacing u^2 by u .

Step 1: Perturbed contraction recursion. Let $V^* := V^{(\alpha)}$ denote the unique fixed point of $\Phi_\tau^{(\alpha)}$. By the contraction property in Lemma D.1,

$$\|\Phi_\tau^{(\alpha)}(V) - \Phi_\tau^{(\alpha)}(V^*)\|_\infty \leq e^{-\beta\tau} \|V - V^*\|_\infty.$$

For the Richardson Picard-Hamiltonian iteration $V_{k+1} := T_{\tau,u}^{R,(\alpha)}(V_k)$,

$$\begin{aligned} \|V_{k+1} - V^*\|_\infty &= \|T_{\tau,u}^{R,(\alpha)}(V_k) - V^*\|_\infty \\ &\leq \|\Phi_\tau^{(\alpha)}(V_k) - \Phi_\tau^{(\alpha)}(V^*)\|_\infty + \|\Phi_\tau^{(\alpha)}(V_k) - T_{\tau,u}^{R,(\alpha)}(V_k)\|_\infty \\ &\leq e^{-\beta\tau} \|V_k - V^*\|_\infty + C(\tau^2 + \tau u^2), \end{aligned}$$

where the last step uses (99). Again, a simple inductive argument gives:

$$\|V_k - V^*\|_\infty \leq e^{-\beta\tau k} \|V_0 - V^*\|_\infty + \frac{C(\tau^2 + \tau u^2)}{1 - e^{-\beta\tau}}. \quad (100)$$

Step 2: q -convergence from value convergence. By the triangle inequality,

$$\|\tilde{q}_{V_k}^u - q_{V^*}\|_\infty \leq \|\tilde{q}_{V_k}^u - \tilde{q}_{V^*}^u\|_\infty + \|\tilde{q}_{V^*}^u - q_{V^*}\|_\infty.$$

The first term is controlled by Lemma E.8:

$$\|\tilde{q}_{V_k}^u - \tilde{q}_{V^*}^u\|_\infty \leq \frac{6}{u} \|V_k - V^*\|_\infty.$$

The second term is the modelling bias, bounded by Lemma E.6:

$$\|\tilde{q}_{V^*}^u - q_{V^*}\|_\infty \leq \tilde{C}_q u^2.$$

Combining these yields

$$\|\tilde{q}_{V_k}^u - q_{V^*}\|_\infty \leq \frac{6}{u} \|V_k - V^*\|_\infty + \tilde{C}_q u^2. \quad (101)$$

Substituting (100) into (101) gives the stated q -bound. \square

Finally, the bound contains the factor $1/u$ multiplying the value error. Thus, to guarantee $\tilde{q}_{V_k}^u \rightarrow q_{V^*}$ as $(\tau, u) \rightarrow (0, 0)$, it suffices that $u \rightarrow 0$ and $\tau/u \rightarrow 0$ so that $\frac{1}{u} \cdot (\tau + u^2) \rightarrow 0$, and the errors in Theorem 4.2 go to 0.

F. Proof of convergence for CT-SAC (Theorem 4.3 and Corollary 4.4)

F.1. From (V_k, q_k) to a single Q_k

We prove that the single-critic update is an algebraic re-expression of the decoupled (V_k, q_k) iteration, hence inherits its convergence guarantees. Fix an algorithmic step size $\tau > 0$ and a holding time $u > 0$ with $\gamma := e^{-\beta u}$. Recall that

$$q_V^u(x, a) := \frac{\gamma \mathbb{E}_x^a[V(X_u)] - V(x)}{u} + r(x, a). \quad (102)$$

We will also use the shorthand

$$\Delta_u V(x, a) := \gamma \mathbb{E}_x^a[V(X_u)] - V(x), \quad q_V^u(x, a) = \frac{\Delta_u V(x, a)}{u} + r(x, a). \quad (103)$$

Lemma F.1 (One-step Q -update induced by (V, q)). *Assume that at iteration k we have a pair (V_k, q_k) and a policy π_k such that*

$$V_{k+1}(x) = V_k(x) + \tau \mathbb{Q}^{(\alpha)}(q_k)(x) \quad (\text{Hamiltonian flow update}), \quad (104)$$

and the finite-horizon approximation q_{k+1} :

$$q_{k+1}(x, a) = \frac{\gamma \mathbb{E}_x^a[V_{k+1}(X_u)] - V_{k+1}(x)}{u} + r(x, a). \quad (105)$$

Define the single critic $Q_k(x, a) := V_k(x) + q_k(x, a)$. Then $Q_{k+1} := V_{k+1} + q_{k+1}$ satisfies the closed-form update

$$\begin{aligned} Q_{k+1}(x, a) &= (1 - \tau)Q_k(x, a) + \tau r(x, a) + \tau \mathbb{E}_{a \sim \pi_k(\cdot|x)} [\tilde{Q}_k(x, a)] \\ &\quad + \tau \frac{\gamma \mathbb{E}_{a' \sim \pi_k(\cdot|X_u)} [\tilde{Q}_k(X_u, a')] - \mathbb{E}_{a \sim \pi_k(\cdot|x)} [\tilde{Q}_k(x, a)]}{u}, \end{aligned} \quad (106)$$

where $\tilde{Q}_k(x, a)$ is defined as $Q_k(x, a) - \alpha \log \pi_k(a|x)$ with $\pi_k(a|x) \sim \exp(q_k(x, a)/\alpha) \sim \exp(Q_k(x, a)/\alpha)$.

Note that this is the same equation as Equation (33). We state the equation again here for convenience reference.

Proof. From Lemma C.6, we immediately have $V_{k+1}(x) = V_k(x) + \tau \mathbb{E}_{a \sim \pi_k(\cdot|x)} [q_k(x, a) - \alpha \log \pi_k(a|x)]$, for $\pi_k(\cdot|x) \sim \exp(q_k(x, \cdot)/\alpha)$. Using $q_k = Q_k - V_k$ gives:

$$\begin{aligned} V_{k+1}(x) &= V_k(x) + \tau \mathbb{E}_{a \sim \pi_k} [Q_k(x, a) - V_k(x) - \alpha \log \pi_k(a|x)] \\ &= (1 - \tau)V_k(x) + \tau \mathbb{E}_{a \sim \pi_k(\cdot|x)} [\tilde{Q}_k(x, a)]. \end{aligned} \quad (107)$$

Plugging Equation (107) into Equation (105) gives

$$\begin{aligned} q_{k+1}(x, a) &= \frac{1}{u} \left(\gamma \mathbb{E}_x^a[V_{k+1}(X_u)] - V_{k+1}(x) \right) + r(x, a) \\ &= \frac{1}{u} \left(\gamma(1 - \tau) \mathbb{E}_x^a[V_k(X_u)] + \gamma \tau \mathbb{E}_x^a [\mathbb{E}_{a'} [\tilde{Q}_k(X_u, a')]] \right. \\ &\quad \left. - (1 - \tau)V_k(x) - \tau \mathbb{E}_a [\tilde{Q}_k(x, a)] \right) + r(x, a). \end{aligned} \quad (108)$$

Rearranging the terms, we get (we drop \mathbb{E}_x^a for the last term for readability):

$$\begin{aligned} q_{k+1}(x, a) &= (1 - \tau) \frac{\gamma \mathbb{E}_x^a[V_k(X_u)] - V_k(x)}{u} + r(x, a) + \frac{\tau}{u} \left(\gamma \mathbb{E}_{a'} [\tilde{Q}_k(X_u, a')] - \mathbb{E}_a [\tilde{Q}_k(x, a)] \right) \\ &= (1 - \tau)(q_k(x, a) - r(x, a)) + r(x, a) + \frac{\tau}{u} \left(\gamma \mathbb{E}_{a'} [\tilde{Q}_k(X_u, a')] - \mathbb{E}_a [\tilde{Q}_k(x, a)] \right). \end{aligned} \quad (109)$$

Finally, add $V_{k+1}(x)$ from Equation (109) to obtain

$$\begin{aligned} Q_{k+1}(x, a) &= V_{k+1}(x) + q_{k+1}(x, a) \\ &= (1 - \tau)V_k(x) + \tau \mathbb{E}_a [\tilde{Q}_k(x, a)] + (1 - \tau)q_k(x, a) + \tau r(x, a) \\ &\quad + \frac{\tau}{u} \left(\gamma \mathbb{E}_{a'} [\tilde{Q}_k(X_u, a')] - \mathbb{E}_a [\tilde{Q}_k(x, a)] \right) \\ &= (1 - \tau)Q_k(x, a) + \tau r(x, a) + \tau \mathbb{E}_a [\tilde{Q}_k(x, a)] + \tau \frac{\gamma \mathbb{E}_{a'} [\tilde{Q}_k(X_u, a')] - \mathbb{E}_a [\tilde{Q}_k(x, a)]}{u}. \end{aligned} \quad (110)$$

This is exactly Equation (106) (or Equation (33)). \square

Note. For implementation, it is convenient to introduce a “fast” update

$$Q_{k+1}^{\text{fast}}(s, a) = \frac{Q_{k+1}(s, a) - (1 - \tau)Q_k(s, a)}{\tau} \quad (111)$$

The full update can then be written as:

$$Q_{k+1}^{\text{fast}}(s, a) = r(s, a) + \mathbb{E}_a [\tilde{Q}_k(s, a)] + \frac{\gamma \mathbb{E}_{a'} [\tilde{Q}_k(s', a')] - \mathbb{E}_a [\tilde{Q}_k(s, a)]}{u} \quad (112)$$

$$Q_{k+1}(s, a) = \tau Q_{k+1}^{\text{fast}}(s, a) + (1 - \tau)Q_k(s, a) \quad (113)$$

Algorithm 2 Continuous-time TD3 (CT-TD3)

- 1: **Input:** discount rate β , Euler step $\tau > 0$, actor delay $d \in \mathbb{N}$, exploration std σ_{expl} , target smoothing std σ_{targ} , clip $c > 0$.
- 2: Initialize twin critics $Q_{\theta_1}, Q_{\theta_2}$ and deterministic actor μ_ϕ .
- 3: Initialize target networks $Q_{\bar{\theta}_1} \leftarrow Q_{\theta_1}, Q_{\bar{\theta}_2} \leftarrow Q_{\theta_2}, \mu_{\bar{\phi}} \leftarrow \mu_\phi$.
- 4: **for** $k = 0, 1, 2, \dots$ **do**
- 5: Collect transitions (x, a, r, x', u) , where $x = X_t, x' = X_{t+u}$, and u can vary across samples. Use behavior action $a = \mu_\phi(x) + \epsilon$ with $\epsilon \sim \mathcal{N}(0, \sigma_{\text{expl}}^2 I)$ (clip to action bounds if needed). Store in an off-policy replay buffer.
- 6: Sample a mini-batch \mathcal{B} of (x, a, r, x', u) from the replay buffer and set $\gamma = e^{-\beta u}$ per sample.
- 7: **Target policy smoothing:**

$$\tilde{a}' = \mu_{\bar{\phi}}(x') + \epsilon', \quad \epsilon' \sim \text{clip}(\mathcal{N}(0, \sigma_{\text{targ}}^2 I), -c, c),$$

- 8: Compute clipped double- Q bootstrap:

$$\bar{Q}_{\bar{\theta}}(x', \tilde{a}') := \min\{Q_{\bar{\theta}_1}(x', \tilde{a}'), Q_{\bar{\theta}_2}(x', \tilde{a}')\}.$$

- 9: **Critic updates:** for $i \in \{1, 2\}$, form the target

$$y_i := (1 - \tau)Q_{\bar{\theta}_i}(x, a) + \tau \bar{Q}_{\bar{\theta}}(x, \mu_{\bar{\phi}}(x)) + \tau r + \tau \frac{\gamma \bar{Q}_{\bar{\theta}}(x', \tilde{a}') - \bar{Q}_{\bar{\theta}}(x, \mu_{\bar{\phi}}(x))}{u},$$

and update θ_i by regression on \mathcal{B} :

$$\theta_i \leftarrow \arg \min_{\theta} \mathbb{E}_{(x, a, r, x', u) \sim \mathcal{B}} (Q_\theta(x, a) - y_i)^2.$$

- 10: **if** $k \bmod d = 0$ **then**

- 11: **Delayed policy update:** update actor using critic Q_{θ_1} :

$$\phi \leftarrow \phi + \eta_\pi \mathbb{E}_{x \sim \mathcal{B}} \left[\nabla_\phi \mu_\phi(x) \nabla_a Q_{\theta_1}(x, a) \Big|_{a=\mu_\phi(x)} \right].$$

- 12: **end if**

- 13: **end for**

When $u = 1$, this reduces to a Q -update closely aligned with the discrete-time counterpart. Below is a deterministic version (CT-TD3) of CT-SAC (See Algorithm 2).

Richardson update. We now state the Richardson version of Q -function update. Fix a holding time $u > 0$ and define $\gamma := e^{-\beta u}$ and $\gamma_{1/2} := e^{-\beta u/2}$. Let $X_{u/2}$ denote the state reached after time $u/2$ when starting from (x, a) . Define the policy-averaged soft value functional

$$S_k(x) := \mathbb{E}_{a \sim \pi_k(\cdot | x)} [\tilde{Q}_k^R(x, a)], \quad \tilde{Q}_k^R(x, a) := Q_k^R(x, a) - \alpha \log \pi_k(a | x), \quad (114)$$

and the Richardson critic decomposition

$$Q_k^R(x, a) := V_k(x) + \tilde{q}_{V_k}^u(x, a), \quad (115)$$

Then the induced single-critic update of Q_k^R has the form:

$$\begin{aligned} Q_{k+1}^R(x, a) &= (1 - \tau)Q_k^R(x, a) + \tau r(x, a) + \tau S_k(x) \\ &\quad + \frac{\tau}{u} \left(4\gamma_{1/2} \mathbb{E}_x^a [S_k(X_{u/2})] - \gamma \mathbb{E}_x^a [S_k(X_u)] - 3S_k(x) \right). \end{aligned} \quad (116)$$

Detailed derivations are given in Lemma I.2. We now continue with the algorithm convergence.

Lemma F.2 (Inductive preservation of $Q_k = V_k + q_k$). *Assume (V_0, q_0) satisfy the finite-horizon relation $q_0 = q_{V_0}^u$ from Equation (102) and define $Q_0 := V_0 + q_0$. Let (V_k, q_k) be generated by Equation (104)–Equation (105) and let Q_k be generated by Equation (106). Then for all $k \geq 0$,*

$$Q_k(x, a) = V_k(x) + q_k(x, a). \quad (117)$$

Proof. By construction, Equation (117) holds for $k = 0$. Assume it holds for some k . By Lemma F.1, the update Equation (106) produced from (V_k, q_k) satisfies $Q_{k+1} = V_{k+1} + q_{k+1}$. This completes the induction. \square

We now show that the single critic converges by combining the value and rate convergence bounds.

Theorem 4.3 (Theoretical Algorithm Convergence). *Consider the exact iterative update of Q_k through Equation (33) with no optimization or statistical error. Then Q_k converge to the optimal value $Q^{(\alpha)} = V^{(\alpha)} + q_{V^{(\alpha)}}$ as $k \rightarrow \infty$.*

Proof. From Lemma F.2, we get:

$$Q_k - Q^{(\alpha)} = (V_k - V^{(\alpha)}) + (q_k - q_{V^{(\alpha)}}), \quad (118)$$

Therefore, by the triangle inequality,

$$\|Q_k - Q^{(\alpha)}\|_\infty \leq \|V_k - V^{(\alpha)}\|_\infty + \|q_k - q_{V^{(\alpha)}}\|_\infty. \quad (119)$$

The terms are controlled by Theorem 4.1 and Theorem 4.2 (with $q_k = q_{V_k}$ in the idealized setting, or $q_k = \tilde{q}_{V_k}^u$ in the model-free setting). Combining the two bounds yields convergence of Q_k to $Q^{(\alpha)} = V^{(\alpha)} + q_{V^{(\alpha)}}$, with the error rates given by Theorem 4.1 and Theorem 4.2. \square

We now sketch a standard finite-sample extension that converts the exact convergence into a statistical bound for the learned critic \hat{Q}_k produced by neural network fitting. We first state standard i.i.d. generalization bounds that we use to control the statistical error of the critic regression step.

F.2. Learning-theoretic ingredients (i.i.d. regression)

Throughout this section, \mathcal{X} denotes an input space, $\mathcal{Y} \subset \mathbb{R}$ a bounded label space, and $\mathcal{Z} = \mathcal{X} \times \mathcal{Y}$. Let \mathcal{H} be a hypothesis class of functions $h : \mathcal{X} \rightarrow \mathcal{Y}$ and let $l(h, (x, y)) = \phi(h(x), y)$ be a loss with $\phi(\cdot, y)$ γ -Lipschitz for all y . For i.i.d. samples $Z_i = (X_i, Y_i) \sim \mathbb{P}$, define the population and empirical risks

$$e(h) := \mathbb{E}[l(h, Z)], \quad E_n(h) := \frac{1}{n} \sum_{i=1}^n l(h, Z_i). \quad (120)$$

Definition F.3 (Rademacher complexity). For $\mathcal{T} \subseteq \mathbb{R}^n$, its Rademacher complexity is

$$\text{Rad}(\mathcal{T}) := \mathbb{E} \left[\sup_{t \in \mathcal{T}} \frac{1}{n} \sum_{i=1}^n B_i t_i \right], \quad (121)$$

where B_i are i.i.d. Rademacher random variables.

Besides Rademacher complexity, we also define the following sets: $\mathcal{H} \circ \{Z_1, \dots, Z_n\} := \{(h(X_1), \dots, h(X_n)), h \in \mathcal{H}\} \subseteq \mathbb{R}^n$, and $\mathcal{L} \circ \{Z_1, \dots, Z_n\} := \{(l(h, Z_1), \dots, l(h, Z_n)), h \in \mathcal{H}\} \subseteq \mathbb{R}^n$. We state the following standard PAC-type results (Rebeschini, 2022):

Lemma F.4 (Lipschitz contraction for losses). *If $\phi(\cdot, y)$ is γ -Lipschitz for all y , then*

$$\mathbb{E} \left[\sup_{h \in \mathcal{H}} (e(h) - E_n(h)) \right] \leq 2 \mathbb{E} [\text{Rad}(\mathcal{L} \circ \{Z_1, \dots, Z_n\})] \leq 2\gamma \mathbb{E} [\text{Rad}(\mathcal{H} \circ \{Z_1, \dots, Z_n\})]. \quad (122)$$

Lemma F.5 (High-probability uniform bound). *Assume $l(h, Z) \in [0, c]$ almost surely. Then with probability at least $1 - \delta$,*

$$\sup_{h \in \mathcal{H}} (e(h) - E_n(h)) \leq 4 \text{Rad}(\mathcal{L} \circ \{Z_1, \dots, Z_n\}) + c \sqrt{\frac{2 \log(1/\delta)}{n}}. \quad (123)$$

Lemma F.6 (Rademacher complexity for bounded neural nets). *For a hypothesis class \mathcal{H} consisting of (regularized) neural networks with bounded weights, there exist constants $C_1, C_2 > 0$ such that for n i.i.d. samples,*

$$\text{Rad}(\mathcal{H} \circ \{Z_1, \dots, Z_n\}) \leq \frac{1}{\sqrt{n}} (C_1 + C_2 \sqrt{\log d}), \quad (124)$$

where d is an ambient dimension parameter of the network class.

F.3. Proof of Corollary 4.4

Definition F.7. With $\tilde{Q}(x, a) := Q(x, a) - \alpha \log \pi(a | x)$, and $\pi(a|x) \sim \exp(Q(x, a)/\alpha)$, we define the single-critic update operator arising from Equation (33):

$$\begin{aligned} (\mathcal{F}_{\tau, u}(Q))(x, a) := & (1 - \tau)Q(x, a) + \tau r(x, a) + \tau \mathbb{E}_{a \sim \pi(\cdot|x)} [\tilde{Q}(x, a)] \\ & + \tau \frac{\gamma \mathbb{E}_{a' \sim \pi(\cdot|x')} [\tilde{Q}(x', a')] - \mathbb{E}_{a \sim \pi(\cdot|x)} [\tilde{Q}(x, a)]}{u} \end{aligned} \quad (125)$$

Definition F.8. With the Richardson q-function $\tilde{q}_V^u := 2q_V^{u/2} - q_V^u$, the single-critic update operator is:

$$\begin{aligned} (\mathcal{F}_{\tau,u}^{\text{Rich}}(Q))(x, a) &:= (1 - \tau)Q(x, a) + \tau r(x, a) + \tau \mathbb{E}_{a \sim \pi(\cdot|x)}[\tilde{Q}(x, a)] \\ &\quad + \frac{\tau}{u} \left(4e^{-\beta u/2} \mathbb{E}_{a' \sim \pi(\cdot|x'_{u/2})}[\tilde{Q}(x'_{u/2}, a')] - e^{-\beta u} \mathbb{E}_{a'' \sim \pi(\cdot|x'_u)}[\tilde{Q}(x'_u, a'')] - 3 \mathbb{E}_{a \sim \pi(\cdot|x)}[\tilde{Q}(x, a)] \right) \end{aligned} \quad (126)$$

where $x'_{u/2} = X_{t+u/2}$ and $x'_u = X_{t+u}$.

Approximation procedure. At each iteration k , we draw n_k i.i.d. transition samples

$$(X_i, A_i, R_i, X'_i, U_i)_{i=1}^{n_k}, \quad (127)$$

from a replay distribution (treated as i.i.d. for analysis), and form a bounded regression target $Y_k(x, a, r, x', u)$ corresponding to the right-hand side of the population update Equation (33). We then fit $\hat{Q}_{k+1} \in \mathcal{H}_Q$ by (approximately) minimizing the empirical loss $\frac{1}{n_k} \sum_{i=1}^{n_k} \phi(\hat{Q}_{k+1}(X_i, A_i), Y_k(Z_i))$. Assume the output range of \mathcal{H}_Q and the targets are uniformly bounded. Let ν denote the state–action sampling distribution induced by the data collection scheme (e.g. replay buffer sampling), and define the $L^2(\nu)$ norm by:

$$\|f\|_{L^2(\nu)} := \left(\mathbb{E}_{(X, A) \sim \nu} [|f(X, A)|^2] \right)^{1/2}.$$

Let Q_k denote the exact iterate and \hat{Q}_{k+1} the learned iterate obtained by regression at iteration $k + 1$. At each step k , the target Y_k is exactly the value $(\mathcal{F}_{\tau,u}(Q))$ on realized samples. As a result, thanks to Lemmas F.4 to F.6, we can estimate the one-step statistical error (which is a random variable):

$$\text{stat}_k := \|\hat{Q}_{k+1} - \mathcal{F}_{\tau,u}(\hat{Q}_k)\|_{L^2(\nu)}.$$

In this case, we have:

$$\text{stat}_k \lesssim \frac{1}{\sqrt{n_k}} \left(1 + \sqrt{\log d} + \sqrt{\log(1/\delta)} \right) \quad \text{with probability } \geq 1 - \delta, \quad (128)$$

Note that the replay buffer sampling distribution $\nu = \nu_k$ can change at each iterations. However, for large enough n_k , we can easily transfer from $L^2(\nu)$ to $L^2(\nu_k)$ given that ν_k is regular enough. Hence, for simplicity, we proceed with a fixed replay buffer sampling ν .

Lemma F.9 (Lipschitz of critic mapping). *Assume the policy $\pi_k(\cdot|x)$ used inside $\hat{Q}_k(x, a) := Q_k(x, a) - \alpha \log \pi_k(a|x)$ is treated as fixed when comparing two critics (policy-evaluation step). Then the mapping $\mathcal{F}_{\tau,u}$ is Lipschitz in $L^2(\nu)$:*

$$\|\mathcal{F}_{\tau,u}(Q) - \mathcal{F}_{\tau,u}(Q')\|_{L^2(\nu)} \leq \left(1 + \frac{\tau}{u} \right) \|Q - Q'\|_{L^2(\nu)}. \quad (129)$$

Proof. The update $\mathcal{F}_{\tau,u}$ is affine in Q through terms of the form $Q(x, a)$, $\mathbb{E}_{a \sim \pi(\cdot|x)}[Q(x, a)]$, and $\mathbb{E}_{a' \sim \pi(\cdot|x')}[Q(x', a')]$, all multiplied by coefficients bounded by $1 + \tau/u$. Using Jensen’s inequality for conditional expectations $\|\mathbb{E}[Q(X, \cdot) | X]\|_{L^2} \leq \|Q(X, \cdot)\|_{L^2}$ yields the stated Lipschitz bound. \square

Corollary 4.4 (Algorithm Convergence). *Suppose at each iteration k , n_k samples are used in the gradient update. Then, for any pair of $(\epsilon, \delta) > 0$, there exists an iteration L together with the sequence n_1, n_2, \dots, n_L so that with the probability of at least δ , $\mathbb{E}[(|Q_L(X, A) - Q^{(\alpha)}(X, A)|^2)] < \epsilon$ for random state-action pair (X, A) . Here $Q^{(\alpha)} = V^{(\alpha)} + q_{V^{(\alpha)}}$ is the optimal function, and Q_L is the learned function from Algorithm 1.*

Proof. Given an $\epsilon > 0$, from Theorem 4.3, given the algorithmic error go to 0, we can choose an iteration L so that $\|Q_L - Q^{(\alpha)}\|_{L^2(\nu)} \leq \|Q_L - Q^{(\alpha)}\|_\infty < \epsilon/2$. Additionally, choose n_j large enough, so that $\text{stat}_j^{(2)} < (1/L_0^{L-1-j}) \frac{\epsilon}{2L}$ for probability of at least $1 - \delta/k$ for $L_0 = 1 + \tau/u$.

Now let Q_k be the exact iteration results and \hat{Q}_k the learned one. Define the statistical deviation in $L^2(\nu)$:

$$\epsilon_k^{(2)} := \|\hat{Q}_k - Q_k\|_{L^2(\nu)}.$$

Then we have the decomposition,

$$\begin{aligned} \epsilon_{k+1}^{(2)} &= \|\hat{Q}_{k+1} - Q_{k+1}\|_{L^2(\nu)} \\ &\leq \|\hat{Q}_{k+1} - \mathcal{F}_{\tau,u}(\hat{Q}_k)\|_{L^2(\nu)} + \|\mathcal{F}_{\tau,u}(\hat{Q}_k) - \mathcal{F}_{\tau,u}(Q_k)\|_{L^2(\nu)}. \end{aligned} \quad (130)$$

The first term is the one-step regression error stat_k . The second term is bounded by Lemma F.9:

$$\|\mathcal{F}_{\tau,u}(\hat{Q}_k) - \mathcal{F}_{\tau,u}(Q_k)\|_{L^2(\nu)} \leq \left(1 + \frac{\tau}{u} \right) \epsilon_k^{(2)}.$$

Hence,

$$\epsilon_{k+1}^{(2)} \leq \text{stat}_k + \left(1 + \frac{\tau}{u}\right) \epsilon_k^{(2)}. \quad (131)$$

Given the same initial point with $\epsilon_0^{(2)} = 0$, an inductive argument gives:

$$\epsilon_L^{(2)} \leq \sum_{j=0}^{L-1} \left(1 + \frac{\tau}{u}\right)^{L-1-j} \text{stat}_j = \sum_{j=0}^{L-1} L_0^{L-1-j} \text{stat}_j \quad (132)$$

Based on the choice of n_k , the RHS can further be bounded by $\sum_{j=0}^{L-1} \epsilon_j^{(2)} / (2L) = \epsilon/2$ with probability of at least $1 - k(\delta/k) = 1 - \delta$. Finally, with probability of at least $1 - \delta$, we have the decomposition:

$$\|\hat{Q}_L - Q^{(\alpha)}\|_{L^2(\nu)} \leq \underbrace{\|Q_L - Q^{(\alpha)}\|_{L^2(\nu)}}_{\text{algorithmic error}} + \underbrace{\|\hat{Q}_L - Q_L\|_{L^2(\nu)}}_{=\epsilon_L^{(2)} \text{ statistical error}} < \epsilon/2 + \epsilon/2 = \epsilon \quad (133)$$

□

We defer the theoretical analysis with more refined control of sample complexity and regret bound to Section H

G. Random time step U

Many environments produce irregular times U , and here we provide similar convergence results for (random time) U . The deterministic finite-horizon approximation results extend directly by conditioning on U and averaging. The key observation is that any deterministic Hamiltonian bias bound in u transfers to random U by replacing u^γ with $\mathbb{E}[U^\gamma]$.

Lemma G.1 (Hamiltonian bias). *Fix $\alpha \geq 0$ and a bounded test function V . Let U be a random variable taking values in $(0, 1]$, independent of the state and control. Assume that for some $\gamma > 0$ and constant $C_H < \infty$,*

$$\|H_u^{(\alpha)}(V) - H^{(\alpha)}(V)\|_\infty \leq C_H u^\gamma, \quad \forall u \in (0, 1]. \quad (134)$$

Define the random Hamiltonian $H_U^{(\alpha)}(V)$ by evaluation at $u = U$, and its averaged version $\bar{H}_U^{(\alpha)}(V) := \mathbb{E}[H_U^{(\alpha)}(V)]$ (expectation over U only). Then,

$$\|\bar{H}_U^{(\alpha)}(V) - H^{(\alpha)}(V)\|_\infty \leq C_H \mathbb{E}[U^\gamma]. \quad (135)$$

The same statement holds if $H_u^{(\alpha)}$ is replaced by the Richardson Hamiltonian $\tilde{H}_u^{(\alpha)}$.

Proof. By Jensen and the deterministic bound (134),

$$\|\bar{H}_U^{(\alpha)}(V) - H^{(\alpha)}(V)\|_\infty = \left\| \mathbb{E}[H_U^{(\alpha)}(V) - H^{(\alpha)}(V)] \right\|_\infty \leq \mathbb{E}[\|H_U^{(\alpha)}(V) - H^{(\alpha)}(V)\|_\infty] \leq C_H \mathbb{E}[U^\gamma].$$

The Richardson case is identical. □

Theorem G.2 (Picard iteration with random time step). *Fix $\alpha \geq 0$ and $\tau > 0$. Let $\Phi_\tau^{(\alpha)}$ be the dynamic-programming semigroup from (55). Consider the averaged Picard operator*

$$(\tilde{T}_\tau^{(\alpha)} V)(x) := V(x) + \tau \bar{H}_U^{(\alpha)}(V)(x) = V(x) + \tau \mathbb{E}[H_U^{(\alpha)}(V)(x)], \quad (136)$$

and the iterates $\tilde{V}_{k+1} := \tilde{T}_\tau^{(\alpha)}(\tilde{V}_k)$.

Assume further that the local expansion error satisfies, for all $V \in \mathcal{D}$,

$$\|\Phi_\tau^{(\alpha)}(V) - (V + \tau H^{(\alpha)}(V))\|_\infty \leq C_{\text{DP}} \tau^p, \quad (137)$$

for some $p > 1$ and constant $C_{\text{DP}} < \infty$.

In addition if the deterministic Hamiltonian bias bound (134) holds for some $\gamma > 0$, then for all $k \geq 0$,

$$\|\tilde{V}_k - V^{(\alpha)}\|_\infty \leq e^{-\rho\tau k} \|\tilde{V}_0 - V^{(\alpha)}\|_\infty + \frac{C_{\text{DP}} \tau^p + \tau C_H \mathbb{E}[U^\gamma]}{1 - e^{-\rho\tau}}. \quad (138)$$

Proof. For any V ,

$$\|\tilde{T}_\tau^{(\alpha)}(V) - (V + \tau H^{(\alpha)}(V))\|_\infty = \tau \|\bar{H}_U^{(\alpha)}(V) - H^{(\alpha)}(V)\|_\infty \leq \tau C_H \mathbb{E}[U^\gamma]$$

by Lemma G.1. Combining with the local semigroup mismatch (137) gives

$$\|\tilde{T}_\tau^{(\alpha)}(V) - \Phi_\tau^{(\alpha)}(V)\|_\infty \leq C_{\text{DP}} \tau^p + \tau C_H \mathbb{E}[U^\gamma].$$

Again, using contraction of $\Phi_\tau^{(\alpha)}$ and the fixed-point identity $\Phi_\tau^{(\alpha)}(V^{(\alpha)}) = V^{(\alpha)}$ yields the recursion

$$\|\tilde{V}_{k+1} - V^{(\alpha)}\|_\infty \leq e^{-\rho\tau} \|\tilde{V}_k - V^{(\alpha)}\|_\infty + C_{\text{DP}} \tau^p + \tau C_H \mathbb{E}[U^\gamma],$$

and a similar inductive argument proves (138). \square

Corollary G.3. *Based on the error estimates from Section E, we can naturally extends to random time settings under the following 3 scenarios:*

(1) **Finite-horizon Picard-Hamiltonian iterations with q_V^u under standard assumption.** If $\|H_u^{(\alpha)}(V) - H^{(\alpha)}(V)\|_\infty \leq Cu^{1/2}$ and $\|\Phi_\tau^{(\alpha)}(V) - (V + \tau H^{(\alpha)}(V))\|_\infty \leq C\tau^{3/2}$, then (138) holds with $(p, \gamma) = (3/2, 1/2)$ and the random bias term becomes $\tau \mathbb{E}[U^{1/2}]$.

(2) **Finite-horizon Picard-Hamiltonian iterations with q_V^u under smoother assumption.** If $\|H_u^{(\alpha)}(V) - H^{(\alpha)}(V)\|_\infty \leq Cu$ and the semigroup mismatch is $\mathcal{O}(\tau^2)$, then $(p, \gamma) = (2, 1)$ and the random bias term becomes $\tau \mathbb{E}[U]$.

(3) **Richardson Picard-Hamiltonian iterations.** If $\|\tilde{H}_u^{(\alpha)}(V) - H^{(\alpha)}(V)\|_\infty \leq Cu^2$ and the semigroup mismatch is $\mathcal{O}(\tau^2)$, then $(p, \gamma) = (2, 2)$ and the random bias term becomes $\tau \mathbb{E}[U^2]$.

G.1. q -convergence

The Hamiltonian transfer in Lemma G.1 is immediate because the bias bound depends only on positive moments $\mathbb{E}[U^\gamma]$. For the advantage-rate q_V^u , an additional stability condition is needed because the finite-horizon definition contains a division by u , making the map $V \mapsto q_V^u$ Lipschitz with constant of order $1/u$.

Lemma G.4 (Random-time Lipschitz stability of q_V^U). *Fix $\beta > 0$ and for $u \in (0, 1]$. Let U be a random variable taking values in $(0, 1]$, independent of the state and control. Then for any bounded V, W ,*

$$\mathbb{E} [\|q_V^U - q_W^U\|_\infty] \leq 2 \mathbb{E} \left[\frac{1}{U} \right] \|V - W\|_\infty, \quad (139)$$

and

$$\mathbb{E} [\|\tilde{q}_V^U - \tilde{q}_W^U\|_\infty] \leq 10 \mathbb{E} \left[\frac{1}{U} \right] \|V - W\|_\infty. \quad (140)$$

In particular, if $U \geq u_{\min} > 0$ almost surely, then the above bounds hold with $\mathbb{E}[1/U] \leq 1/u_{\min}$.

Proof. Fix $u \in (0, 1]$. Using definitions of q^u and cancelling $r(x, a)$, we have:

$$|q_V^u(x, a) - q_W^u(x, a)| \leq \frac{1}{u} \left(e^{-\beta u} |\mathbb{E}_x^a[V(X_u^a) - W(X_u^a)]| + |V(x) - W(x)| \right) \leq \frac{2}{u} \|V - W\|_\infty.$$

Taking the supremum over (x, a) yields $\|q_V^u - q_W^u\|_\infty \leq \frac{2}{u} \|V - W\|_\infty$. Evaluating at $u = U$ and taking expectation gives (139). For Richardson, apply the same bound to u and $u/2$:

$$\|\tilde{q}_V^u - \tilde{q}_W^u\|_\infty \leq 2 \|q_V^{u/2} - q_W^{u/2}\|_\infty + \|q_V^u - q_W^u\|_\infty \leq \left(2 \cdot \frac{4}{u} + \frac{2}{u} \right) \|V - W\|_\infty = \frac{10}{u} \|V - W\|_\infty,$$

and again evaluate at $u = U$ and take expectation to obtain (140). \square

Theorem G.5 (Random holding times: averaged q -convergence). *Let $V^* := V^{(\alpha)}$ be the optimal value function. Assume the random-time averaged Picard iteration $(\tilde{V}_k)_{k \geq 0}$ satisfy the value error bound*

$$\|\tilde{V}_k - V^*\|_\infty \leq e^{-\rho\tau k} \|\tilde{V}_0 - V^*\|_\infty + \frac{C_{\text{DP}} \tau^p + \tau C_H \mathbb{E}[U^\gamma]}{1 - e^{-\rho\tau}}. \quad (141)$$

If $\mathbb{E}[1/U] < \infty$, then the corresponding random-time rates obey

$$\mathbb{E} [\|q_{\tilde{V}_k}^U - q(V^*)\|_\infty] \leq 2 \mathbb{E} \left[\frac{1}{U} \right] \|\tilde{V}_k - V^*\|_\infty + C_q \mathbb{E}[U^\gamma], \quad (142)$$

and, if Richardson is used,

$$\mathbb{E} [\|\tilde{q}_{\tilde{V}_k}^U - q(V^*)\|_\infty] \leq 10 \mathbb{E} \left[\frac{1}{U} \right] \|\tilde{V}_k - V^*\|_\infty + C'_q \mathbb{E}[U^2]. \quad (143)$$

Proof. Decompose and apply triangle inequality:

$$\mathbb{E} [\|q_{V_k}^U - q(V^*)\|_\infty] \leq \mathbb{E} [\|q_{V_k}^U - q_{V^*}^U\|_\infty] + \mathbb{E} [\|q_{V^*}^U - q(V^*)\|_\infty].$$

The first term is controlled by Lemma G.4. The second term is the modelling bias, which follows from the deterministic bias bound $\|q_{V^*}^u - q(V^*)\|_\infty \leq C_q u^\gamma$ and averaging over U : $\mathbb{E} [\|q_{V^*}^U - q(V^*)\|_\infty] \leq C_q \mathbb{E}[U^\gamma]$. The Richardson case is identical, using the Richardson modelling bias $\|\tilde{q}_{V^*}^u - q(V^*)\|_\infty \leq C'_q u^2$ and the Lipschitz bound (140). \square

Note. If $U \in [u_{\min}, 1]$ almost surely, then $\mathbb{E}[1/U] \leq 1/u_{\min}$ and the q -bounds (142)–(143) hold with explicit constants. This matches the typical irregular-timestep setting where the environment enforces a minimum timestep.

H. Regret bound and sample complexity

This section provides a more refined statistical analysis of the practical single-critic learning algorithm in Algorithm 1. Recall that Q_k denotes the analytic iteration results without statistical error, and the \hat{Q}_k is the function produced by sample-based estimates (with statistical error). The goal is to control the cumulative gap $\sum_{k=0}^{L-1} \|\hat{Q}_k - Q^{(\alpha)}\|_\infty$. The main technique that allows a more refined error analysis is a geometric argument that upgrades $L^2(\nu)$ control to uniform $\|\cdot\|_\infty$ control for Lipschitz functions on a compact domain.

At iteration k , recall the update operator $\mathcal{F}_{\tau,u}$ Equation (125) that defines the regression target on \mathcal{Z} :

$$\begin{aligned} (\mathcal{F}_{\tau,u}(Q))(x, a) := & (1 - \tau)Q(x, a) + \tau r(x, a) + \tau \mathbb{E}_{a \sim \pi(\cdot|x)}[\tilde{Q}(x, a)] \\ & + \tau \frac{\gamma \mathbb{E}_{a' \sim \pi(\cdot|x')}[\tilde{Q}(x', a')] - \mathbb{E}_{a \sim \pi(\cdot|x)}[\tilde{Q}(x, a)]}{u} \end{aligned}$$

Recall the statistical error $\text{stat}_k := \|\hat{Q}_{k+1} - \mathcal{F}_{\tau,u}(\hat{Q}_k)\|_{L^2(\nu)}$. Also recall that thanks to Lemmas F.4 to F.6, we have:

$$\text{stat}_k \lesssim \frac{1}{\sqrt{n_k}} \left(1 + \sqrt{\log d} + \sqrt{\log(1/\delta)} \right) \quad \text{with probability } \geq 1 - \delta, \quad (144)$$

Setup and assumptions Let $\mathcal{X} \subset \mathbb{R}^d$ ($d = d_{\mathcal{X}}$) be the state space and $\mathcal{A} \subset \mathbb{R}^{d_{\mathcal{A}}}$ the action space. Define the state–action domain with dimension m :

$$\mathcal{Z} := \mathcal{X} \times \mathcal{A}, \quad m := d_{\mathcal{X}} + d_{\mathcal{A}}.$$

We write $z = (x, a) \in \mathcal{Z}$, equip \mathcal{Z} with the Euclidean metric $d(z, z') := \|z - z'\|_2$, and denote the sup norm on \mathcal{Z} by $\|f\|_\infty = \sup_{z \in \mathcal{Z}} |f(z)|$. Throughout, we fix an algorithmic step size $\tau > 0$ and a holding time $u > 0$, with $\gamma := e^{-\beta u}$.

Assumption H.1 (Compact domain and boundedness). We have the following assumptions. First, we assume state-action space $\mathcal{Z} = \mathcal{X} \times \mathcal{A}$ is compact and has diameter $\text{diam}(\mathcal{Z}) \leq R$ for some $R > 0$. Additionally, assume the rewards are bounded: $|r(x, a)| \leq r_{\max}$.

Assumption H.2 (Coverage density lower bound). At each critic regression step k , training samples $Z_i = (X_i, A_i)$ are drawn i.i.d. from a distribution ν_k supported on \mathcal{Z} whose density is bounded below by $\nu_{\min} > 0$ with respect to Lebesgue measure on \mathbb{R}^m . Equivalently, for any measurable $E \subseteq \mathcal{Z}$,

$$\nu_k(E) \geq \nu_{\min} \text{Vol}(E).$$

Assumption H.3 (Lipschitz critic). All critics considered are uniformly bounded and Lipschitz on \mathcal{Z} : there exist constants $B_Q, L_Q > 0$ such that for every iterate Q (population or learned),

$$\|Q\|_\infty \leq B_Q, \quad |Q(z) - Q(z')| \leq L_Q \|z - z'\|_2, \quad \forall z, z' \in \mathcal{Z}.$$

Moreover, for each fixed Q , the population mapping $\mathcal{F}_{\tau,u}(Q)$ is also Lipschitz with

$$\|\mathcal{F}_{\tau,u}(Q)\|_\infty \leq B_F, \quad \text{Lip}(\mathcal{F}_{\tau,u}(Q)) \leq L_F,$$

for constants B_F, L_F that do not depend on k . (The same holds for the Richardson mapping $\mathcal{F}_{\tau,u}^{\text{Rich}}$.)

This Assumption H.3 holds true by a similar argument to the proof of Lemma F.9

H.1. A norm-transfer argument from L^2 to $\|\cdot\|_\infty$

We start with a few lemmas from a standard norm-transfer argument.

Lemma H.4 (Uniform lower bound on ball mass). *Under Assumption H.2, for any $z \in \mathcal{Z}$ and any $r > 0$ with $B_r(z) \subseteq \mathcal{Z}$,*

$$\nu(B_r(z)) \geq \nu_{\min} \text{Vol}(B_r(z)) = \nu_{\min} c_m r^m, \quad (145)$$

where $c_m := \text{Vol}(B_1(0))$ is the volume of the unit ball in \mathbb{R}^m .

Lemma H.5 ($L^2(\nu)$ to sup-norm). *Let $g : \mathcal{Z} \rightarrow \mathbb{R}$ be L_g -Lipschitz and suppose $\|g\|_{L^2(\nu)} \leq \varepsilon$. Under Assumption H.2, one has*

$$\|g\|_\infty \leq \left(\frac{2^{m+2} L_g^m}{\nu_{\min} c_m} \right)^{\frac{1}{m+2}} \varepsilon^{\frac{2}{m+2}}. \quad (146)$$

Proof. Let $z^* \in \arg \max_{z \in \mathcal{Z}} |g(z)|$ and set $M := \|g\|_\infty = |g(z^*)|$. Choose $r := M/(2L_g)$. By Lipschitzness, for any $z \in B_r(z^*)$,

$$|g(z)| \geq |g(z^*)| - L_g \|z - z^*\|_2 \geq M - L_g r = M/2.$$

Therefore,

$$\varepsilon^2 \geq \int_{\mathcal{Z}} g(z)^2 \nu(dz) \geq \int_{B_r(z^*)} g(z)^2 \nu(dz) \geq (M/2)^2 \nu(B_r(z^*)).$$

By Lemma H.4, $\nu(B_r(z^*)) \geq \nu_{\min} c_m r^m = \nu_{\min} c_m (M/(2L_g))^m$. Substituting gives

$$\varepsilon^2 \geq \frac{M^2}{4} \nu_{\min} c_m \left(\frac{M}{2L_g} \right)^m = \frac{\nu_{\min} c_m}{2^{m+2} L_g^m} M^{m+2}.$$

Rearranging yields Equation (146). \square

Aggregate bounds. Now we summarize the inequality ingredients for the main bound. Because of Lemma H.5, there exists a universal constant C_∞ so that, with probability of at least $1 - \delta$:

$$\|\hat{Q}_{k+1} - \mathcal{F}_{\tau,u}(\hat{Q}_k)\|_\infty \leq C_\infty \text{stat}_k^{\frac{2}{m+2}} \leq C_\infty \left(\frac{1 + \sqrt{\log d} + \sqrt{\log(1/\delta)}}{\sqrt{n_k}} \right)^{\frac{2}{m+2}} \quad (147)$$

Additionally, recall that $Q^{(\alpha)}$ is the optimal soft critic $Q^{(\alpha)}(x, a) = V^{(\alpha)}(x) + q_{V^{(\alpha)}}(x, a)$. By Theorem 4.2, there exist $\rho > 0$ and $C > 0$ such that:

$$\|Q_k - Q^{(\alpha)}\|_\infty \leq \frac{e^{-\rho\tau k}}{u} \|Q_0 - Q^{(\alpha)}\|_\infty + C(\tau/u + u), \quad (148)$$

H.2. Main bound

Define the one-step sup-norm statistical deviation

$$\zeta_k := \|\hat{Q}_{k+1} - \mathcal{F}_{\tau,u}(\hat{Q}_k)\|_\infty, \quad (149)$$

Lemma H.6 (Cumulative sup-norm bound). *Suppose the update operator $\mathcal{F}_{\tau,u}$ is $(1 - \alpha)$ -Lipschitz for $\alpha < 1$ where α depends on τ and u . Under Assumption H.1 and H.2 (Assumption H.3 is satisfied), for any $L \geq 1$,*

$$\sum_{k=0}^{L-1} \|\hat{Q}_k - Q^{(\alpha)}\|_\infty \leq \frac{1}{(1 - e^{-\rho\tau})u} \|\hat{Q}_0 - Q^{(\alpha)}\|_\infty + CL(\tau/u + u) + \frac{1}{\alpha} \left(\sum_{k=0}^{L-1} \zeta_k \right) \quad (150)$$

Proof. The bias (algorithmic) error $\|Q_k - Q^{(\alpha)}\|_\infty$ makes up the first 2 terms in Equation (150). This is clear from Equation (148). Now we bound the statistical error with $E_k := \|\hat{Q}_k - Q_k\|_\infty$. We have:

$$\begin{aligned} E_{k+1} &= \|\hat{Q}_{k+1} - \mathcal{F}_{\tau,u}(\hat{Q}_k)\|_\infty \leq \|\hat{Q}_{k+1} - \mathcal{F}_{\tau,u}(\hat{Q}_k)\|_\infty + \|\mathcal{F}_{\tau,u}(\hat{Q}_k) - \mathcal{F}_{\tau,u}(Q_k)\|_\infty \\ &\leq \zeta_k + (1 - \alpha) \|\hat{Q}_k - Q_k\|_\infty = \zeta_k + (1 - \alpha) E_k \end{aligned}$$

Hence, through an inductive argument, the running gap $\sum_{k=0}^{L-1} E_k$ is bounded by $\sum_k \zeta_k (1 + (1 - \alpha) + \dots + (1 - \alpha)^{L-1})$, leading to the third term of Equation (150). \square

Note that the terms in the update operators (see Equation (125)) can be rearranged so that it consists of 3 components with Lipschitz coefficients $(1 - \tau)$, $\frac{\gamma\tau}{u}$ and $(\tau - \frac{\tau}{u})$. In case if $u \geq 1$, this yields a $(1 - \alpha)$ Lipschitz operator with $\alpha = (1 - \gamma) \frac{\tau}{u}$

Theorem H.7 (Sample complexity and regret bounds). *Given the probability confidence level $\delta \in (0, 1)$ and maximum number of iteration L_{\max} . Suppose the update operator is $(1 - \alpha)$ -Lipschitz with $\alpha \geq C_0 \frac{\tau}{u}$. Then there exists (q-function discretization) timestep u ,*

the Hamiltonian flow discretization step τ , a sequence of numbers of samples $\{n_k\}$, and an universal constants C_1 and C_2 (independent of L , L_{\max} , τ or u), such that for every iteration $L_{\max}/2 \leq L \leq L_{\max}$, with probability at least $1 - \delta$, the running gap satisfies:

$$\sum_{k=0}^{L-1} \|\hat{Q}_k - Q^{(\alpha)}\|_{\infty} \leq C_1 L^{3/4} \quad (151)$$

Additionally, in both cases, the total sample size in the first L iteration satisfies

$$K = K(L) := \sum_{k=0}^{L-1} n_k = C_2 L^{m+3}. \quad (152)$$

Consequently, for any given fixed L , ignore the log-terms, we get $\text{Regret}(K) = \mathcal{O}(K^{\frac{4m+11}{4m+12}})$ (sub-linear regret rate).

Proof. Choose $\tau = L_{\max}^{-1/2}$, $u = L_{\max}^{-1/4}$. Choose the number of samples $n_k = (k+1)^{m+2}$ for all $k \geq 0$.

Now we choose per-iteration confidence $\delta_k := \delta/L$ for $k \in \overline{0, L-1}$. Through the statistical bound derived above, with probability $\geq 1 - \delta$ (via union bound over k using $\delta_k = \delta/L$), we have for all $k \in \overline{0, L-1}$:

$$\zeta_k \leq \left(\text{stat}_k \right)^{\frac{2}{m+2}} \leq C_{\infty} \left(\frac{1 + \sqrt{\log d} + \sqrt{\log(L/\delta)}}{\sqrt{n_k}} \right)^{\frac{2}{m+2}}.$$

Now we analyze each error term within the large bracket of Equation (150). First, with $n_k = (k+1)^{m+2}$, the right-hand side for the inequality of ζ_k can be upper-bounded by $C_3 (\log(L/\delta)^{\frac{1}{m+2}} / (k+1))$. Hence $\sum_{k=0}^{L-1} \zeta_k \leq C_4 (\log(L/\delta)^{\frac{1}{m+2}} \times \log L)$, and the statistical part is then only multiply by $1/\alpha = u/\tau = C_5 L^{1/4}$.

Second, due to the choice of τ and u , the bias part Equation (150) from can be bounded by $C_6 \frac{1}{\tau u} + CL(\tau/u + u) = C_7 L^{3/4}$, which dominates the statistical part and yields the overall error rate in Equation (151). The sample complexity follows from $\sum_{k=1}^L k^{m+2} \leq C_1 L^{m+3}$ for some universal constant C_1 .

Finally, regarding the regret bound, which can be defined by sum of gaps $Q^{(\alpha)}(Z) - \hat{Q}_k(Z)$ over starting points Z of all episodes. Thus, up to iteration L (for any $L \leq L_{\max}$), the regret can be over-estimated by:

$$\begin{aligned} \text{Regret} &\leq \sum_{\text{all samples } Z} \mathbb{E} \|\hat{Q}_k(Z) - Q^{(\alpha)}(Z)\| \leq \sum_{k=0}^{L-1} n_k \|\hat{Q}_k - Q^{(\alpha)}\|_{\infty} \\ &\leq \left(\max_{k \in \overline{0, L-1}} n_k \right) \sum_{k=0}^{L-1} \|\hat{Q}_k - Q^{(\alpha)}\|_{\infty} \leq C_1 L^{m+2} L^{3/4} = \mathcal{O}(L^{m+11/4}) \end{aligned}$$

As $K = \mathcal{O}(L^{m+3})$, $\mathcal{O}(L^{m+11/4}) = \mathcal{O}(K^{\frac{m+11/4}{m+3}}) = \mathcal{O}(K^{\frac{4m+11}{4m+12}})$, yielding the desired regret bound. Here all C_i 's are universal constants independent of L , L_{\max} , τ or u . \square

Notes. For random time step $U \in (0, 1]$, independent of (x, a) , the only change is the bias term, which becomes a moment of U : $\mathbb{E}[\text{bias}(U)]$. In particular: $\text{bias}(U) = \mathbb{E}[U^{1/2}]$ for standard case, and $\text{bias}(U) = \mathbb{E}[U^2]$ for Richardson-version. Additionally, an improved variant with sharper regret and complexity guarantees will be studied in subsequent work. The proof techniques developed here extend naturally to adaptive step sizes $(\tau_k)_{k \geq 0}$; we also plan to derive explicit rates for such schedules in the future.

I. Further Theoretical Details For Main Paper

I.1. Further explanations for the main paper

Variational representation for Hamiltonian. For the Hamiltonian function, by a standard variational argument (see Lemma C.6), one can equivalently write:

$$H^{(\alpha)}(V)(x) = \sup_{\pi(\cdot|x)} \int_{\mathcal{A}} \left(r(x, a) + (L^a V)(x) - \beta V(x) - \alpha \log \pi(a|x) \right) \pi(da|x) \quad (153)$$

As $\alpha \rightarrow 0$, $H^{(\alpha)}$ recovers $H^{(0)}$ and, for $\alpha > 0$, the policy π that maximize the above variational form is exactly the Boltzmann policy

$$\pi_V^{(\alpha)}(a | x) \propto \exp\left(\frac{1}{\alpha}(r(x, a) + (L^a V)(x) - \beta V(x))\right) \quad (154)$$

Distinction between u and τ . We emphasize that our framework separates two distinct discretizations: (i) the environment produces transitions with potentially irregular durations u , and (ii) the algorithm updates V using a flow step size τ , which controls value-iteration stability and convergence and is not tied to u . This separation is one reason the method remains stable under small or irregular time steps. Additionally, in this work, we make two concrete modeling choices for simplicity and scalability. First, we discretize the value flow Equation (26) using a single forward-Euler (Picard) step. More accurate ODE solvers (e.g., higher-order Runge–Kutta schemes) could be substituted to improve numerical stability. Second, we implement the decoupled iteration with a single critic by using the algebraic representation $Q = V + 1 \cdot q$ in Equation (32). This choice is viewed as selecting a nominal unit time scale for combining a value-like term and an instantaneous rate term. More generally, one may consider $Q = V + c q$ for other scalings $c > 0$, which may trade off learning signal, conditioning, and empirical performance. Exploring such optimal discretization and scaling strategies is the scope for future work.

I.2. Discrete MDP with noise converge to SDE

Here we explain and rigorously prove the statement we mentioned in Section 2.1 regarding the convergence of discrete-MDP to stochastic differential equation (SDE) when the time step converges to 0.

Lemma I.1 (Convergence of MDP to SDE). *Fix $T > 0$ and let the time step $\Delta_n \rightarrow 0$. Define grid times $t_k = k\Delta_n$ and $\bar{t} := t_k$ be the left endpoint mapping for $t \in [t_k, t_{k+1})$. Assume $f(\cdot, u)$ and $\sigma(\cdot, u)$ are globally Lipschitz and of linear growth in x , and let X_t solve the SDE:*

$$dX_t = f(X_t, U_t) dt + \sigma(X_t, U_t) dW_t, \quad X_0 = x.$$

Define (discretized) MDP process $X_k^{(n)}$ with discretized time step Δ_n :

$$X_{k+1}^{(n)} = X_k^{(n)} + f(X_k^{(n)}, U_{t_k})\Delta_n + \sigma(X_k^{(n)}, U_{t_k})(W_{t_{k+1}} - W_{t_k}), \quad X_0^{(n)} = x,$$

and let $X_t^{(n)} := X_k^{(n)}$ for $t \in [t_k, t_{k+1})$ (piecewise-constant interpolation), and similarly $U_{\bar{t}} := U_{t_k}$. Then there exists a constant $C = C(T, L, K, x)$ such that

$$\mathbb{E}\left[\sup_{0 \leq t \leq T} \|X_t^{(n)} - X_t\|^2\right] \leq C \Delta_n.$$

In particular, $\sup_{t \leq T} \|X_t^{(n)} - X_t\| \rightarrow 0$ in L^2 (and hence in probability).

Proof. First by the proof of Lemma C.5, $\mathbb{E}\|X_t - X_s\|^2 \leq C|t - s|$. Therefore, for any $u \in [0, T]$ with \bar{u} its left gridpoint, $|u - \bar{u}| \leq \Delta_n$ and $\mathbb{E}\|X_u - X_{\bar{u}}\|^2 \leq C \Delta_n$. Now, the piecewise-constant Euler process can be written as

$$X_t^{(n)} = x + \int_0^t f(X_{\bar{s}}^{(n)}, U_{\bar{s}}) ds + \int_0^t \sigma(X_{\bar{s}}^{(n)}, U_{\bar{s}}) dW_s.$$

Subtracting the SDE gives the error process $e_t := X_t^{(n)} - X_t$:

$$e_t = \int_0^t [f(X_s^{(n)}, U_{\bar{s}}) - f(X_s, U_s)] ds + \int_0^t [\sigma(X_s^{(n)}, U_{\bar{s}}) - \sigma(X_s, U_s)] dW_s.$$

Let $E_t := \sup_{0 \leq r \leq t} \|e_r\|$.

Drift term. With $g_s = f(X_s^{(n)}, U_{\bar{s}}) - f(X_s, U_s)$, using Lipschitzness, we get:

$$\|g_s\| \leq L\|X_s^{(n)} - X_s\| \leq L(\|X_s^{(n)} - X_{\bar{s}}\| + \|X_{\bar{s}} - X_s\|) \leq L(E_s + \|X_{\bar{s}} - X_s\|).$$

As a result,

$$\mathbb{E}\left[\sup_{0 \leq r \leq t} \left\| \int_0^r g_s ds \right\|^2\right] \leq C \int_0^t \mathbb{E}[E_s^2] ds + C \int_0^t \mathbb{E}\|X_s - X_{\bar{s}}\|^2 ds. \quad (155)$$

Diffusion term. By the Burkholder–Davis–Gundy inequality (for $p = 2$),

$$\mathbb{E}\left[\sup_{0 \leq r \leq t} \left\| \int_0^r h_s dW_s \right\|^2\right] \leq C_{\text{BDG}} \mathbb{E} \int_0^t \|h_s\|_F^2 ds.$$

With $h_s = \sigma(X_{\bar{s}}^{(n)}, U_{\bar{s}}) - \sigma(X_s, U_s)$ and Lipschitzness,

$$\|h_s\|_F \leq L \|X_{\bar{s}}^{(n)} - X_s\| \leq L(E_s + \|X_{\bar{s}} - X_s\|),$$

so that

$$\mathbb{E} \left[\sup_{0 \leq r \leq t} \left\| \int_0^r h_s dW_s \right\|^2 \right] \leq C \int_0^t \mathbb{E}[E_s^2] ds + C \int_0^t \mathbb{E}\|X_s - X_{\bar{s}}\|^2 ds. \quad (156)$$

Now combining (155)–(156) together with triangle inequality,

$$\mathbb{E}[E_t^2] \leq C \int_0^t \mathbb{E}[E_s^2] ds + C \int_0^t \mathbb{E}\|X_s - X_{\bar{s}}\|^2 ds.$$

As proved earlier, $\mathbb{E}\|X_s - X_{\bar{s}}\|^2 \leq C\Delta_n$ for all $s \leq T$, so that

$$\mathbb{E}[E_t^2] \leq C \int_0^t \mathbb{E}[E_s^2] ds + C t \Delta_n.$$

Finally, Gronwall's lemma gives $\mathbb{E}[E_T^2] \leq C\Delta_n$, proving the claim with the error go to 0 as $\Delta_n \rightarrow 0$. \square

Note that instead of $(W_{t_{k+1}} - W_{t_k})$, we can replace it by i.i.d normal random variable ξ_{t_k} , and all the inequalities derived in the proof still holds in expectation as they has the same distribution due to the property of the Brownian motion.

I.3. Exact Richardson single-critic update equation.

Lemma I.2 (Algebraic derivation of the Richardson single-critic update). *Fix $u > 0$ and define $\gamma := e^{-\beta u}$ and $\gamma_{1/2} := e^{-\beta u/2}$. Let V_k be updated by the entropy-regularized expectation step*

$$V_{k+1}(x) = (1 - \tau)V_k(x) + \tau S_k(x), \quad S_k(x) := \mathbb{E}_{a \sim \pi_k(\cdot|x)} [\tilde{Q}_k^R(x, a)], \quad (157)$$

where $Q_k^R(x, a) := V_k(x) + \tilde{q}_V^u(x, a)$ and $\tilde{Q}_k^R(x, a) := Q_k^R(x, a) - \alpha \log \pi_k(a|x)$. Then the induced single-critic iteration satisfies the closed-form update:

$$\begin{aligned} Q_{k+1}^R(x, a) &= (1 - \tau)Q_k^R(x, a) + \tau r(x, a) + \tau S_k(x) \\ &+ \frac{\tau}{u} \left(4\gamma_{1/2} \mathbb{E}_x^a [S_k(X_{u/2})] - \gamma \mathbb{E}_x^a [S_k(X_u)] - 3S_k(x) \right). \end{aligned} \quad (158)$$

Proof. We start with definition of $q_V^{u/2}$:

$$q_V^{u/2}(x, a) = \frac{\gamma_{1/2} \mathbb{E}_x^a [V(X_{u/2})] - V(x)}{u/2} + r(x, a) = \frac{2(\gamma_{1/2} \mathbb{E}_x^a [V(X_{u/2})] - V(x))}{u} + r(x, a).$$

Hence

$$\begin{aligned} \tilde{q}_V^u(x, a) &= 2q_V^{u/2}(x, a) - q_V^u(x, a) \\ &= \frac{4\gamma_{1/2} \mathbb{E}_x^a [V(X_{u/2})] - \gamma \mathbb{E}_x^a [V(X_u)] - 3V(x)}{u} + r(x, a). \end{aligned} \quad (159)$$

Now apply Equation (159) to V_{k+1} :

$$\tilde{q}_{V_{k+1}}^u(x, a) = \frac{4\gamma_{1/2} \mathbb{E}_x^a [V_{k+1}(X_{u/2})] - \gamma \mathbb{E}_x^a [V_{k+1}(X_u)] - 3V_{k+1}(x)}{u} + r(x, a). \quad (160)$$

Substitute the value update Equation (157) inside each term. Since the update is pointwise in the state, for any random state Y we have $V_{k+1}(Y) = (1 - \tau)V_k(Y) + \tau S_k(Y)$, and therefore

$$\mathbb{E}_x^a [V_{k+1}(X_h)] = (1 - \tau) \mathbb{E}_x^a [V_k(X_h)] + \tau \mathbb{E}_x^a [S_k(X_h)], \quad h \in \{u/2, u\}.$$

Also $V_{k+1}(x) = (1 - \tau)V_k(x) + \tau S_k(x)$. Plugging these into Equation (160) and collecting the corresponding terms gives:

$$\begin{aligned} \tilde{q}_{V_{k+1}}^u(x, a) &= (1 - \tau) \frac{4\gamma_{1/2} \mathbb{E}_x^a [V_k(X_{u/2})] - \gamma \mathbb{E}_x^a [V_k(X_u)] - 3V_k(x)}{u} \\ &+ \tau \frac{4\gamma_{1/2} \mathbb{E}_x^a [S_k(X_{u/2})] - \gamma \mathbb{E}_x^a [S_k(X_u)] - 3S_k(x)}{u} + r(x, a). \end{aligned} \quad (161)$$

The first fraction is exactly $\tilde{q}_{V_k}^u(x, a) - r(x, a)$ by Equation (159). Thus

$$\begin{aligned}\tilde{q}_{V_{k+1}}^u(x, a) &= (1 - \tau)(\tilde{q}_{V_k}^u(x, a) - r(x, a)) + r(x, a) \\ &\quad + \frac{\tau}{u} \left(4\gamma_{1/2} \mathbb{E}_x^a[S_k(X_{u/2})] - \gamma \mathbb{E}_x^a[S_k(X_u)] - 3S_k(x) \right) \\ &= (1 - \tau)\tilde{q}_{V_k}^u(x, a) + \tau r(x, a) + \frac{\tau}{u} \left(4\gamma_{1/2} \mathbb{E}_x^a[S_k(X_{u/2})] - \gamma \mathbb{E}_x^a[S_k(X_u)] - 3S_k(x) \right).\end{aligned}\quad (162)$$

Finally, add the value update $V_{k+1}(x) = (1 - \tau)V_k(x) + \tau S_k(x)$ to both sides, we get

$$\begin{aligned}Q_{k+1}^R(x, a) &= (1 - \tau)V_k(x) + \tau S_k(x) + (1 - \tau)\tilde{q}_{V_k}^u(x, a) + \tau r(x, a) + \frac{\tau}{u} \left(\dots \right) \\ &= (1 - \tau)(V_k(x) + \tilde{q}_{V_k}^u(x, a)) + \tau r(x, a) + \tau S_k(x) + \frac{\tau}{u} \left(\dots \right) \\ &= (1 - \tau)Q_k^R(x, a) + \tau r(x, a) + \tau S_k(x) + \frac{\tau}{u} \left(4\gamma_{1/2} \mathbb{E}_x^a[S_k(X_{u/2})] - \gamma \mathbb{E}_x^a[S_k(X_u)] - 3S_k(x) \right),\end{aligned}$$

which is exactly Equation (158). \square

I.4. Decoupled continuous-time policy evaluation

For a fixed policy π , standard stochastic control arguments imply that the value function $V^{(\alpha)}(\cdot; \pi)$ in (51) satisfies the linear elliptic PDE:

$$\beta V^{(\alpha)}(x; \pi) - (L^\pi V^{(\alpha)}(\cdot; \pi))(x) - \tilde{r}^{(\alpha)}(x, \pi) = 0 \quad (163)$$

Fix a Markov policy $\pi(a | x)$ and temperature $\alpha \geq 0$. For a value function $V \in \mathcal{D} \subset C_b^2(\mathbb{R}^d)$, define the *instantaneous q-rate* for (π, α) as

$$q_V^{(\pi, \alpha)}(x, a) := r(x, a) - \alpha \log \pi(a | x) + (L^a V)(x) - \beta V(x). \quad (164)$$

This corresponds to the infinitesimal temporal-difference

$$q_V^{(\pi, \alpha)}(x, a) = \lim_{\Delta t \rightarrow 0} \frac{e^{-\beta \Delta t} \mathbb{E}[V(X_{\Delta t})] - V(x)}{\Delta t} + r(x, a) - \alpha \log \pi(a | x) \quad (165)$$

This policy-dependent *q*-function $q_V^{(\pi, \alpha)}$ can be estimated from short rollouts by:

$$q_V^{u, (\pi, \alpha)}(x, a) := \frac{e^{-\beta u} V(X_{t+u}) - V(x)}{u} + r(x, a) - \alpha \log \pi(a | x) \quad (166)$$

Given $q_V^{(\pi, \alpha)}$, the policy-evaluation PDE satisfies

$$(L^\pi V)(x) + \tilde{r}^{(\alpha)}(x, \pi) - \beta V(x) = 0$$

And can be equivalently written as:

$$\int_{\mathcal{A}} q_V^{(\pi, \alpha)}(x, a) \pi(da | x) = 0, \quad \forall x. \quad (167)$$

Following a similar idea as in Section 3, we obtain the following flow update for V under a fixed π :

$$\frac{d}{d\tau} V_\tau(x) = \int_{\mathcal{A}} q_{V_\tau}^{(\pi, \alpha)}(x, a) \pi(da | x). \quad (168)$$

A single explicit Euler step of (168) with step size $\tau > 0$ is

$$T_\tau^{(\pi, \alpha)}(V)(x) := V(x) + \tau \int_{\mathcal{A}} q_V^{(\pi, \alpha)}(x, a) \pi(da | x), \quad (169)$$

This yields an analogous Picard–Hamiltonian iteration for policy evaluation. The corresponding theoretical guarantees follow by applying the same argument as in the original setting, with only notational changes.

Table 6. Compute resources used in our experiments. “Cores” and “Memory” are per node.

Node class	CPU vendor (cores)	GPU vendor (count \times memory)	Host memory
CPU-only (high core)	NVIDIA (144)	–	237 GB
GPU node (single GPU)	NVIDIA (72)	NVIDIA (1 \times 96 GB)	116 GB
CPU-only (general)	AMD (128)	–	256 GB
GPU node (multi-GPU)	AMD (128)	NVIDIA (3 \times 40 GB)	256 GB
CPU-only (baseline)	Intel (48)	–	192 GB
CPU-only (HBM)	Intel (112)	–	128 GB (HBM)
CPU-only (large memory)	Intel (80)	–	4 TB (NVDIMM)

J. Further experiment details

J.1. Visualization on the trading task

We provide additional (qualitative) visualizations for the trading task in Figure 7. These plots complement the quantitative metrics by illustrating representative trajectories under the same evaluation market paths.

J.2. Visualization on control tasks

We provide additional qualitative results on the control tasks under two evaluation settings.

Irregular-time evaluation. We first evaluate on a held-out irregular-time setting and compare CT-SAC against (i) continuous-time baselines and (ii) discrete-time baselines. See Figures 8 and 9 for the corresponding images.

Regular-time evaluation. We also evaluate the same policies under the standard regular-time setting (which differs from the irregular-time training distribution) and again compare against continuous-time and discrete-time baselines. See Figures 10 and 11 for qualitative results.

J.3. Compute resources

All experiments were executed on High-Performance Computing infrastructure. We used a *mixture* of CPU-only and GPU-accelerated nodes with different hardware characteristics in order to support both large-scale sweeps and computationally intensive deep RL training. Each run used a single node. We report details in Table 6.

J.4. Ablation-study hyperparameters

For completeness, we list the hyperparameter configurations used in the ablation study. Table 7, 8, 9, and 10 provide the configuration dictionary for each algorithm group, with **top/second/third** referring to the ranked settings used in the ablation tables. Due to space limit, we only list differing hyperparameters for these configurations. Please refer to the codebase to get a complete set of hyperparameters.

K. Benchmarking algorithms

K.1. Coupled-style q -learning

As the step size $u \rightarrow 0$, the drift contribution scales as $O(u)$ while the stochastic increment is $O(\sqrt{u})$, so a squared TD residual can be dominated by martingale variation rather than the Bellman drift. To address this mismatch, Jia & Zhou (2023) characterize optimality via a martingale condition: for any start time t_0 , the process:

$$M_t := e^{-\beta t} V(X_t) + \int_{t_0}^t e^{-\beta s} (r(X_s, a_s) - q(X_s, a_s)) ds$$

must be a martingale. Two practical relaxations follow from this characterization: (i) a *martingale-loss* objective built from squared pathwise residuals (involving an outer integral over t and an inner integral over future s), and (ii) *martingale orthogonality* conditions of the form $\mathbb{E} \int_0^T \omega_t (dV(X_t) + ((r - q) - \beta V) dt) = 0$ for suitable test processes ω_t . To implement both criteria, we consider an (irregular) grid $t_0 < t_1 < \dots < t_K = T$ with $\Delta_{t_i} := t_{i+1} - t_i$, and samples $(x_{t_i}, a_{t_i}, r_{t_i})$. Define the discounted martingale increment over $[t_k, T]$:

$$G_{t_k:T}(V, q) := e^{-\beta(T-t_k)} h(x_{t_K}) - V(x_{t_k}) + \sum_{i=k}^{K-1} e^{-\beta(t_i-t_k)} [r_{t_i} - q(x_{t_i}, a_{t_i})] \Delta_{t_i}.$$

Two commonly used enforcement criteria are:

Table 7. Hyperparameter dictionary (CT-SAC vs SAC). For each environment, **top/second/third** correspond to the ranked configurations used in Table 2.

Task	CT-SAC			SAC		
	top	second	third	top	second	third
Cheetah	lr=0.00073, tau=0.04	lr=0.00073, tau=0.02	lr=0.00146, tau=0.04	lr=0.00073, train_freq=4, gradient_steps=4	lr=0.00073, train_freq=1, gradient_steps=1	lr=0.00146, train_freq=4, gradient_steps=4
Walker	lr=0.00073, train_freq=1, gradient_steps=1, tau=0.02	lr=0.00073, train_freq=4, gradient_steps=4, tau=0.02	lr=0.00146, train_freq=4, gradient_steps=4, tau=0.01	lr=0.00146, train_freq=1, gradient_steps=1	lr=0.00073, train_freq=4, gradient_steps=4	lr=0.00292, train_freq=1, gradient_steps=1
Humanoid	train_freq=1, gradient_steps=1, tau=0.01	train_freq=4, gradient_steps=4, tau=0.005	train_freq=1, gradient_steps=1, tau=0.005	log_std_init=-0.5, lr=0.0003, tau=0.0025	log_std_init=0.5, lr=0.0003, tau=0.005	log_std_init=-0.5, lr=0.0012, tau=0.005
Quadruped	train_freq=4, gradient_steps=4, tau=0.02	train_freq=1, gradient_steps=1, tau=0.04	train_freq=1, gradient_steps=1, tau=0.02	lr=0.000182	lr=0.00292	lr=0.00146
Trading	lr=0.001, train_freq=4, gradient_steps=4, tau=0.02	lr=0.0005, train_freq=1, gradient_steps=1, tau=0.02	lr=0.001, train_freq=1, gradient_steps=1, tau=0.005	log_std_init=-3.0, lr=0.002, train_freq=1, gradient_steps=1	log_std_init=-1.0, lr=0.002, train_freq=4, gradient_steps=4	log_std_init=-3.0, lr=0.001, train_freq=1, gradient_steps=1

Abbreviation: lr=learning_rate; tau=soft-update rate; train_freq=update frequency; gradient_steps=number of gradient steps per update; log_std_init=initial policy log-std.

1. **Martingale loss (pathwise squared residual)** (See Algorithm 3):

$$\mathcal{L}_{\text{mg}}(V, q) := \sum_{k=0}^{K-1} G_{t_k:T}(V, q)^2 \Delta_{t_k}.$$

2. **Martingale orthogonality (test-function TD):** define the one-step residual

$$\delta_k := V(x_{t_{k+1}}) - V(x_{t_k}) + (r_{t_k} - q(x_{t_k}, a_{t_k}) - \beta V(x_{t_k})) \Delta_{t_k},$$

and enforce $\mathbb{E}[\omega(x_{t_k}, a_{t_k}) \delta_k] = 0$ for a class of test functions ω (value gradient in this case), yielding simple SGD-style updates (See Algorithm 4).

K.2. Policy gradient

We denote a regularizer by $p(x, a; \pi)$ (for entropy regularization, $p(x, a; \pi) = -\log \pi(a|x)$) and the performance $\eta(\pi) := \int_{\mathcal{S}} V(x; \pi) \mu(dx)$. Below are two continuous-time policy gradient where CPPO (see Algorithm 6) is an upgraded version over the (vanilla) CPG (see Algorithm 5). For CPPO, due to its instability, we use 1.5 instead of 2 for penalty adaptation.

Table 8. Hyperparameter dictionary (CT-TD3 vs TD3). For each environment, **top/second/third** correspond to the ranked configurations used in Table 2.

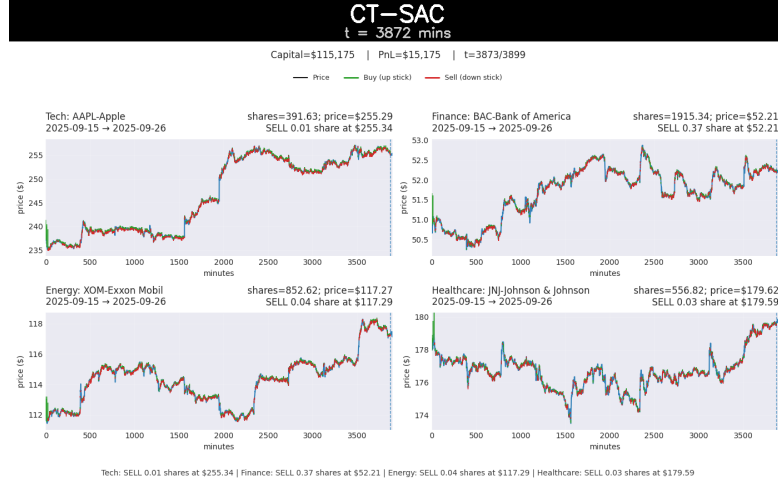
Task	CT-TD3			TD3		
	top	second	third	top	second	third
Cheetah	noise_sigma=0.1, policy_noise=0.4, noise_clip=1.0	noise_sigma=0.2, policy_noise=0.2, noise_clip=0.5	noise_sigma=0.1, policy_noise=0.2, noise_clip=0.3	lr=0.00073, policy_noise=0.3, noise_clip=0.6	lr=0.00073, policy_noise=0.1, noise_clip=0.2	lr=0.00146, policy_noise=0.1, noise_clip=0.2
Walker	lr=0.000365, policy_noise=0.2, noise_clip=0.5	lr=0.00073, policy_noise=0.2, noise_clip=0.5	lr=0.000365, policy_noise=0.1, noise_clip=0.2	lr=0.001, policy_noise=0.1, noise_clip=0.2	lr=0.0006, policy_noise=0.1, noise_clip=0.2	lr=0.0003, policy_noise=0.1, noise_clip=0.2
Humanoid	policy_noise=0.2, noise_clip=1.0	policy_noise=0.2, noise_clip=0.5	policy_noise=0.1, noise_clip=0.2	lr=0.0003, policy_noise=0.1, noise_clip=0.2	lr=0.0003, policy_noise=0.2, noise_clip=0.5	lr=0.0006, policy_noise=0.2, noise_clip=0.5
Quadruped	noise_sigma=0.1, policy_noise=0.4, noise_clip=1.0	noise_sigma=0.1, policy_noise=0.2, noise_clip=0.5	noise_sigma=0.2, policy_noise=0.2, noise_clip=0.5	lr=0.00073, policy_noise=0.4, noise_clip=1.0	lr=0.0003, policy_noise=0.2, noise_clip=0.5	lr=0.00073, policy_noise=0.2, noise_clip=0.5
Trading	noise_sigma=0.1, policy_noise=0.4, noise_clip=1.0	noise_sigma=0.1, policy_noise=0.1, noise_clip=0.2	noise_sigma=0.2, policy_noise=0.2, noise_clip=0.5	lr=0.001, policy_noise=0.2, noise_clip=0.3	lr=0.002, policy_noise=0.2, noise_clip=0.5	lr=0.001, policy_noise=0.3, noise_clip=0.6

Abbreviation: lr=learning_rate; policy_noise=noise std for target action; noise_clip=clip range for that noise; noise_sigma=exploration/target noise scale.

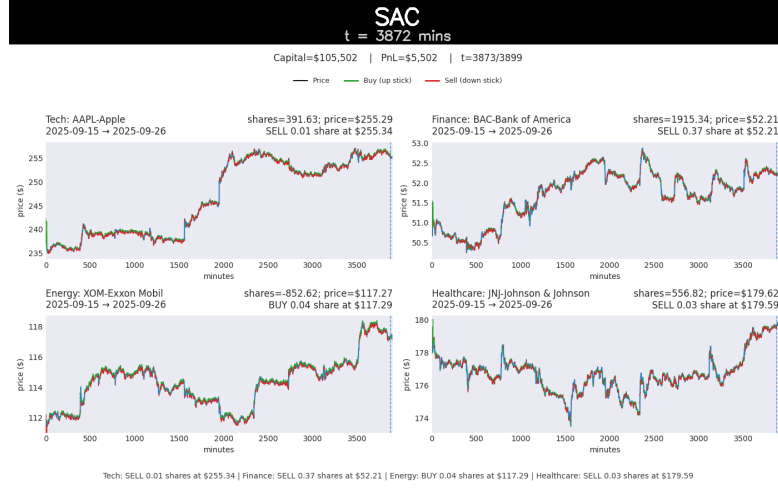
Table 9. Hyperparameter dictionary (CPPO vs PPO). For each environment, **top/second/third** correspond to the ranked configurations used in Table 2.

Task	CPPO			PPO		
	top	second	third	top	second	third
Cheetah	lr=0.00073, alpha=0.004, clip_ratio=False, clip_range=0.2, kl_coef_init=1.0	lr=0.00073, alpha=0.004, clip_ratio=True, clip_range=0.1, kl_coef_init=0.3	lr=0.00146, alpha=0.004, clip_ratio=False, clip_range=0.2, kl_coef_init=1.0	lr=0.000365, clip_range=0.2, vf_coef=0.5, gae_lambda=0.95	lr=0.000365, clip_range=0.1, vf_coef=0.5, gae_lambda=0.95	lr=0.000365, clip_range=0.2, vf_coef=1.0, gae_lambda=0.8
Walker	lr=0.00073, alpha=0.004, clip_ratio=False, clip_range=0.2, kl_coef_init=1.0	lr=0.000365, alpha=0.004, clip_ratio=False, clip_range=0.2, kl_coef_init=1.0	lr=0.00146, alpha=0.004, clip_ratio=False, clip_range=0.2, kl_coef_init=1.0	lr=0.000365, clip_range=0.2, vf_coef=1.0, gae_lambda=0.95	lr=0.000365, clip_range=0.2, vf_coef=0.5, gae_lambda=0.95	lr=0.000365, clip_range=0.2, vf_coef=0.5, gae_lambda=0.8
Humanoid	log_std_init=-0.5, alpha=0.004	log_std_init=-1.0, alpha=0.004	log_std_init=-1.0, alpha=0.004	lr=0.0003, clip_range=0.2, vf_coef=0.5	lr=0.0003, clip_range=0.3, vf_coef=0.5	lr=0.0006, clip_range=0.2, vf_coef=0.5
Quadruped	log_std_init=-3.0, clip_ratio=False, clip_range=0.3	log_std_init=-3.0, clip_ratio=False, clip_range=0.2	log_std_init=-1.0, clip_ratio=False, clip_range=0.2	lr=0.000365, clip_range=0.2, vf_coef=0.5, gae_lambda=0.95	lr=0.000182, clip_range=0.2, vf_coef=0.5, gae_lambda=0.95	lr=0.000365, clip_range=0.2, vf_coef=0.5, gae_lambda=0.8
Trading	alpha=0.0004, sqrt_kl=0.02	alpha=0.04, sqrt_kl=0.02	alpha=0.0004, sqrt_kl=0.01	lr=0.002, clip_range=0.2, clip_range_vf=0.2, vf_coef=0.5	lr=0.001, clip_range=0.3, clip_range_vf=0.3, vf_coef=0.5	lr=0.001, clip_range=0.2, clip_range_vf=0.2, vf_coef=1.0

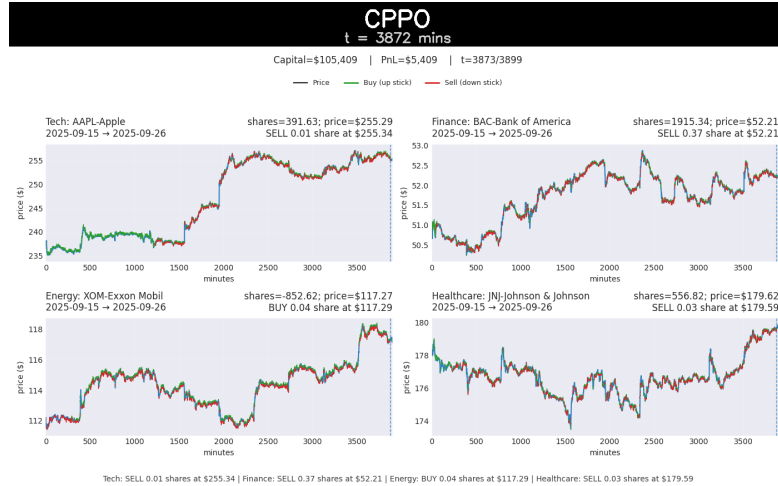
Abbreviation: lr=learning_rate; alpha=entropy coefficient; clip_range=PPO clipping range; clip_range_vf=value-function clipping; vf_coef=value loss coefficient; gae_lambda=GAE λ ; log_std_init=initial policy log-std; sqrt_kl=target \sqrt{KL} constraint (CPPO).



(a) CT-SAC on trading task



(b) SAC on trading task



(c) PPO on trading task

Figure 7. CT-SAC vs. two competitive baselines CT-SAC and CPPO on trading task with two-week trading episode under irregular time steps. During these 2-weeks, CT-SAC made a profit of \$15,000 while other two methods only make about \$5,500.

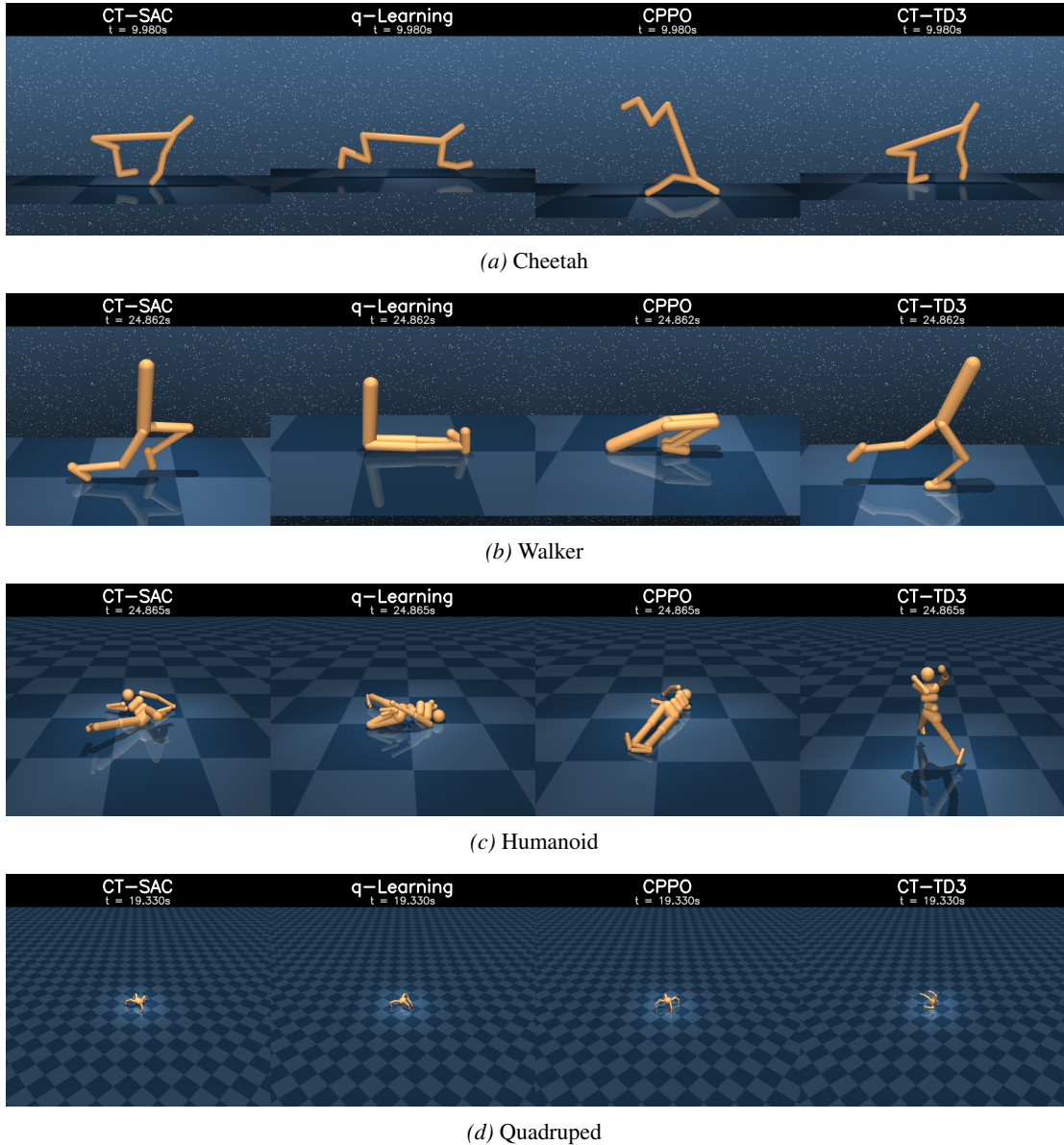


Figure 8. CT-SAC vs. continuous-time baselines under irregular time steps.

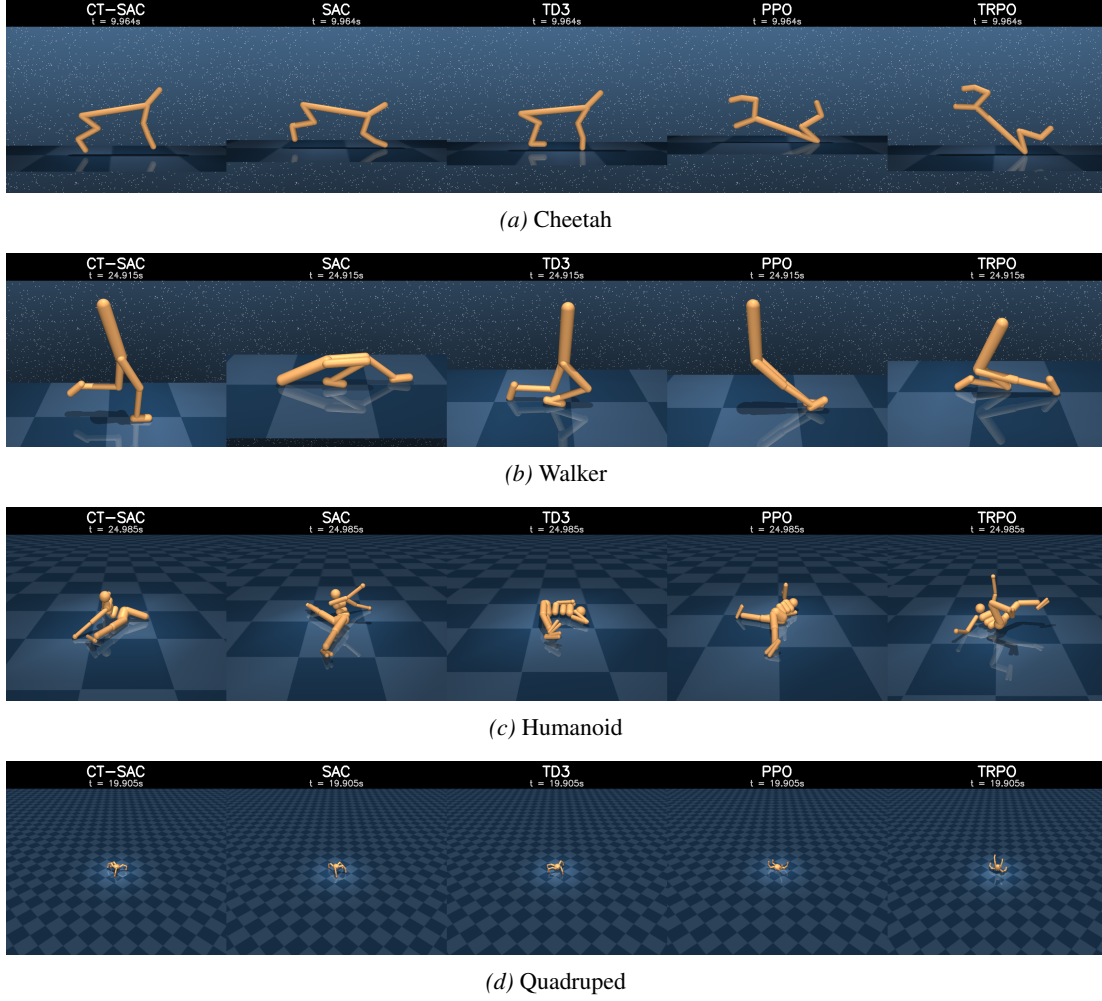


Figure 9. CT-SAC vs. discrete-time baselines under irregular time steps.

 Table 10. Hyperparameter dictionary (TRPO vs q-learning). For each environment, **top/second/third** correspond to the ranked configurations used in Table 2.

Task	TRPO			q-learning		
	top	second	third	top	second	third
Cheetah	lr=0.000365, gae_lambda=0.95, cg_damping=0.1	lr=0.000182, gae_lambda=0.95, cg_damping=0.1	lr=0.000365, gae_lambda=0.8, cg_damping=0.1	train_freq=1, gradient_steps=1, max_grad_norm=0.5	train_freq=4, gradient_steps=4, max_grad_norm=0.5	train_freq=4, gradient_steps=4, max_grad_norm=1.0
Walker	lr=0.000365, gae_lambda=0.95, cg_damping=0.1	lr=0.000182, gae_lambda=0.95, cg_damping=0.1	lr=0.000365, gae_lambda=0.8, cg_damping=0.1	log_std_init=-3, lr=0.000365	log_std_init=-1, lr=0.000365	log_std_init=-3, lr=0.000182
Humanoid	lr=0.0006, target_kl=0.01	lr=0.0003, target_kl=0.01	lr=0.001, target_kl=0.01	log_std_init=-1, lr=0.000365	log_std_init=-3, lr=0.000365	log_std_init=-1, lr=0.000182
Quadruped	lr=0.000365, gae_lambda=0.95, cg_damping=0.1	lr=0.000182, gae_lambda=0.8, cg_damping=0.1	lr=0.000365, gae_lambda=0.8, cg_damping=0.1	lr=0.000365, log_std_init=-3	lr=0.00073, log_std_init=-3	lr=0.00146, log_std_init=-3
Trading	lr=0.001, target_kl=0.005	lr=0.002, target_kl=0.01	lr=0.0005, target_kl=0.01	lr=0.004, max_grad_norm=1.0, log_std_init=-3	lr=0.002, max_grad_norm=0.5, log_std_init=-3	lr=0.001, max_grad_norm=1.0, log_std_init=-1

Abbreviation: lr=learning_rate; gae_lambda=GAE λ ; target_kl=TRPO KL constraint; cg_damping=conjugate-gradient damping; max_grad_norm=gradient clipping threshold; train_freq=update frequency; gradient_steps=number of gradient steps per update; log_std_init=initial policy log-std.

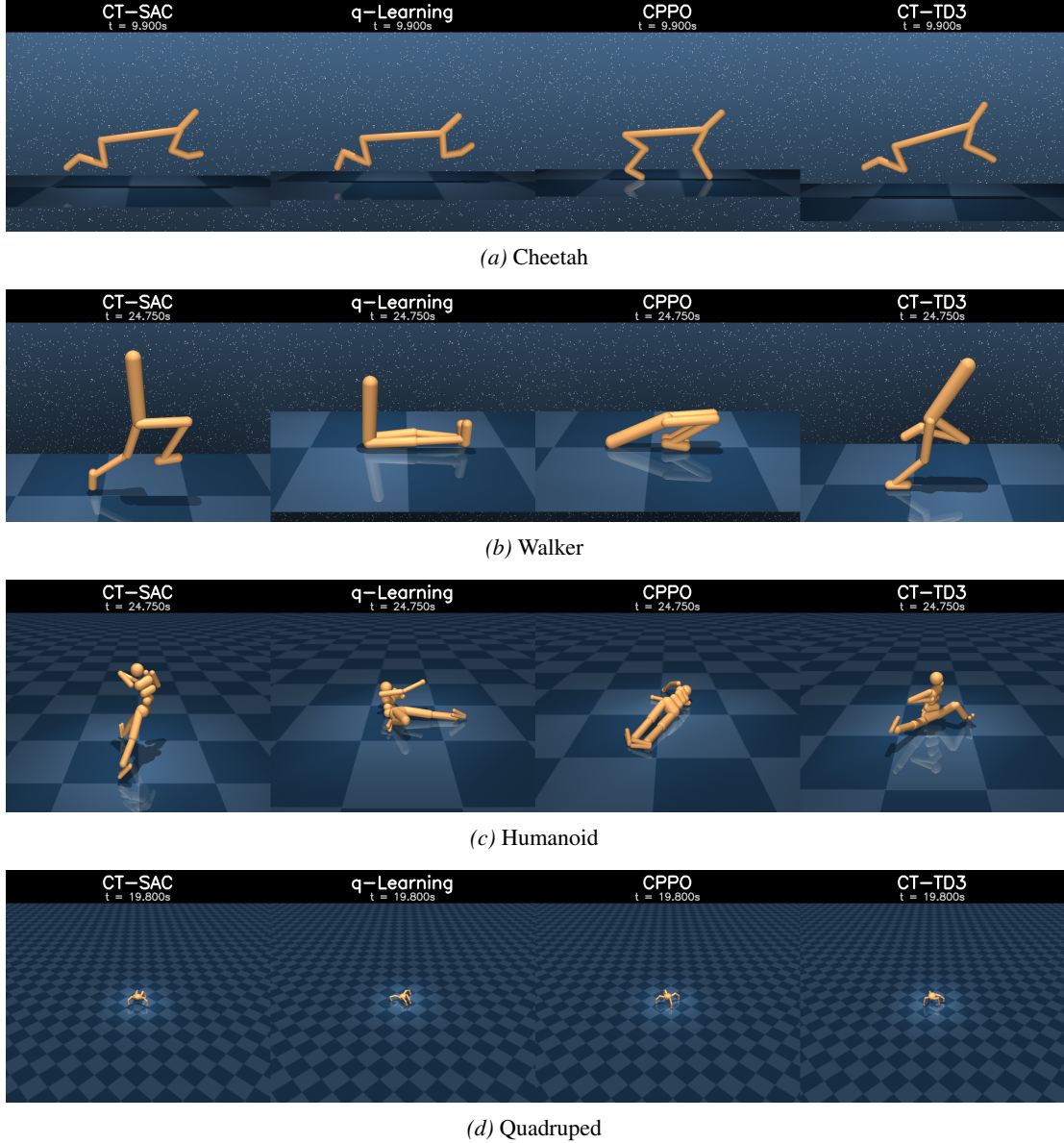


Figure 10. CT-SAC vs. continuous-time baselines under **regular** time steps. Note that the model is trained under irregular time settings.

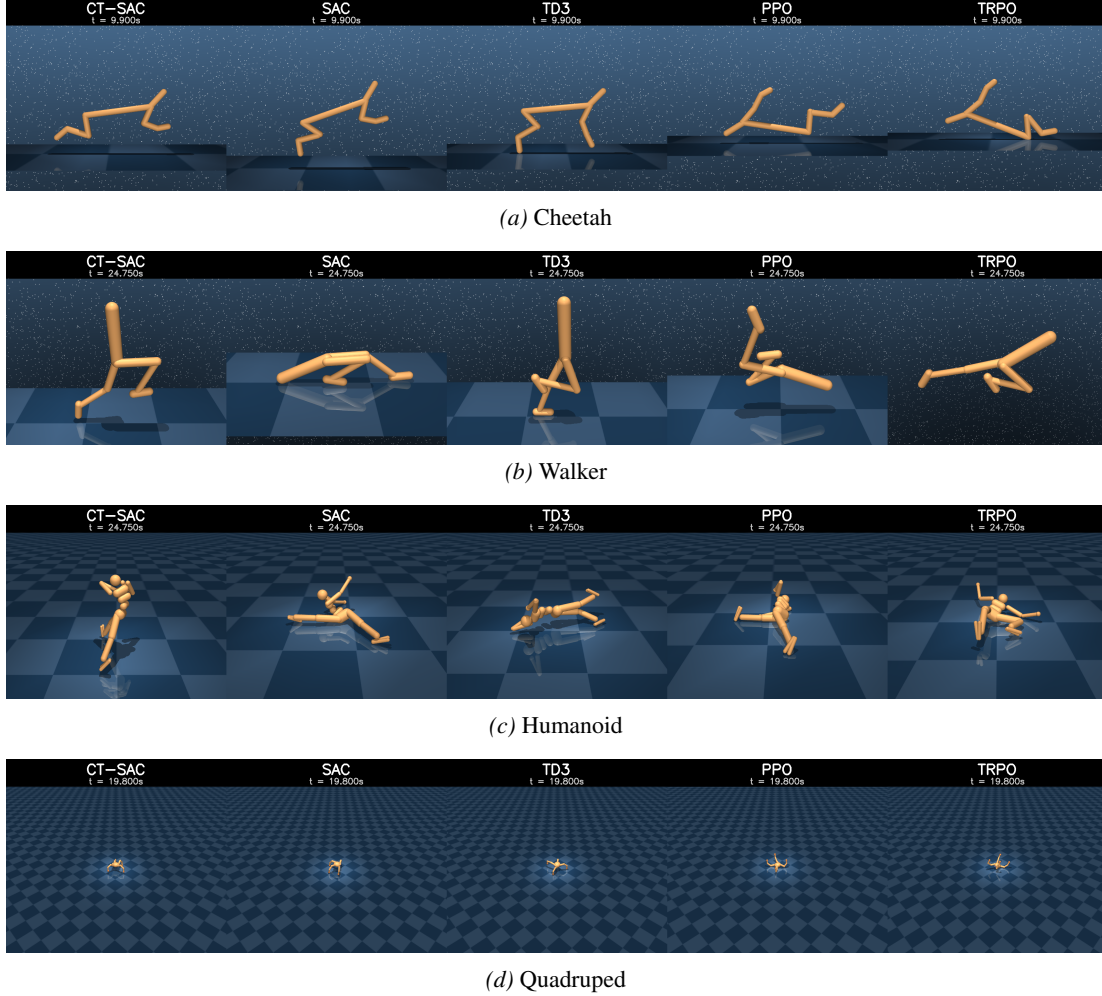


Figure 11. CT-SAC vs. discrete-time baselines under **regular** time steps. Note that the model is trained under irregular time settings.

Algorithm 3 Coupled-style q -learning (Martingale loss)

- 1: **Input:** discount β , terminal time $T = t_K$, learning rates η_V, η_q .
- 2: Initialize parameters θ for value V_θ and ψ for advantage-rate q_ψ .
- 3: **for** $k_{\text{iter}} = 0, 1, 2, \dots$ **do**
- 4: Collect rollouts under a behavior policy, producing irregular grid samples $\{(x_{t_i}, a_{t_i}, r_{t_i}, \Delta_{t_i})\}_{i=0}^{K-1}$ and terminal payoff $h(x_{t_K})$.
- 5: Sample a mini-batch of trajectories (or segments) from the dataset/buffer.
- 6: **for** each trajectory in the mini-batch **do**
- 7: **for** $k = 0, 1, \dots, K-1$ **do**
- 8: Compute
$$G_{t_k:T}(V_\theta, q_\psi) := e^{-\beta(T-t_k)}h(x_{t_K}) - V_\theta(x_{t_k}) + \sum_{i=k}^{K-1} e^{-\beta(t_i-t_k)}[r_{t_i} - q_\psi(x_{t_i}, a_{t_i})]\Delta_{t_i}.$$
- 9: **end for**
- 10: Form loss $\mathcal{L}_{\text{mg}}(\theta, \psi) := \sum_{k=0}^{K-1} G_{t_k:T}(V_\theta, q_\psi)^2 \Delta_{t_k}$.
- 11: Update critics (SGD): $\theta \leftarrow \theta - \eta_V \nabla_\theta \mathcal{L}_{\text{mg}}(\theta, \psi)$, $\psi \leftarrow \psi - \eta_q \nabla_\psi \mathcal{L}_{\text{mg}}(\theta, \psi)$.
- 12: **end for**
- 13: **end for**

Algorithm 4 Coupled-style q -learning (Martingale orthogonality)

```

1: Input: discount  $\beta$ , learning rates  $\eta_V, \eta_q$ .
2: Initialize parameters  $\theta$  for value  $V_\theta$  and  $\psi$  for advantage-rate  $q_\psi$ .
3: for  $k_{\text{iter}} = 0, 1, 2, \dots$  do
4:   Collect transitions with irregular increments  $(x, a, r, x', \Delta)$  and store in a buffer.
5:   Sample a mini-batch  $\mathcal{B}$  of transitions from the buffer.
6:   for each  $(x, a, r, x', \Delta)$  in  $\mathcal{B}$  do
7:     Compute one-step residual

$$\delta := V_\theta(x') - V_\theta(x) + (r - q_\psi(x, a) - \beta V_\theta(x))\Delta.$$

8:     Update value (test function  $\omega_1 = \nabla_\theta V_\theta$ ):  $\theta \leftarrow \theta + \eta_V \nabla_\theta V_\theta(x) \delta$ .
9:     Update advantage-rate (test function  $\omega_2 = \nabla_\psi q_\psi$ ):  $\psi \leftarrow \psi + \eta_q \nabla_\psi q_\psi(x, a) \delta$ .
10:    end for
11:   end for

```

Algorithm 5 Continuous-time policy gradient (CPG)

```

1: Input: discount  $\beta$ , temperature  $\alpha$ , learning rates  $\eta_V, \eta_\pi$ .
2: Models: value  $V_\phi$ , policy  $\pi_\theta$ .
3: for  $k = 0, 1, 2, \dots$  do
4:   Collect transitions  $(x, a, r, x', \Delta)$  from rollouts under current policy  $\pi_\theta$ , where  $\Delta = t' - t$  can vary.
5:   Critic update (martingale orthogonality):

```

$$\delta_V := V_\phi(x') - V_\phi(x) + \Delta(r(x, a) + \alpha p(x, a; \pi_\theta)) - \beta V_\phi(x)\Delta,$$

and perform SGD: $\phi \leftarrow \phi + \eta_V \nabla_\phi V_\phi(x) \delta_V$.

```

6:   Advantage-rate estimate (one-step / GAE-style):

$$\hat{q}(x, a) := r + \frac{e^{-\beta\Delta} V_\phi(x') - V_\phi(x)}{\Delta}.$$


```

```

7:   Policy gradient step: update  $\theta$  using a mini-batch estimator of

```

$$\nabla_\theta \eta(\theta) \approx \frac{1}{\beta} \nabla_\theta \log \pi_\theta(a|x) (\hat{q}(x, a) + \alpha p(x, a; \pi_\theta)) + \frac{\alpha}{\beta} \nabla_\theta p(x, a; \pi_\theta).$$

```

8:    $\theta \leftarrow \theta + \eta_\pi \widehat{\nabla_\theta \eta}(\theta).$ 
9:   end for

```

Algorithm 6 Continuous-time proximal policy optimization (CPPO, KL-penalty)

- 1: **Input:** discount β , temperature α , target KL δ_{KL} , tolerance ϵ , initial penalty C_{pen} , actor epochs E .
- 2: **Models:** value V_ϕ , policy π_θ .
- 3: **for** $k = 0, 1, 2, \dots$ **do**
- 4: Collect a batch $\mathcal{B} = \{(x, a, r, x', \Delta)\}$ from rollouts under current policy π_{θ_k} .
- 5: Update critic V_ϕ using the CPG martingale-orthogonality step (Algorithm 5, line 5).
- 6: Compute advantage-rate estimates $\hat{q}(x, a)$ on \mathcal{B} (Algorithm 5, line 6) and (optionally) normalize.
- 7: Set $\theta \leftarrow \theta_k$.
- 8: **for** epoch $e = 1, \dots, E$ **do**
- 9: For mini-batches from \mathcal{B} , compute importance ratio $w_\theta(x, a) := \pi_\theta(a|x)/\pi_{\theta_k}(a|x)$.
- 10: Define penalized surrogate objective

$$J(\theta) := \mathbb{E}_{(x,a) \sim \mathcal{B}} [w_\theta(x, a)(\hat{q}(x, a) + \alpha p(x, a; \pi_\theta))] - C_{\text{pen}} \bar{D}_{\text{KL}}(\theta \parallel \theta_k),$$

where $\bar{D}_{\text{KL}}(\theta \parallel \theta_k) := \mathbb{E}_{x \sim \mathcal{B}} \left[\sqrt{D_{\text{KL}}(\pi_{\theta_k}(\cdot|x) \parallel \pi_\theta(\cdot|x))} \right]$.

- 11: Update actor by gradient ascent on $J(\theta)$.
- 12: **end for**
- 13: Set $\theta_{k+1} \leftarrow \theta$.
- 14: **Penalty adaptation:** if $\bar{D}_{\text{KL}}(\theta_{k+1} \parallel \theta_k) \geq (1 + \epsilon)\delta_{\text{KL}}$, set $C_{\text{pen}} \leftarrow 2C_{\text{pen}}$; else if $\bar{D}_{\text{KL}}(\theta_{k+1} \parallel \theta_k) \leq \delta_{\text{KL}}/(1 + \epsilon)$, set $C_{\text{pen}} \leftarrow \frac{1}{2}C_{\text{pen}}$.
- 15: **end for**
